MOJIM RODITELJIMA

PREFACE

This thesis is concerned with a reinvestigation of the kinetics and mechanism of the mercury-photosensitized decomposition of propane. In spite of a considerable amount of previous work, many details of the kinetics have remained obscure. The pressure dependence of the rates of formation of various products has not been previously examined in detail. The activation energy and the pressure dependence of the first-order rate constant for the unimolecular decomposition of propyl radicals were unsettled, since there were discrepancies in the previous literature. The present work was undertaken to investigate the influence of pressure on the mercury-photosensitized decomposition of propane at various temperatures.

ACKNOWLEDGMENTS

I wish to express my sincere thanks for having had the privilege of working under the direction of Professor K. J. Laidler, who has been most willing to assist in all aspects of this work. His patience and encouragement throughout the course of this research are most gratefully acknowledged.

Thanks are also due to Drs. M. H. Back and J. L. Holmes from the University of Ottawa and to Dr. R. A. Back from the National Research Council of Canada for their helpful suggestions. Appreciation is also extended to my colleagues for many useful discussions.

To my wife I wish to express a special gratitude for her constant help, understanding and moral support.

TABLE OF CONTENTS

Page No.

LIST OF TABLES

LIST OF FIGURES

ABSTRACT

The mercury-photosensitized decomposition of propane was investigated at 252°C, 276°C, 301°C, 325°C and 350°C and over the pressure range from 5 mm Hg to 700 mm Hg. The initial rates of formation of H_2, CH_4, C_2H_4, C_2H_6, $(CH_3)_2CHCH(CH_3)_2$, $(CH_3)_2CHCH_2CH_2CH_3$ and n-C_6H_{14} were measured. The rate of formation of all the measured products increased with increasing pressure of propane at low propane pressures and approached constant values at high pressures of propane. The propane pressure at which the rates of formation of hydrogen and of the three isomeric hexanes became pressure independent is about 150 to 160 mm Hg, and is approximately independent of temperature. The limiting pressure of propane for methane, ethene and ethane, on the other hand, depends on the temperature and increases with increasing temperature.

The pressure dependence of the rates of formation of the products is discussed in the light of the proposed mechanism. The influence of the CO_2 as inert gas was briefly examined, and its effect on the quenching of the excited mercury atoms is discussed.

In the low temperature region (252 and 276°C) the rate of hydrogen production was found to be independent of temperature, and is greater than the rate of production of any other product. At high temperatures, where the decomposition of propyl radicals is an additional source of hydrogen, the rate of hydrogen production increases with increasing temperature. At high propane pressures, the activation energy of hydrogen production by decomposition of propyl radicals is 38.7 kcal.mole^{-1}.

The rates of production of methane, ethene and ethane are strongly dependent on temperature. Their energies of activation increase with increasing pressure of propane and become constant at high pressures of propane. At high propane pressures, the activation energies are 29.5 kcal.mole^{-1}, 29.7 kcal.mole^{-1}, and 24.0 kcal.mole^{-1}, respectively.

No significant change in the rate of 2,3-dimethylbutane formation was detected when the temperature was increased from 250 to 350°C, whereas the rates of 2-methylpentane and n-hexane diminished on raising the temperature. This implies that the concentration of i-propyl radicals remains essentially constant, while the concentration of n-propyl radicals decreases when the temperature is raised.

The concentrations of n-propyl and i-propyl radicals as a function of temperature are given by: $[n\text{-}C_3H_7] = \text{const.}\exp(2.9/RT)$ and $[i\text{-}C_3H_7] = \text{const.}\exp(-0.2/RT)$. The ratio of their concentrations is given by the expression $[i\text{-}C_3H_7]/[n\text{-}C_3H_7] = 1.7 \times 10^2 \exp(-3.1/RT)$.

The products of the combination reactions of propyl radicals revealed the ratio $k_{ab}/(k_{aa}k_{bb})^{1/2}$ to be near 2, in agreement with the theoretical predictions.

The decomposition of the n-propyl radical into the methyl radical and ethene has been investigated as a function of temperature and propane pressure. The high-pressure rate constant is given by the expression $k_{20b} = 2.5 \times 10^{14}\exp(-32.6/RT)\text{sec}^{-1}$. The limiting value of the low-pressure rate constant obtained from the slopes of the Lindemann plots is given by $k^{o}_{20b} = 2.5 \times 10^{7}\exp(-17.0/RT)$cc. mole^{-1}sec^{-1}.

With the high-pressure value of E_{20b} the standard dissociation energy of the C-C bond in the n-propyl radical was obtained: $DH^{o}(n\text{-}CH_3\text{-}CH_2CH_2) = 24.3$ kcal.mole^{-1}. The standard heat of formation for the n-propyl radical is then $\Delta H_f^{o}(n\text{-}C_3H_7) = 20.2$ kcal.mole^{-1} and the primary C-H standard bond dissociation energy in propane is $DH^{o}(CH_3CH_2CH_2\text{-}H) = 97.1$ kcal.mole^{-1}. The entropy change for the decomposition reaction of the n-propyl radical into a methyl radical and ethene is $\Delta S_{20b} = 10.6$ cal.deg.$^{-1}$mole^{-1}, the standard state being 1 mole cc^{-1} of ideal gas. The entropy of activation for this reaction is $\Delta S^{\neq}_{20b} = 5.4$ cal.deg.$^{-1}$mole^{-1} at 25°C.

The decomposition of the i-propyl radical into a hydrogen atom and propene has been investigated over the temperature range 250 to 350°C and the pressure range 5 mm Hg to 700 mm Hg. The unimolecular rate coefficient for this decomposition, k_{21a}, does not show any regular dependence on the propane pressure at pressures above about 10 mm Hg. If there is a fall off of k_{21a} with decreasing propane pressure it must then take place in the pressure region below 10 mm Hg. The high-pressure rate constant is given by $k_{21a} = 2.0 \times 10^{14} \exp(-38.7/RT)\text{sec}^{-1}$.

With the high-pressure value of E_{21a} the standard bond dissociation energy of the C-H bond in the i-propyl radical was obtained: $DH^{o}(i\text{-}CH_3CHCH_2\text{-}H) = 38.1$ kcal.mole^{-1}. The standard heat of formation for the i-propyl radical has been then estimated $\Delta H_f^{o}(i\text{-}C_3H_7) = 18.9$ kcal.mole^{-1}, and the secondary C-H standard bond dissociation energy in propane, $DH^{o}[(CH_3)_2)CH\text{-}H] = 95.8$ kcal.mole^{-1}. The entropy change for the decomposition reaction of the i-propyl radical into a hydrogen atom and propene is $\Delta S_{21a} = 6.0$ cal.deg.$^{-1}$mole^{-1}, the standard state being 1 mole cc^{-1} of ideal gas. The entropy of activation for this reaction is $\Delta S^{\neq}_{21a} = 5.0$ cal.deg.$^{-1}$mole^{-1} at 25°C.

CHAPTER I

INTRODUCTION

1.1 Object of the Investigation

The aim of the present work is to study the kinetics and mechanism of the mercury-photosensitized decomposition of propane over a wide range of pressure and temperature, special attention being paid to the decomposition of propyl radicals.

The main types of elementary reactions of univalent free radicals which may occur in the system are (1, 2):

(1) The splitting of a bond in a stable molecule, with the formation of free radicals:

$$R_1R_2 + Hg^* \rightarrow R_1 + R_2 + Hg$$

(2) A substitution reaction:

$$R_1 + R_2R_3 \rightarrow R_1R_2 + R_3$$

where R_1, R_2 and R_3 are atoms or radicals. R_2 is a single atom in the majority of substitution reactions which have so far been studied. The most common type is that in which the species transferred, R_2, is a hydrogen atom.

(3) The decomposition of a radical to form a molecule and a smaller radical:

$$RM_1 - M_2 \rightarrow R + A_1 = A_2$$

(4) The addition of radicals to multiple bonds (i.e. the inverse of (3);

$$R + M_1 = M_2 \rightarrow RM_1 - M_2$$

(5) A radical-radical (or atom) interaction, involving recombination and disproportionation:

$$2C_3H_7 \rightarrow C_6H_{14} \text{ and } 2C_3H_7 \rightarrow C_3H_6 + C_3H_8$$

(6) An isomerization reaction such as:

$$CH_3 - CH_2 - CH_2 \rightarrow CH_3 - CH - CH_3$$

These elementary reactions may be either unimolecules or bimolecular. The rates of these processes are given by the formulae:

$$v_1 = A_1 \exp(-E_1/RT)[R]$$

(unimolecular decomposition or isomerization of the radical of concentration [R]) , and

$$v_2 = A_2 \exp(-E_2/RT)[R][M]$$

(bimolecular reaction). In these equations, A_1 and A_2 are the frequency factors and E_1 and E_2 the activation energies; R is the gas constant.

It is only in recent years that techniques have become available to study the elementary processes in a reaction mechanism and to examine the effects of temperature, pressure and foreign gases on the individual steps. In some case it is now possible to observe the kinetic behavior of a unimolecular reaction that is one step of an overall mechanism. The most easily accessi ble examples for the study of unimolecular reactions are the thermal isomerization reactions such as the isomerization of cyclopropane to propene. A number of isomerizations have been studied so far, as have many molecular decompositions. Decompositions of radicals have been studied to a much less extent.

The unimolecular decomposition of a radical is frequently one of the chain-propagating steps; an understanding of radical decompositions is thus of considerable importance in understanding the overall reaction mechanism of a chain reaction. The activation energies for the decomposition of some radicals have been obtained from the study of the reactions at different temperatures. These studies have often been made at one pressure and involve an assumption about the kinetic order of the decomposition at this pressure. Although the assumption of a certain order of reaction is sometimes justified, there is some uncertainty because the order of the radical decomposition may be a function of pressure. The most frequently used radicals in pyrolysis and photolysis investigations containing 4 to 10 atoms are likely to show a variation in the order of reaction with pressure over the pressure range from 10 to 600 mm Hg. For larger species the pressure dependence is observed at lower pressures, while smaller species will show second-order kinetics over this range of pressure, and the kinetics will change to first order only at several atmospheres pressure. The determination of the kinetic parameters of the radical decomposition reaction is often difficult, and very divergent kinetic parameters are sometimes obtained. Values for the activation energy and the rate constant at 300°K for the decomposition of n-C_3H_7 radical into $CH_3 + C_2H_4$ for example, varied from 20 to 35 kcal per mole and from 16 to 268 sec^{-1}, respectively, as obtained in seven separate studies (3, 4, 5, 6, 7, 8, 9).

It is also possible to arrive at values of activation energies from thermochemical data. In the case of the propyl radical we can set up the sequence:

$$C_3H_8 \rightarrow C_2H_4 + CH_4 - 18 \text{ kcal} \quad [1]$$

$$CH_4 \rightarrow CH_3 + H - 104 \text{ kcal} \quad [2]$$

$$H + C_3H_7 \rightarrow C_3H_8 + 98 \text{ kcal} \quad [3]$$

$$C_3H_7 \rightarrow C_2H_4 + CH_3 - 24 \text{ kcal} \quad [4]$$

The heat of reaction [1] could be calculated from thermochemical values of heats of formation. The heat of reaction [4] can thus be obtained if the heats of [2] and [3] are known, i.e. if we know DH° (CH_3-H) and DH° (C_3H_7-H). DH° (CH_3-H) seems to be well established, but DH° (C_3H_7-H) is not certain and a value of 98 ± 2 kcal seems to be accepted at present. On this basis, $\Delta H_4^\circ = 24 \pm 3$ kcal. The activation energy of the reverse of [4], i.e. the addition of a methyl radical to ethene, is certainly small and is assumed to be 4 ± 2 kcal. Hence we may put $E_4 = 28 \pm 5$ kcal.

The study described in this thesis was initiated to examine the thermal decomposition of propyl radicals over a wide range of pressure and temperature. Propyl radicals are known to decompose to ethene and a methyl radical, and to propene and a hydrogen atom. The activation energy and the pressure dependence of the first-order rate constant for the unimolecular decomposition are uncertain, a number of different values having been obtained in previous investigations. The thermochemical discussion of the correlation of the observed activation energies with the thermochemistry of the corresponding reactions was also uncertain, for similar reasons.

1.2 Review of Earlier Work

It seems that the first work on the mercury photosensitized reactions of propane was reported in 1940 by E. W. R. Steacie and D.J. Dewar (10). An investigation was made of the mercury-photosensitized reactions of propane at temperatures from 25 to 323°C and at a constant pressure of propane of 14 cm Hg. The pressure of mercury in the reaction vessel was controlled by a trap kept at 25°C. The products detected and measured were hydrogen and hexanes. The authors concluded that the primary step was the C-H bond split and proposed the following mechanism which accounts for the products found:

$$C_3H_8 + Hg(^3P_1) \rightarrow C_3H_7 + H + Hg(^1S_o) \quad [1]$$

$$2C_3H_7 \rightarrow C_6H_{14} \quad [2]$$

$$H + C_3H_8 \rightarrow C_3H_7 + H_2 \quad [3]$$

$$C_3H_7 + C_3H_8 \rightarrow C_6H_{14} + H \quad [4]$$

$$H + H \rightarrow H_2 \quad [5]$$

$$H_2 + Hg(^3P_1) \rightarrow 2H + Hg(^1S_o) \quad [6]$$

The products from propane (and also from ethane and butanes) are in accord with the assumption of a C-H split as the initial act. Since the strengths of the C-H bonds in the lower saturated hydrocarbons (91 to 104 kcal/mole) are known to be considerably greater than those of the C-C bonds (78 - 88 kcal/mole), the fact that there is a C-H split indicates that the reaction is of a specific nature. The possibility of formation of singlet excited propane is eliminated on energetic grounds (the energy of excitation is about 185 kcal/mole) and by the spin conservation rule (11), and that of triplet excited

propane on energetic grounds. The only feasible chemical quenching of alkanes would therefore appear to take place by direct dissociation or by the formation of hydride. Mercury hydride has been suggested as an unstable intermediate (12,13) but there is no direct evidence for its formation. Masson and Steacie (14) attempted to obtain resonance emission of HgH bands in a propane-mercury-vapor mixture illuminated with 2537A light. No resonance emission was obtained, and it was concluded that if HgH is formed it must possess excess energy and largely dissociate immediately. Resonance emission of CdH bands has been detected (15) in the cadmium-photosensitized reaction.

Little is known about the intimate aspects of the actual act of energy transfer from the excited mercury atom to the alkane, and the mechanistic path by which the dissociation of the C-H bond is effected is still not fully understood (16,17,18). It was shown that in the mercury photosensitization of aliphatic hydrocarbons a tertiary hydrogen atom is roughly 500 times, and a secondary hydrogen atom roughly 50 times, more reactive than a primary hydrogen atom (19,20). In the case of propane it was found that the primary products of the quenching reaction $RH + Hg\ (^3P_1) \rightarrow R + H + Hg\ (^1S_o)$ are 90% i-propyl and 10% n-propyl radicals and that the secondary hydrogen atoms are 27 times as reactive as the primary hydrogen atoms (19). Separate studies of the primary step in the mercury photosensitization of propane indicated ratios of i-propyl to n-propyl to be approximately 1:1 (21,22), but it seems that these results should be disregarded on the basis of later re-examination (18). It seems established that at least 90% of the quenching efficiency of propane is due to the secondary hydrogen atoms in the molecule (23,24). It was found that the isomeric distribution of primary radicals in the mercury photosensitization of propane

was dependent on the pressure of propane and on the intensity of incident light (18). The maximum values for the i-propyl/n-propyl ratios obtained at high pressures (3 mm Hg) and low light intensities (i.e. low conversions) are considered to be a good approximation of the true primary radical ratios. For propane this ratio is i-propyl/n-propyl = 9.1.

Reactions of hydrogen atoms with hydrocarbons (C_2H_6, C_3H_8, n-C_4H_{10}, i-C_4H_{10}) lead to the production of much methane, when hydrogen atoms are present in high concentrations. This is to be expceted since at high concentrations of hydrogen atoms the sequence of "atomic cracking" reactions such as

$$H + C_3H_8 \rightarrow C_3H_7 + H_2$$

$$H + C_3H_7 \rightarrow C_2H_5 + CH_3$$

$$H + C_2H_5 \rightarrow 2CH_3$$

$$H + CH_3 \rightarrow CH_4$$

is favored (ref. 1, p. 464).

In the case of the mercury-photosensitized reactions, methane arises from reactions involving hydrogen atoms (25). However, there is a considerable difference between ethane on the one hand, and propane and the butanes on the other.

Darwent and Steacie (25) found that in the case of the mercury-photosensitized decomposition of ethane at room temperature, with the mercury saturator at room temperature, the quantum yield of hydrogen production increased strongly with increasing pressure of ethane, while that of methane approached zero at higher pressures (600 mm). Addition of molybdenum oxide, which effectively removed

hydrogen atoms, almost completely inhibited the formation of methane. The decrease of methane production with increasing pressure of ethane led these authors to believe that atomic cracking actually proceeded via the formation of an active molecule, $C_2H_6^*$. They proposed the following mechanism:

$$Hg(^3P_1) + C_2H_6 \rightarrow C_2H_5 + H + Hg(^1S_o) \quad [1]$$

$$H + C_2H_6 \rightarrow C_2H_5 + H_2 \quad [2]$$

$$H + C_2H_5 \rightarrow C_2H_6^* \quad [3]$$

$$C_2H_6^* \rightarrow 2CH_3 \quad [4]$$

$$C_2H_6^* + M \rightarrow C_2H_6 + M \quad [5]$$

$$2C_2H_5 \rightarrow C_4H_{10} \quad [6]$$

At temperatures above 400°C the ethyl radical decomposes

$$C_2H_5 \rightarrow C_2H_4 + H \quad [7]$$

and gives rise to a chain reaction (26).

The investigation by Darwent and Steacie (27) of the mercury-photosensitized decomposition of propane in a conventional circulating system at room temperature, with the mercury saturator at room temperature, showed that, at high pressure of propane, methane production was negligible, the products consisting almost entirely of hydrogen and hexanes. However, at low pressures, of 3 - 10 mm, methane and C_2 and C_4 hydrocarbons were produced in increasing amounts, although the production of methane was much less than in the similar reactions of ethane. The results with propane at low pressures qualitatively agree with those for ethane, but with

ethane a marked change occurred at pressures of about 150 mm. The rate of disappearance of propane decreased with decreasing pressure of propane. The yield of hydrogen (cc produced per cc C_3H_8 reacted) and of heavy fraction (C_5 hydrocarbons and higher) decreased with decreasing pressure of propane, while the yields of CH_4, C_2 and C_4 hydrocarbons increased as the propane pressure was decreased. In the absence of a cold trap, to remove the heavy products and to provide a constant working pressure of propane, the yield of hydrogen increased with decreasing pressure of propane. This effect is opposite to that found when a cold trap was used. The absence of a cold trap did not influence the production of CH_4, C_2 and C_4 hydrocarbons or the disappearance of C_3H_8. Rates of decomposition of propane, and of production of hydrogen and methane, were found to be independent of time. The following series of reactions was proposed to explain the products of the reaction of propane with Hg ($^3P_1$) atoms at low temperatures:

$$C_3H_8 + Hg(^3P_1) \rightarrow C_3H_7 + H + Hg(^1S_o) \quad [1]$$

$$H + C_3H_8 \rightarrow C_3H_7 + H_2 \quad [2]$$

$$H_2 + Hg(^3P_1) \rightarrow 2H + Hg(^1S_o) \quad [3]$$

$$2C_3H_7 \rightarrow C_6H_{14} \quad [4]$$

$$2H + M \rightarrow H_2 + M \quad [5]$$

$$H + C_3H_7 \rightarrow C_2H_5 + CH_3 \quad [6]$$

$$H + C_2H_5 \rightarrow 2CH_3 \quad [7]$$

$$C_2H_5 + C_3H_8 \rightarrow C_2H_6 + C_3H_7 \quad [8]$$

$$H + CH_3 + M \rightarrow CH_4 + M \quad [9]$$

$$2C_2H_5 \rightarrow C_4H_{10} \quad [10]$$

$$C_2H_5 + C_3H_7 \rightarrow C_5H_{12} \quad [11]$$

$$CH_3 + C_3H_8 \rightarrow C_3H_7 + CH_4 \quad [12]$$

At higher pressures only reactions [1], [2], [3] and [4] are of much importance. At low pressures of propane the rate of reaction [6] increases relative to [2], and methane is therefore produced at the expense of hexane. The above mechanism indicates that the mercury-photosensitized reactions of propane and ethane are of the same type. However, there is a big difference in the extent of atomic cracking with ethane and propane at a given pressure. To explain this difference Darwent and Steacie (27) considered the possibility of formation of an "active complex" in the first stage of the process.

$$R.CH_3 + Hg(^3P_1) \rightarrow R.CH_3.Hg^* \quad [13]$$

This complex can either react

$$R.CH_3.Hg^* \rightarrow R.CH_2 + HgH \quad [14]$$

or return to its original state

$$R.CH_3.Hg^* \rightarrow R.CH_3^* + Hg(^1S_o) \quad [15]$$

The portion which reacts by a C-H split follows the course of the original mechanism. The excited molecule formed in reaction [15] may be deactivated and it may also decompose by a C-C split. The probability of deactivation is supposedly greater at high pressures of propane, and that of decomposition at low pressures, thus causing the formation of methane. One also expects a relatively

greater extent of C-H bond split with propane, and with the butanes containing secondary and tertiary C-H bonds, than with ethane containing only primary C-H bonds. Moreover it is likely that the active molecules formed in reaction [15] from propane and the butanes, because of the larger number of vibrational degrees of freedom in those molecules, would be longer lived than $C_2H_6^*$ and would thus have greater chances of deactivation. Therefore one would expect less C-C bond split to occur with propane and butane than with ethane at the same pressures. Darwent and Steacie (27) concluded that there was no clear-cut evidence available to help in deciding whether these reactions proceed entirely by a C-H split or by a combination of a C-H split and the formation of an activated molecule.

The experiments carried out in the presence of added hydrogen showed that at low pressures (0.25 to 3 mm) of propane the rate of disappearance of propane decreased with increasing hydrogen pressure. The rate of production of methane increased to a maximum and then decreased, attaining a constant value when larger amounts of hydrogen are added. The yield of methane per cc of propane decomposed increased on the addition of hydrogen. The rate of production of C_2 and C_4 hydrocarbons decreased on the addition of hydrogen. All these effects of added hydrogen were less pronounced at higher pressure of propane. The explanation for such behavior was given by the assumption that with increased hydrogen pressure the rate of reaction [1] decreased, owing to quenching of mercury with hydrogen, and this decrease more than compensated for the increase in the rate of reaction [2]; as a result, the rate of the overall production of propyl radicals in [1] and [2] was decreased, which means that the rate of disappearance of propane was also decreased. The increased rate of production of methane with small amounts of hydrogen was due to an increase in the

rate of reaction [6], which more than compensated for the decreased rate of the overall production of propyl radicals in [1] and [2]. The addition of larger amounts of hydrogen beyond the pressure required for complete quenching increased the concentration of third bodies and so lowered the stationary H atom concentratinn by reaction [5], thus causing a decrease in the rates of reactions [2] and [6], and consequently a decrease in the rate of methane production.

Bywater and Steacie (28) investigated the mercury photosensitized decomposition of propane in a conventional static system, with a mercury saturator at room temperature, in the temperature range from 25 to 450°C and at pressures between 4 and 300 mm Hg.

High propane-pressure (14 and 30 cm Hg) results at lower temperatures (below 200°C) were consistent with the earlier proposed mechanism (27). The high pressure - low temperature hydrogen production was found to be a linear function of time; its rate was directly proportional to the light intensity and independent of the pressure of propane above 20 cm Hg. The energy of activation for total hydrogen formation in this high pressure - low temperature region was 0.5 kcal, and was attributed to reaction [1]. The quantum yield of hydrogen production was found to be 0.46 at room temperature and 14 cm pressure, rising to 0.50 at high pressures. It should be unity according to the proposed mechanism. This lower quantum yield was attributed to the quenching of mercury to the metastable (^3P_o) state with subsequent dissipation of energy. Methane production was also a linear function of time. Above 300°C at high pressures of propane (14 and 30 cm Hg), hydrogen and methane production increased rapidly still being linear functions of time. The amount of ethene produced was roughly equivalent to that of methane. The rate of methane was the same at both

14 cm Hg and 30 cm Hg total pressure. The increase in hydrogen and methane production at higher temperatures was attributed to the decomposition reactions of propyl radicals:

$$C_3H_7 \rightarrow C_3H_6 + H \qquad [16]$$

and

$$C_3H_7 \rightarrow C_2H_4 + CH_3 \qquad [17]$$

The observed energies of activation for hydrogen and methane formation were E_{16} = 38 kcal mole^{-1}, and E_{17} = 20 kcal mole^{-1}, respectively. These energies, according to the authors' interpretation, probably correspond to some intermediate value between the true values for normal and isopropyl radicals. The reaction [17] was supposed to be followed by [12], whose energy of activation E_{12} = 8 kcal.

Low propane-pressure (4 mm Hg) results at lower temperatures (below 200°C) were consistent with the earlier proposed mechanism (27). The low pressure - low temperature methane production was supposed to be due to atomic cracking reactions [6] and [7]. The activation energies had been estimated at less than 5 kcal. Methane formation at low pressures of propane was a linear function of time up to 400°C. The apparent activation energy for methane formation at low pressure varied with temperature. Below 300°C a value of approximately 8 kcal was obtained, whereas at higher temperatures, the value approached that value obtained at high pressure of propane (20 kcal). If methane was produced by reaction [12], which has an activation energy of 8 kcal, this would be the rate-determining step, and the high activation energy (20 kcal) for methane formation observed at high temperatures should drop to 8 kcal at low temperatures, as was in fact observed. At low pressures of propane at temperatures from 300°C to 400°C the hydrogen production was proportional to the square root of

both light intensity and reaction time after an initial period of about one hour. The fall off in the rate of hydrogen production was attributed to the quenching of mercury by the hydrogen produced. Bywater and Steacie (28) supposed that in the unobserved initial period the hydrogen production was linearly dependent on reaction time.

A number of experiments were carried out between room temperature and 200°C in the presence of added propene, in order to determine the relative reactivity of hydrogen atoms formed in the system for propane and propene. The difference in the activation energies for the reactions of hydrogen atoms with propane and propene was found to be 4 kcal (28). Consequently, the ratio of corresponding rate constants is too large for propene to be stable at low temperatures. At 300°C, however, propene formed by a disproportionation reaction ought to be detectable. No propene could be detected at 250°C and 300°C, so that there is no indication of a disproportionation reaction between two propyl radicals at those temperatures.

The mercury photosensitized decomposition of propane in a conventional static system at 24°C and at pressures of 300 and 600 mm Hg, with the mercury saturator at room temperature, was re-investigated by Back (29).at very low conversions (up to 1%). Hydrogen was the only product identified and measured. The rate of hydrogen production decreased with increasing reaction time, at first rapidly, slowing down subsequently and eventually reaching a constant value at about 0.6% to 1.6% of the reaction. This behavior was interpreted as being due to the accumulation of propene formed by the disproportionation of propyl radicals, and the scavenging of hydrogen atoms by it. The constant rate of hydrogen production finally achieved.

was thought to correspond to a steady-state concentration of the unsaturate. The addition of small amounts of propene ($\sim 10^{-3}$ times that of propane) to the system caused a marked decrease in the rate of hydrogen production. Back proposed the following "self-scavenging" mechanism:

$Hg + h\nu$	$\rightarrow$	Hg^*	[1]
$C_3H_8 + Hg^*$	$\rightarrow$	$C_3H_7 + H + Hg$	[2]
$H + C_3H_8$	$\rightarrow$	$H_2 + C_3H_7$	[3]
$2C_3H_7$	$\rightarrow$	C_6H_{14}	[4]
$2C_3H_7$	$\rightarrow$	$C_3H_8 + C_3H_6$	[5]
$H + C_3H_6$	$\rightarrow$	C_3H_7	[6]
$H + C_3H_6$	$\rightarrow$	$H_2 + C_3H_5$	[7]
$C_3H_7 + C_3H_6$	$\rightarrow$	C_6H_{13}	[8]
$C_3H_7 + C_3H_5$	$\rightarrow$	C_6H_{12}	[9]

On the basis of this mechanism the rate of hydrogen production is:

$$\frac{dH_2}{dt} = \emptyset I_a \frac{k_3[C_3H_8] + k_7[C_3H_6]}{k_3[C_3H_8] + (k_6+k_7)[C_3H_6]}$$

where I_a is the intensity of light absorbed and $\emptyset$ is the quantum yield for reaction [2].

According to this expression, $\frac{dH_2}{dt}$ is equal to $\emptyset I_a$ initially, decreases as C_3H_6 accumulates, and becomes constant if C_3H_6 attains a steady-state concentration before depletion of C_3H_8 becomes appreciable. The above equation can be written in the form:

$$(\phi I_a - \frac{dH_2}{dt}) \frac{[C_3H_8]}{[C_3H_6]} = \frac{k_6+k_7}{k_3} \frac{dH_2}{dt} - \frac{k_7}{k_3} \phi I_a$$

From the slope and the intercept of the plot of this equation Back was able to obtain the ratios of the rate constants $\frac{k_6+k_7}{k_3}$ and $\frac{k_7}{k_3}$. If loss of C_3H_6 via reaction [8] is neglected, the reduction of the rate of hydrogen production is a measure of the rate of disappearance of C_3H_6, and of the rate of the steady-state production of C_3H_6 by reaction [5]. Thus the ratio of k_5/k_4 could be obtained. These ratios are given in the following table:

T	$P_{C_3H_8}$	$(k_6+k_7)/k_3$	k_7/k_3	k_6/k_3	$k_7/(k_6+k_7)$	k_5/k_4
24°C	300 mm	1565	50.1	1515	0.032	0.80
24°C	600 mm	1389	84.7	1304	0.061	0.54

The decrease in the rate of hydrogen formation could be observed only at low conversion because of large value of k_6/k_3. The previous measurements (26, 28) were made at higher conversions, apparently in the steady-state region, and no dependence of the rate of hydrogen production on time was observed. It is probable that olefin was present from the beginning as an impurity. Back suggested that the reported pressure-independent quantum yield of 0.5 should be corrected upwards by the factor $(k_4+k_5)/k_4$. In this way the initial quantum yields of 0.90 and 0.77 at 300 mm Hg and 600 mm Hg respectively could be obtained. The decrease of the initial quantum yield with increasing pressure suggested that the intermediate formation of an excited propane molecule of appreciable life time might take place in the primary process. However, all the relative rate constants

measured were dependent upon the values of ϕI_a, the initial rate of hydrogen formation, obtained from the extrapolation to zero time of the rate of hydrogen formation. The sharply rising curves made this extrapolation inaccurate. The high values of the k_5/k_4 ratios might be caused by inaccuracy of extrapolating to zero time, and may be attributed to preferential disproportionation of "hot" radicals formed in reaction [6] in the steady state.

Similar trends in the rates of hydrogen production were observed by Back with ethane (29) and n-pentane (30).

The apparent low quantum yield of hydrogen in the mercury-photosensitized decompositions of hydrocarbons was confirmed by Cvetanovic (31) through the measurements of the relative overall efficiencies of quenching in binary mixtures of hydrocarbons (C_2H_6, n-C_4H_{10}, C_2H_4) with N_2O. The reactions were studied at low temperatures (23°C and 120°C) and higher pressures ($\approx 10^2$ mm RH + 100 mm N_2O) with the mercury saturator at room temperature. In the case of n-butane it was found that $\phi_{H_2}/\phi_{N_2} = 0.72$ and this fraction represented an upper limit for ϕ_{H_2}. In a subsequent study of this process with n-butane and propane (32) an increase in the rate of hydrogen production was found when going towards lower and lower conversions. However, in experiments at very low conversions ($\approx 10^{-2}$%), approaching the initial conditions, no time dependence of the rate of hydrogen production was observed. Under these conditions the ratio ϕ_{H_2}/ϕ_{N_2} was found to be 0.94. The quantum yield of hydrogen at constant conversion was found to increase with increasing pressure of n-butane, reaching a constant value at about 300 mm Hg.

At very low conversions this constant value was about 0.94, and for "normal conversions" about 0.72. There was no decline in ϕ_{H_2} with increasing pressure, as was the case with olefins, indicating that there was no initial formation of vibrationally-excited paraffin which could be deactivated. Slight corrections for initial self-scavenging caused by small olefin impurity at very low conversions brought the ratio ϕ_{H_2}/ϕ_{N_2} to unity within the experimental error. The absolute values of these quantum yields have remained uncertain. It was provisionally assumed that ϕ_{N_2} is unity. If this is correct there is no need to postulate the occurrence of physical quenching. If, on the other hand, ϕ_{N_2} and ϕ_{H_2} are indeed smaller than unity, then there is a loss of light energy and the mechanism responsible for it is probably of a physical nature. Cvetanovic suggested that self-scavenging was an important feature of the mercury-photosensitized decompositions of hydrocarbons. The general mechanism can be written as follows:

$$Hg + h\nu \rightarrow Hg^* \quad [1]$$

$$RH + Hg^* \rightarrow R + H + Hg \quad [2]$$

$$H + RH \rightarrow H_2 + R \quad [3]$$

$$R + R \rightarrow R_2 \quad [4]$$

$$R + R \rightarrow RH + Ol \quad [5]$$

$$H + Ol \rightarrow R \quad [6]$$

$$H + Ol \rightarrow H_2 + R' \quad [7]$$

$$R + R' \rightarrow RR' \quad [8]$$

Ol = Olefin

Scavenging of hydrogen atoms by reaction [6] may be of importance if $k_6 \gg k_3$ and the ratio k_5/k_4 is not too small. With the assumption that $k_7/(k_6+k_7) \approx 0.1$. The following ratios were obtained:

Hydrocarbon	T	P	$(k_6+k_7)/k_3$	k_5/k_4	k_6/k_7
C_3H_8	25°C	140 mm	920	0.54	9
n-C_4H_{10}	25°C	200 mm	533	1.07	9

It was pointed out that no quantitative significance should be attached to these values, and that they only served to illustrate the importance of self-scavenging processes.

It should be mentioned that the "chemical method" to determine relative quenching cross-section values for mercury 6 ($^3P_1$) atoms has recently been questioned (33). This, however, does not affect the present discussion.

Back and Takamuku (34) investigated the mercury-photosensitized decomposition of propane in a circulating system at temperatures between 33°C and 400°C and at a pressure of about 300 mm Hg, with the mercury saturator at 0°C. Hydrogen and methane were the only products measured. Conversion was low enough that true initial yields of H_2 and CH_4 were measured, and addition of H or CH_3 to propene produced in the reaction was negligible. This included the assumption that the rate of hydrogen production was independent of time under these conditions, in agreement with the present investigation. The light intensity was low enough that the concentrations of H and C_3H_7 formed were low and their interaction was unimportant. Low light intensity also favors first-order decomposition of radicals over the second-order combination reactions, and causes decomposition to set in at lower temperatures.

It was found that the rate of hydrogen production in the temperature range from 33°C to about 300°C was approximately constant, showing a slight decrease from lower to higher temperatures. Methane was not detected in this region. Above 300°C the rate of hydrogen production increased rapidly, as did the rate of methane production. Back and Takamuku discussed their results obtained below 300°C in the light of the following mechanism:

$$Hg^* + C_3H_8 \rightarrow Hg + C_3H_7 + H \quad [1]$$

$$H + C_3H_8 \rightarrow H_2 + C_3H_7 \quad [2]$$

$$2C_3H_7 \rightarrow C_6H_{14} \quad [3]$$

$$2C_3H_7 \rightarrow C_3H_8 + C_3H_6 \quad [4]$$

Above 300°C they suggested that methane and additional hydrogen are formed by the following reactions:

$$C_3H_7 \rightarrow CH_3 + C_2H_4 \quad [5]$$

$$C_3H_7 \rightarrow H + C_3H_6 \quad [6]$$

followed by

$$CH_3 + C_3H_8 \rightarrow CH_4 + C_3H_7 \quad [7]$$

and reaction [2].

An equilibrium between n-C_3H_7 and i-C_3H_7 was proposed:

$$n\text{-}C_3H_7 + C_3H_8 \underset{8r}{\overset{8f}{\rightleftharpoons}} i\text{-}C_3H_7 + C_3H_8 \quad [8]$$

At low temperatures there was no decomposition of radicals, and $v_{H_2} = v_2 = v_1 = v_3 + v_4$. Above 300°C reaction pairs [5] and [7], and [6] and [2] constitute reaction chains producing methane

and hydrogen without a net consumption of propyl radicals. If v_1, v_3 and v_4 were approximately independent of temperature, simple Arrhenius plots of v_{CH_4} and $v_{H_2} - v_1$ would yield activation energies for reactions [5] and [6]. From the relationships $v_{CH_4} = v_5 = k_5[C_3H_7]$, $v_{H_2} - v_1 = v_6 = k_6[C_3H_7]$ and $[C_3H_7]^2 = (v_3 + v_4)/(k_3 + k_4) = v_1/(k_3 + k_4)$ taking $k_3 + k_4 = 10^{11}$ mole^{-1} l sec^{-1} the absolute values of k_5 and k_6 could be obtained. From Arrhenius plots of these values the relationships $k_5 = 10^{9.6} \exp(-22/RT)$ sec^{-1} and $k_6 = 10^{14.0}\exp(-37/RT)$ sec^{-1} were obtained. Arrhenius parameters for reaction [6] seem to be in agreement with those obtained by others, but those for reaction [5] are lower than the values obtained by other methods (3, 5, 6, 7, 8). The low absolute values for k_5 might be due to the fact that methane comes almost exclusively from the decomposition of the n-propyl radical, whereas in the calculation the total concentration of propyl radicals was used. By applying the steady-state treatment to the n-propyl radical, with the assumption that loss of i-propyl by reaction [5] and n-propyl by reaction [6] was negligible, Back and Takamuku estimated the concentration of n-propyl radicals. The concentration of n-propyl radicals in equilibrium with i-propyl radicals at temperatures between 300°C and 400°C amounted to between 3 and 6% of the total radical concentration. Values for k_5 derived from the estimated n-propyl concentration were higher, but agreement with the values obtained by other methods (3, 5, 6, 7, 8) was not achieved.

At the end of this review of the earlier work on the mercury-photosensitized decomposition of propane it may be concluded that although our knowledge of the mercury-photosensitized reactions of propane presents a coherent pattern, there are still many questions waiting to be answered. Present techniques enable the rates of different processes to be measured with greater precision. The values of the pre-exponential factors and the activation energies may be estimated with greater certainty. The present work has been an attempt to examine the mechanism of the mercury-photosensitized decomposition of propane over a range of pressure and temperature, and to establish the kinetic parameters for the decomposition of propyl radicals created by the mercury-photosensitization.

Mercury-photosensitization as a means of producing free radicals has certain marked advantages over the other methods. In the first place, a definite amount of energy is transferred to the reactant molecule. Also, a wide range of temperatures is available for the investigation, which is not the case with thermal decompositions and chemical sensitizations. Furthermore, photosensitization provides clean reaction conditions since no other radicals are added to the system, in contrast with direct photolysis and chemical sensitization methods. The main disadvantage of mercury-photosensitization is the degree of conversion that can be used. Certain products, as hydrogen and alkenes, which have high quenching cross-section can be lost through further reaction by a mercury-photosensitized reaction. Furthermore, the parent molecules are the same as the products of sometimes interesting reactions of the radicals. When using mercury-photosensitization to generate radicals, one must also consider the possibility of primary steps other than the removal of a hydrogen atom and the possible formation of hot radicals.

CHAPTER II

EXPERIMENTAL METHODS AND TECHNIQUE

2.1 Apparatus

The reaction was studied in a conventional static system. The scheme of the apparatus is shown in Figure 1. The entire system could be evacuated by means of a mercury diffusion pump D_1 which was in series with a double stage rotary pump supplied by the Welsh Manufacturing Company.

The reaction vessel (R. V.) was a quartz cylinder about 10 cm in length and about 5 cm in diameter, with plane windows at each end; its volume was 166 cm^3. The reaction vessel was wrapped with five layers of asbestos paper and placed inside a cylindrical iron collar 23 cm in length, 6 cm in diameter, with walls 0.5 cm thick to ensure even heating. The iron conductor was wrapped with three layers of asbestos paper, on which resistance wire was wound, followed by three more layers of asbestos paper. The whole furnace was wrapped with asbestos string and placed in a box filled with asbestos flakes.

In order to minimize dead space the leads to the vessel were made of 3 mm capillary tubing.

The heating of the furnace was regulated by a Thermo Electronic Co. signalling controller potentiometer connected with the control relay. The controller was activated by means of a chromel-alumel thermocouple (C_4) placed half way along the reaction vessel and between the first and second asbestos layers around the vessel. With this device the temperature could be maintained constant within a degree. A schematic diagram of the temperature controlling device is shown in Figure 2.

Figure 1

A schematic diagram of the apparatus:

R.V.	Reaction vessel
F.	U.V. filter
L.	U.V. lamp
C.	Thermocouple
V.	Variac
T.	Trap
M.	Manometer
S.	Stopcock
D.	Mercury diffusion pump
T.P.	Toepler pump
Mc.	McLeod gauge
B.	Storage bulb

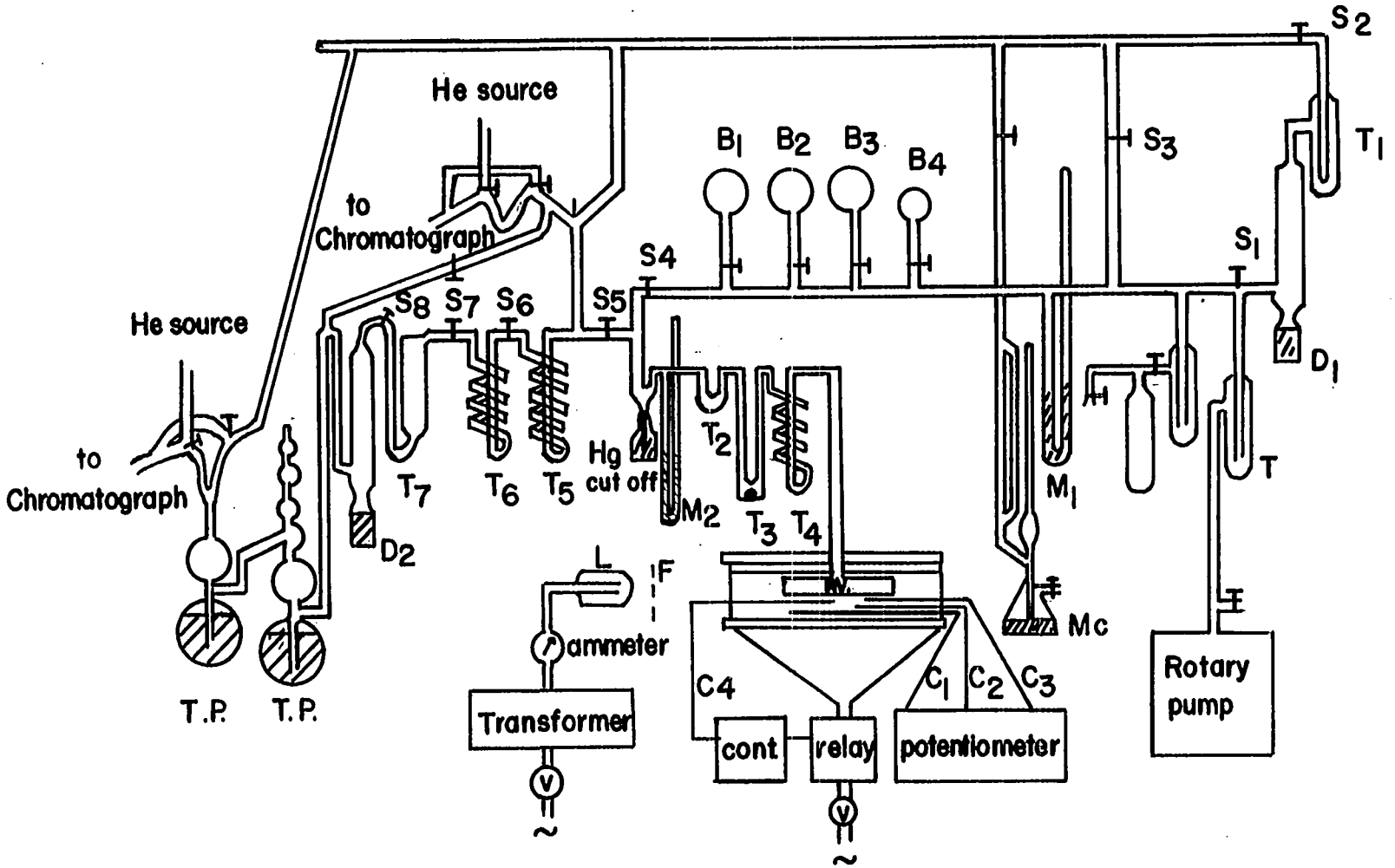
He source
to Chromatograph
He source
to Chromatograph
T.P.
T.P.
S8
S7
S6
S5
S4
S2
S3
S1
B1
B2
B3
B4
T1
T7
T6
T5
Hg cut off
T2
T3
T4
M2
M1
Mc
D1
D2
T
L
F
ammeter
Transformer
V
C4
C1
C2
C3
cont
relay
potentiometer
Rotary pump

Figure 2

A schematic diagram of the temperature-controlling device

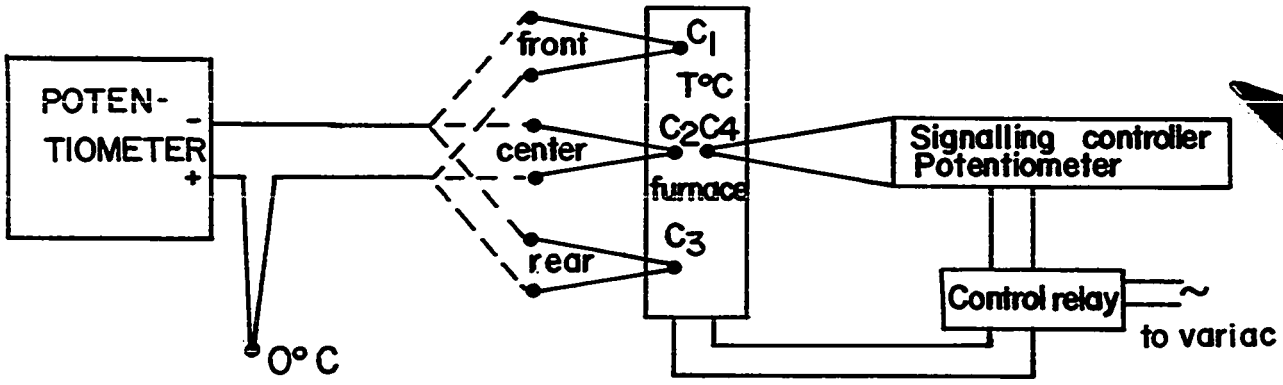
POTEN-
TIOMETER
-
+
0° C
front
center
rear
C1
T°C
C2C4
furnace
C3
Signalling controller
Potentiometer
Control relay
~
to variac

The temperature of the reaction vessel was measured by means of three chromel-alumel thermocouples (C_1, C_2, C_3) suitably placed between the first and second asbestos layers and connected to a Croydon Precision Instrument Co. portable D.C. Potentiometer, type P-3 (see Figure 2). The reference temperature was $0^{\circ}C$. In this way the temperature could be measured at both sides and in the middle of the reaction vessel.

The concentration of mercury in the reaction zone was controlled by the temperature of a spiral trap (T_4) in the lead to the reaction vessel. The temperature of the trap was kept constant at $-33^{\circ}C$ by means of 1, 3-dibromopropane slush. The concentration of the mercury in the reaction zone was assumed to correspond to the equilibrium vapor pressure of mercury at $-33^{\circ}C$, which amounts to about 3.5×10^{-6} mm Hg.

The low-pressure mercury "resonance" lamp (L) of low light intensity was used as a source of U.V. light. It was maintained at about 30 cm distance from the incident face of the reaction vessel. The power for the activation of the lamp was supplied through a transformer with maximum output of 2000 V. The lamp was operated at a constant current at 9.0 mA adjusted by a variac (V) in the primary circuit of the transformer. Between the lamp and the reaction vessel was placed a Corning glass U.V. color filter C.S. No. 9-54, which was non-transparent for the light of wavelength shorter than 2000 A. In this way the mercury 1849 A line was eliminated.

The reaction products were analyzed by a gas chromatograph assembled from commercially available units. As a detection unit the Gow-Mac Co. thermal conductivity cell for gas chromatography Model A-9283 was used, supplied by power from Trygon Electronics Inc. power supply Model HR 40-750. The output used was 12 V D. C.

The current through the filament in the detector was 250 mA. In order to obtain high sensitivity the signal from the detector was pre-amplified by means of a Leeds and Northrup Co. stablized D.C. micro-volt amplifier Model 9835-A. The amplified signal was put through a 10 mV Leeds and Northrup Co. Speedomax recorder, Model S. A schematic diagram of the chromatograph assembly is shown in Figure 3.

The high sensitivity requires minimal fluctuation of pressure between the helium source and the detector, in order to have a stable base line. For that reason Edwards Vacuum Ltd. vacuum and pressure controllers, Model V. P. C. -1, were inserted in both the reference flow and the sample flow of the chromatograph. The flow of the helium carrier gas was measured by a home-made flow meter.

2.2 Materials

The propane used was obtained from Phillips Petroleum Company with stated research grade purity of 99.99 mole %. This was subjected to several trap-to-trap distillations at -160° (isopentane slush). The first and final 20% of the sample were rejected and only the middle fraction was stored for further work. Gas-chromatographic analysis of such a sample showed no impurities. The purified propane was stored in a black-painted storage-bulb and was degassed from time to time.

The hydrogen, methane, ethene and ethane used for calibrations of the chromatograph were obtained from the Phillips Petroleum Company. Their purity was stated as research grade, and they were not subjected to further purification. 2, 3-Dimethylbutane and 2-methylpentane were supplied by the Phillips Petroleum Company. Their purity was stated as pure grade of 99 mole%. n-Hexane was obtained from the Matheson Company. The purity was stated as spectro-quality reagent. 2, 3-Dimethylbutane, 2-methylpentane and n-hexane were subjected to thorough degassing at -130°C to eliminate the air impurity.

Figure 3

A schematic diagram of the gas-chromatographic system

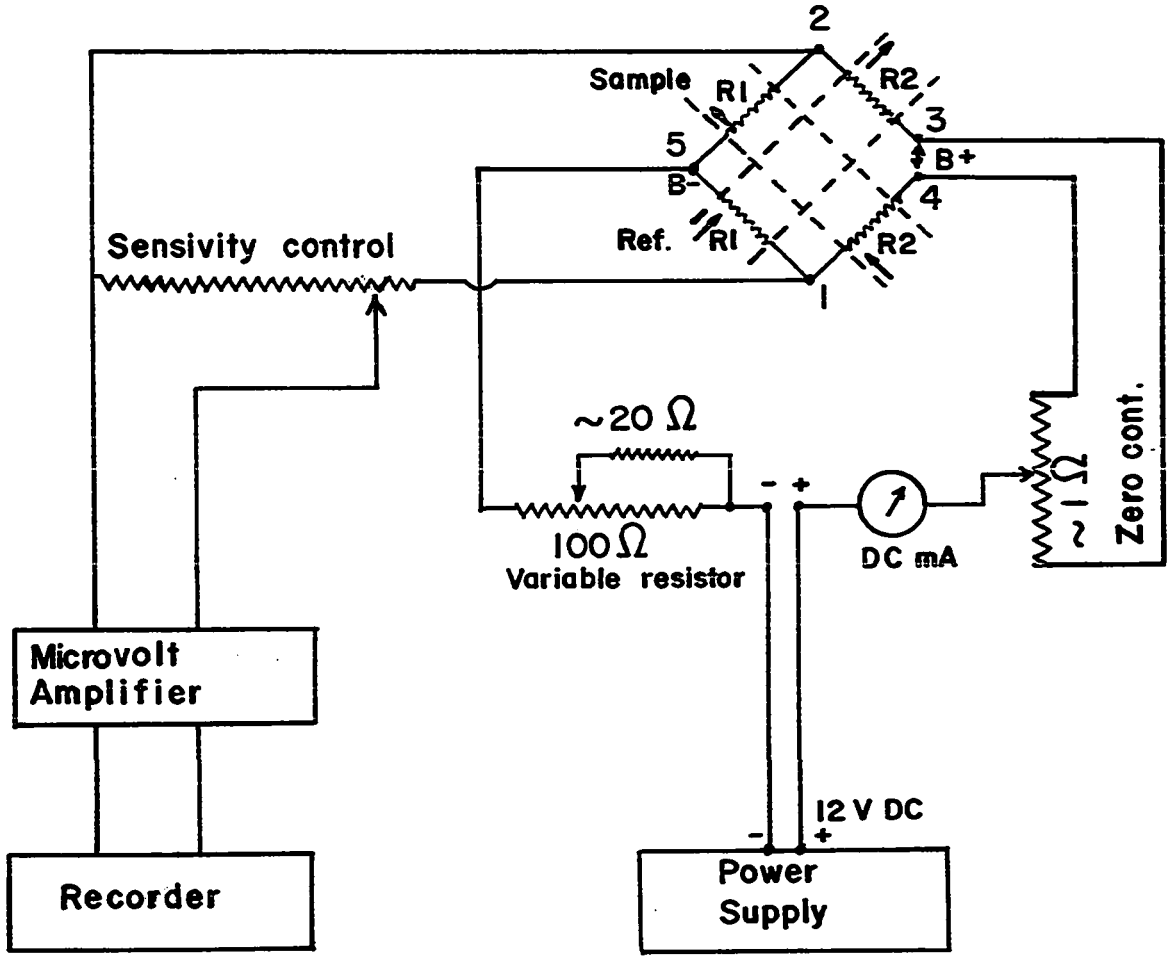
2
Sample
R1
R2
3
5
B+
B-
4
Ref.
R1
R2
1
Sensivity control
~20 Ω
100 Ω
Variable resistor
- +
DC mA
~1 Ω
Zero cont.
Microvolt
Amplifier
12 V DC
- +
Recorder
Power
Supply

Carbon dioxide for investigation of the influence of foreign gas was obtained from the Matheson Company.

Helium carrier gas was obtained from the Union Carbide Inc.

Ascarite used for the adsorption of CO_2 was obtained from the Arthur H. Thomas Company.

Practical n-pentane and iso-pentane used for -130°C and -160°C low-temperature baths respectively were obtained from the Matheson Company. 1,3-Dibromopropane used for -33°C bath was obtained from Aldrich Chemical Co.

Porapak Q solid adsorbent used for the preparation of gas-chromatographic columns was supplied by the Waters Assoc. Inc.

Chromosorb P a.w. used as a solid support in gas-chromatographic columns was obtained from the Johns-Manville Company.

α-Chloronaphthalene used as a liquid phase in gas-chromatographic columns was obtained from the Fisher Scientific Company.

Di-2-ethylhexylsebacate used as a liquid phase in gas-chromatographic columns was obtained from Chromatographic Specialties Ltd.

Chloroform used as solvent in preparing of gas-chromatographic columns was obtained from Fisher Scientific Company.

High vacuum silicone grease used for all stopcocks was obtained from Dow Corning Corp.

2.3 Procedure and Analysis

Before each experiment the system was evacuated to 10^{-5} mm Hg. The trap T_3 with mercury was immersed in liquid nitrogen during the night, and whenever a run was not being performed. Prior to each experiment the trap T_4 was also immersed in liquid nitrogen for about 30 min, and then in a bath at -33°C immediately before the experiment started. A sample of propane was then admitted to the manifold from the storage bulb. The mercury cut-off was then opened, and by means of a stopcock S_4 propane was allowed slowly to diffuse to the trap T_2 immersed in liquid nitrogen. When this operation was completed stopcock S_4 and the mercury cut-off were closed and liquid nitrogen from the trap T_3 was removed so as to allow the mercury in it to warm up to room temperature.

The liquid nitrogen at T_2 was allowed to evaporate, and propane slowly diffused over the mercury at room temperature in T_3, through saturation trap T_4 at -33°C into the reaction vessel. The pressure was measured by the manometer M_2. The mercury lamp was switched on about 30 min before use; the reaction was started by the removal of a shutter and was stopped by switching off the lamp. The residual propane and the reaction products were immediately trapped in the trap T_2 immersed in liquid nitrogen. The 1, 3-dibromopropane slush was removed from T_4, the mercury cut-off opened and liquid nitrogen removed from T_2. The stopcocks S_5, S_6, S_7 and S_8 were then successively opened and the reaction products pumped through traps T_5, T_6 and T_7 by means of a mercury diffusion pump (D_2) followed by a Toepler pump (T. P.). After 30 min of pumping, the mercury cut-off and the stopcocks S_5, S_6, S_7 and S_8 were closed since the separation into fractions was completed.

The products of the reaction were separated into three fractions: (1) non-condensable; (2) condensable at -210°C and -196°C (solid nitrogen and liquid nitrogen respectively) in traps T_7 and T_6 respectively, and (3) condensable at -130°C (n-pentane slush) in trap T_5. The non-condensable products, which comprised hydrogen and methane, were collected in a sample tube by a Toepler pump. They were analyzed on a 6.0 m long column filled with 80-100 mesh Porapak Q operating at 0°C with helium flow of 50 cc min^{-1}. On this column hydrogen could be separated from air. This is important since small quantities of air eventually collected during pumping of products could cause big errors in the analysis of hydrogen because of the much greater difference in thermal conductivity between air and the helium carrier gas than between helium and hydrogen. The traps at -210°C and -190°C retained ethene and ethane (and C_3 and C_4 hydrocarbons which were not analyzed). Ethene and ethane were analyzed on a 3.5 m long column filled with 80-100 mesh Porapak Q operating at 35°C with a helium flow of 100 cc min^{-1}. The characteristics of this column have been described elsewhere (35). The traps at -130°C (there were actually two such traps in tandem) retained 2, 3-dimethylbutane, 2-methylpentane and n-hexane (and some of the C_4 hydrocarbons which were not analyzed). 2, 3-Dimethylbutane and 2-methylpentane were anzlyed on a 7.0 m long column filled with 4% α-chloronaphthalene on chromosorb P a.w., 45-60 mesh operating at 0°C, with helium flow at 120 cc min^{-1}. The retention time of n-hexane on this column was too long (42 min) and the amounts of n-hexane were considerably smaller than those of the other two C_6 isomers. For this reason separate runs were made and n-hexane was analyzed on a 2.0 m long column filled with 20% di-2-ethylhexylsebacate on Chromosorb P a.w., 45-60 mesh operating at 25°C with helium flow of 150 cc min^{-1}. 2, 3-Dimethylbutane could not be separated from 2-methylpentane on this column.

Peak-height measurements provided good calibration curves for all products except for C_6 hydrocarbons, for which it was necessary to make area measurements.

All columns were made from copper tubing with an inner diameter of 4 mm.

Helium was the carrier gas used for all chromatographic analyses.

In the experiments where the effect of CO_2 as a foreign gas was studied, CO_2 was first trapped together with ethene and ethane at -210°C and -196°C and then removed from the product mixture by adsorbing it on ascarite.

2.4 Reaction Conditions

The mercury-photosensitized decomposition of propane has been investigated at five different temperatures, i.e. at 252°C, 276°C, 301°C, 325°C and 350°C in the range of propane pressure from about 5 mm Hg to about 700 mm Hg. Preliminary investigation of a dark reaction with no U.V. illumination showed that above 350°C considerable thermal decomposition of propane is taking part. This would interfere with the photosensitized reaction and make results unreliable. For that reason the highest temperature under which the mercury-photosensitized decomposition of propane was investigated was 350°C.

Mercury vapor in the reaction zone was at its equilibrium vapor pressure at -32°C, which is about 3.5×10^{-6} mm Hg. The low concentration of mercury in the reaction zone was necessary in order to approach a homogeneous absorption of light throughout the reaction vessel. The reaction conditions in the reaction vessel about 10 cm long with mercury saturator at -32°C should be fairly homogeneous

as shown by Loucks and Laidler (36). Any effects of inhomogeneous absorption should have been very much less than in earlier work by Bywater and Steacie (28) and by Back and Takamuku (34) in which the mercury saturator was kept at room temperature and at $0^{\circ}C$ respectively.

The low-pressure mercury "resonance" lamp of low light intensity was used so that the concentration of radicals produced was not too high.

Under these conditions the reaction could be investigated at very low conversions of about 10^{-1} - 10^{-2}%. A very low percent conversion is required in order that true initial yields of products are measured, and that addition of hydrogen atoms and radicals to olefins produced can be neglected.

CHAPTER 3

RESULTS AND INTERPRETATION

3.1 Products of Reaction

The reaction products analyzed were hydrogen methane, ethene, ethane, 2, 3-dimethylbutane (2, 3-DMB), 2-methylpentane (2-MP) and n-hexane (n-C_6H_{14}). The C_4 hydrocarbons could not be separated from propane by distillation and the huge peak of propane made gas-chromatographic analysis impossible. The original data for the mercury-photosensitized decomposition of propane are shown in Table 1 and are plotted in Figures 4 - 10. The results may be considered in the light of their relation to the pressure of propane and may also be presented with reference to two temperature regions.

It may be noted that the rates of formation of products at low pressures of propane increase with increasing propane pressure and then become constant and independent of propane pressure after a certain limiting pressure of propane has been reached. The limiting propane pressure for hydrogen, 2, 3-DMB, 2-MP and n-C_6H_{14} is about 150-160 mm Hg and is approximately independent of temperature. The limiting pressure of propane for methane, ethene and ethane production on the other hand, depends on temperature and is higher at higher temperatures. At 350°C, for example, the limiting pressure is reached at about 650 mm Hg. This behavior could be explained as follows. At low propane pressures the rate of quenching of excited mercury atoms increases with increasing concentration of the quencher propane molecules. At a certain propane pressure complete quenching of the excited mercury is achieved, and further increase of the quencher

TABLE 1

Original data for the mercury-photosensitized decomposition of propane at 252°C, 276°C, 301°C, 325°C and 350°C in the pressure range from 5 mm Hg to 700 mm Hg. All rates are quoted in mole cc^{-1} sec^{-1} x 10^{13} except the rate of n-hexane which is quoted in mole cc^{-1} sec^{-1} x 10^{15}

TABLE 1

T = 252°C

$P_{C_3H_8}$	v[moles cc^{-1} sec^{-1}] x 10^{13}						v x 10^{15}
mm Hg	H_2	CH_4	C_2H_4	C_2H_6	2, 3-DMB	2-MP	n-C_6H_{14}
6	0.9	0.24	0.20	0.02	1.0	0.20	
7							1.1
10	1.4	0.33	0.30	0.03	1.2	0.25	
11	1.8		0.31	0.04			
16	2.4	0.46	0.42	0.05	1.5	0.31	1.8
19	3.0	0.50	0.45	0.06	1.8	0.40	
22	3.2	0.58	0.50	0.06	1.9	0.39	
28	4.0	0.67	0.60	0.08	2.0	0.48	
29							2.3
33	4.5	0.60	0.64	0.08	2.4	0.55	
40	5.2	0.70	0.70	0.09	2.5	0.56	
47							2.8
49	5.2	0.64	0.79	0.08	2.6	0.60	
60	5.3	0.76	0.80	0.10	3.1	0.65	
63	5.8		0.84	0.10	3.4	0.72	
68	5.4	0.80		0.10	3.4	0.71	
69							3.5
72	6.0	0.70	0.86	0.08	3.3	0.72	
88	5.7	0.60	0.87	0.09	3.7	0.84	
91							4.5
102	6.2	0.78	0.84	0.08	4.3	0.91	
113							4.7
117							4.4
126	6.0	0.80	0.88	0.08	4.0	0.94	
132							4.7
156	5.6	0.76	0.80	0.10	4.4	0.98	
160							4.9
186	6.0	0.63	0.86	0.09	5.0	1.03	
191							5.3
193							5.1
217	6.3	0.81	0.82	0.08	4.7	1.06	4.9
242	5.8	0.60	0.79	0.11	4.2	0.97	
247							5.2
269	6.0	0.80	1.0	0.09	4.2	0.98	
300	5.9	0.78	1.0	0.07	4.5	0.99	4.9
382	5.8	0.64	0.95	0.10	4.6	1.01	
446	5.7	0.60	0.90	0.09			
548	6.8	0.69	1.0	0.10			
636	6.3	0.75	0.83	0.08			

TABLE 1 (ctd.)

T = 276°C

$P_{C_3H_8}$	v[moles cc^{-1} sec^{-1}] x 10^{13}						v x 10^{15}
mm Hg	H_2	CH_4	C_2H_4	C_2H_6	2,3-DMB	2-MP	n-C_6H_{14}
6	1.0	0.50	0.40	0.05	0.94	0.17	
9							1.0
10	1.5	0.70	0.51	0.07	1.2	0.22	
12	1.8	0.80	0.68	0.08	1.4	0.23	
16	2.3	0.90	0.80	0.10	1.6	0.30	
20							1.4
21	3.2	1.1	1.1	0.13	2.0	0.34	
24	3.7		1.3	0.14	2.0	0.35	
26	3.7	1.4	1.1	0.14	2.2	0.36	
32							1.8
33	4.8				2.3	0.41	
34	4.4	1.6	1.4	0.15	2.5	0.44	
43	5.3	1.8	1.8	0.18	2.9	0.48	
45							2.3
54	5.8	1.9	2.1	0.20	3.1	0.57	
66	5.5	2.1	2.0	0.20	3.3	0.65	
68							3.1
69	5.9	2.3	2.3	0.22	3.1	0.63	
78							3.0
81	5.5	2.1	2.1	0.22	3.6	0.65	
100	6.1	2.3	2.4	0.25	4.2	0.72	
101							3.4
102	5.6	2.4	2.6	0.24	4.0	0.74	
124							3.6
126	5.8	2.6	2.7	0.26	4.4	0.80	
148							3.7
154	5.5	2.3	2.8	0.24	4.9	0.85	
176							4.1
179	6.3	2.6	3.1	0.24	4.5	0.85	
200							3.9
201	6.0	2.4	2.9	0.25	4.7	0.83	
226	6.5	2.7	3.4	0.28	4.4	0.84	
227							3.8
251							4.0
252	5.8	2.3	3.3	0.26	5.2	0.87	
271	5.7	2.6	3.4	0.27	4.5	0.81	
297	6.0	2.7	3.3	0.23	4.3	0.86	
298							4.1
404	5.9	2.4	3.0	0.22	4.9	0.87	
516	5.7	2.5	3.1	0.24			
632	6.0	2.7	3.0	0.27			

TABLE 1 (ctd.)

T = 301°C

$P_{C_3H_8}$	v[moles cc^{-1} sec^{-1}] x 10^{13}						v x 10^{15}
mm Hg	H_2	CH_4	C_2H_4	C_2H_6	2,3-DMB	2-MP	n-C_6H_{14}
4	0.9	0.70	0.54	0.07	0.79	0.12	
7	1.1	1.0	0.90	0.09	0.98	0.16	
10	1.9	1.3	1.0	0.13	1.1	0.19	0.86
11	2.0	1.3	1.1	0.14	1.3	0.21	
12	2.0	1.4	1.5	0.17	1.3	0.21	
15	2.7	1.7	1.7	0.20	1.4	0.25	
18							1.1
20	3.4	2.1	1.9	0.22	1.5	0.31	
21	3.6			0.25			
22	3.8	2.3	2.1	0.24	1.7	0.30	
26	4.3	2.5	2.4	0.25	2.0	0.31	
29							1.5
31	4.7	2.7	2.8	0.26	2.3	0.40	
39	5.5	3.4	3.4	0.36	2.4	0.42	
42							1.7
45	5.4	3.5	3.4	0.36	2.5	0.45	
56	6.2	3.9	4.3	0.46	2.8	0.47	1.9
66	5.6	4.9	4.6	0.45	3.0	0.55	
72		5.3	4.8	0.53	3.5	0.52	2.5
74	6.4	4.9	5.2	0.55	3.5	0.59	
89	6.3	5.4	5.4	0.49	3.4	0.65	
94							2.6
100	6.2	5.6	5.7	0.50	3.8	0.65	
112	6.3	6.2	6.8	0.55	4.0	0.67	
118	6.1	6.2	6.9	0.56	3.8	0.69	3.1
120	6.8	6.7	6.9	0.59	4.5	0.73	
139	6.6	6.5	7.6	0.61	4.1	0.75	
144							2.8
157	6.0	7.3	7.8	0.60	4.3	0.77	
173							2.8
186	6.4	7.0	8.6	0.58	4.2	0.74	
195							3.1
223	6.3	7.7	9.1	0.64	4.0	0.72	
224							3.3
249							2.9
250	5.8				4.2	0.72	
254	6.4	8.0	9.9	0.70	4.6	0.76	
274	6.8	7.6	10.3	0.67	4.2	0.75	
301	6.5	8.7	10.4	0.72	4.7	0.73	3.0
314		7.9	10.1	0.64	3.9	0.77	
346	6.4	7.3	10.3	0.61	4.4	0.74	
394	6.5	8.0	10.1	0.62	4.5	0.77	
484	6.2	8.5	10.9	0.65			
558	6.2	7.9	10.8	0.70			
627	6.6	7.6	10.4	0.68			

TABLE 1 (ctd.)

T = 325°C

$P_{C_3H_8}$ mm Hg	H_2	CH_4	C_2H_4	C_2H_6	2,3-DMB	2-MP	n-C_6H_{14}
4	1.1	1.1	1.0	0.10	0.80	0.11	
7	2.0	2.0	1.7	0.17	1.1	0.14	
9	2.2	2.1	1.7	0.20	1.2	0.16	
11	2.5	2.3	2.1	0.28	1.2	0.20	0.77
13	3.0	2.7	2.6	0.28	1.3	0.22	
15	3.9	3.2	3.0	0.32	1.4	0.22	
19							1.0
20	4.7	3.9	3.5	0.37	1.6	0.27	
24	5.4	4.5	4.0	0.46	1.8	0.28	
30							1.2
33	6.5	5.4	5.4	0.58	2.4	0.36	
39	6.9	6.4	6.7	0.65	2.7	0.40	
41							1.5
42	7.3		6.5	0.64	2.7	0.39	
47	6.6	6.4	6.9	0.65	2.8	0.39	
54	6.7	7.9	7.8	0.68	2.8	0.45	1.7
64	7.2	9.5	9.2	0.78	3.1	0.45	
69							2.1
74	7.8	9.8	10.5	0.88	3.6	0.53	
87							2.1
88	8.2	11.0	11.0	0.93	3.4	0.55	
102	7.3	11.4	12.6	1.00	3.9	0.59	
109							2,1
124	7.7	13.4	15.8	1.19	4.7	0.63	
132							2.4
157							2.6
176	7.6	16.5	19.5	1.33	4.6	0.66	
182							2.7
201	7.4	18.1	21.8	1.43	4.6	0.60	
206							2,4
224	8.2	18.7	23.0	1.50	4.7	0.67	
231							2.4
252	7.9	19.0	25.1	1.45	4.3	0.64	
274							2.6
276	7.8	20.9	26.8	1.50	5.1	0.70	
299	8.1	20.7	27.7	1.50	4.4	0.65	
338	7.7	20.8	29.4	1.49	4.2	0.63	
380	8.0	22.1	31.1	1.60	4.8	0.62	
415	7.5	21.5	30.7	1.53			
450	7.7	22.0	30.9	1.58			
484	7.6	21.9	30.5	1.55			
523	8.0	21.8	31.7	1.61			
574	7.9	22.5	30.9	1.53			
618	7.6	22.0	31.6	1.57			
686	8.1	21.6	30.6	1.51			

TABLE 1 (ctd.)

T = 350°C

$P_{C_3H_8}$	v[moles cc^{-1} sec^{-1}] x 10^{13}						v x 10^{15}
mm Hg	H_2	CH_4	C_2H_4	C_2H_6	2,3-DMB	2-MP	n-C_6H_{14}
3	1.8	1.8	1.3	0.15	0.66		
5	3.0	2.4	2.0	0.30	0.90	0.11	
8	4.3	3.2	2.9	0.35	1.2	0.15	0.57
12	6.0	4.6	3.7	0.43	1.4	0.20	
15	7.4	5.2	5.2	0.50	1.6	0.21	
18	9.2	6.5	6.3	0.61	1.5	0.26	
21	10.5				1.7	0.26	
22	10.0	6.6	6.6	0.71	1.8	0.28	0.90
27	10.6	8.5	8.2	0.75	2.0	0.30	
35							1.2
40	12.2	11.7	13.0	1.06	2.8	0.35	
49	11.3	13.4	15.1	1.15	2.7	0.38	1.4
60	12.0	14.7	17.0	1.32	2.9	0.43	1.5
68	12.5	18.0	19.8	1.48	3.0	0.48	
71	12.1	17.2	19.9	1.48	3.7	0.45	
76							1.7
80	12.3	18.8	22.0	1.58	3.7	0.53	
91	12.6	21.0	25.5	1.79	4.0	0.53	
95		22.0	26.0	1.80	4.1	0.57	
98							1.8
115	13.0	24.0	29.6	1.94	4.3	0.57	
120							2.2
124	12.5	26.4	31.6	2.05	3.9	0.56	
144							1.9
145	13.1	28.0	37.0	2.24	4.7	0.62	
173							2.2
182	12.6	33.2	42.8	2.47	4.6	0.59	
202							2.1
208	13.3	37.4	46.0	2.61	5.0	0.65	
226							1.8
229	12.8	39.0	49.9	2.70	5.1	0.62	
262	12.6	42.6	55.0	3.00	4.3	0.55	
297	13.2	45.9	59.9	3.06	4.4	0.59	
299							2.1
340	12.7	49.0	63.1	3.15	4.7	0.59	
386	12.5	53.2	67.2	3.25	4.8	0.63	
422	12.4	55.0	71.1	3.31			
468	12.6	58.1	74.0	3.30			
501	12.6	59.2	75.0	3.36			
536	13.1	59.9	77.7	3.41			
565	12.8	60.8	79.4	3.44			
610	13.2	60.9	80.1	3.37			
648	13.0	61.0	79.5	3.36			
692	12.5	60.7	79.8	3.39			

FIGURE 4

Plots of the rates of hydrogen production as a function of propane pressure at five different temperatures

A	252°C
B	276°C
C	301°C
D	325°C
E	350°C

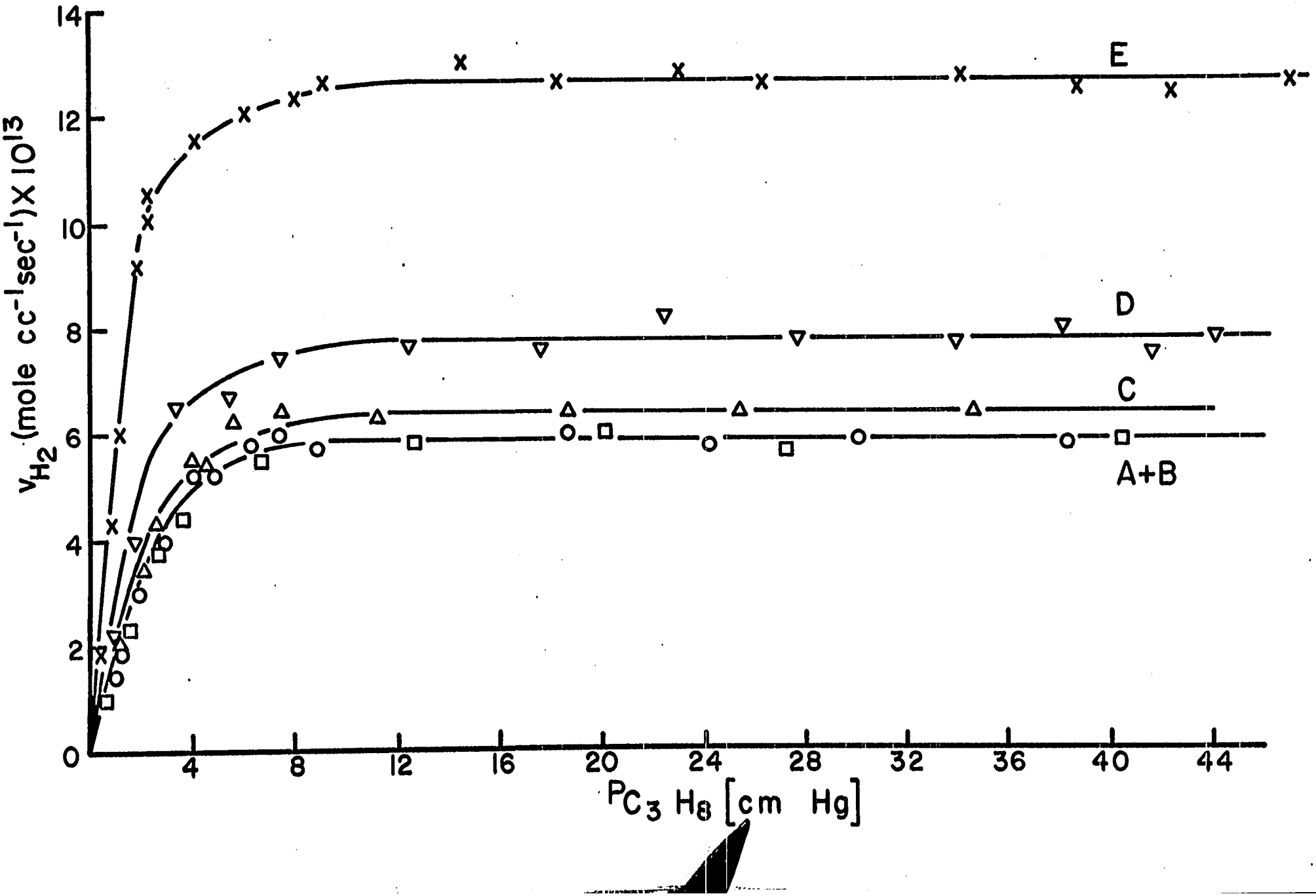
14
12
10
8
6
4
2
0
v_{H_2} (mole cc^{-1}sec^{-1}) X 10^{13}
E
D
C
A+B
4
8
12
16
20
24
28
32
36
40
44
$P_{C_3H_8}$ [cm Hg]

FIGURE 5

Plots of the rates of methane production as a function of propane pressure at five different temperatures

A	252°C
B	276°C
C	301°C
D	325°C
E	350°C

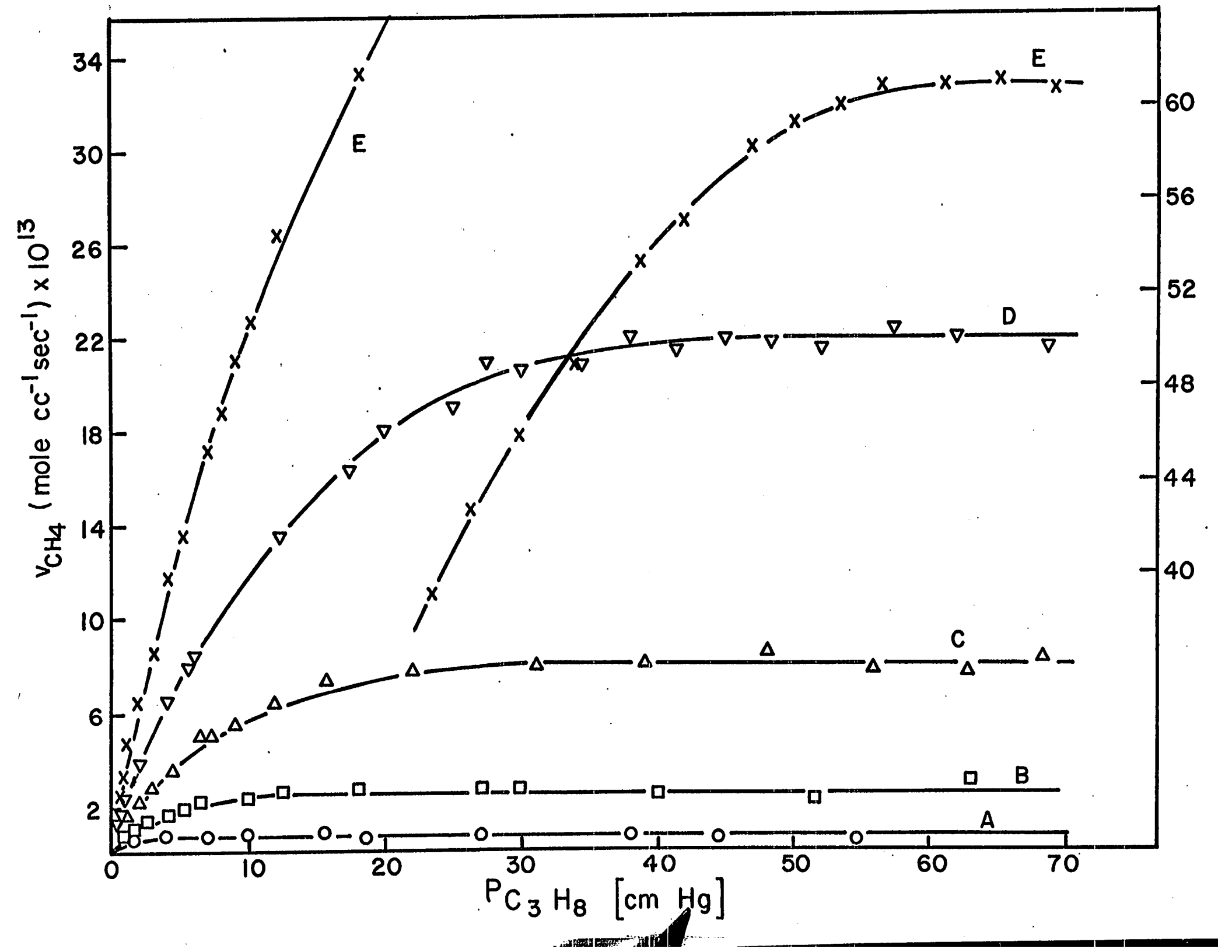
34
30
26
22
18
14
10
6
2
0
10
20
30
40
50
60
70
60
56
52
48
44
40
E
E
D
C
B
A
v_{CH_4} (mole $cc^{-1}sec^{-1}$) x 10^{13}
$P_{C_3H_8}$ [cm Hg]

FIGURE 6

Plots of the rates of ethene production as a function of propane pressure at five different temperatures

A	252°C
B	276°C
C	301°C
D	325°C
E	350°C

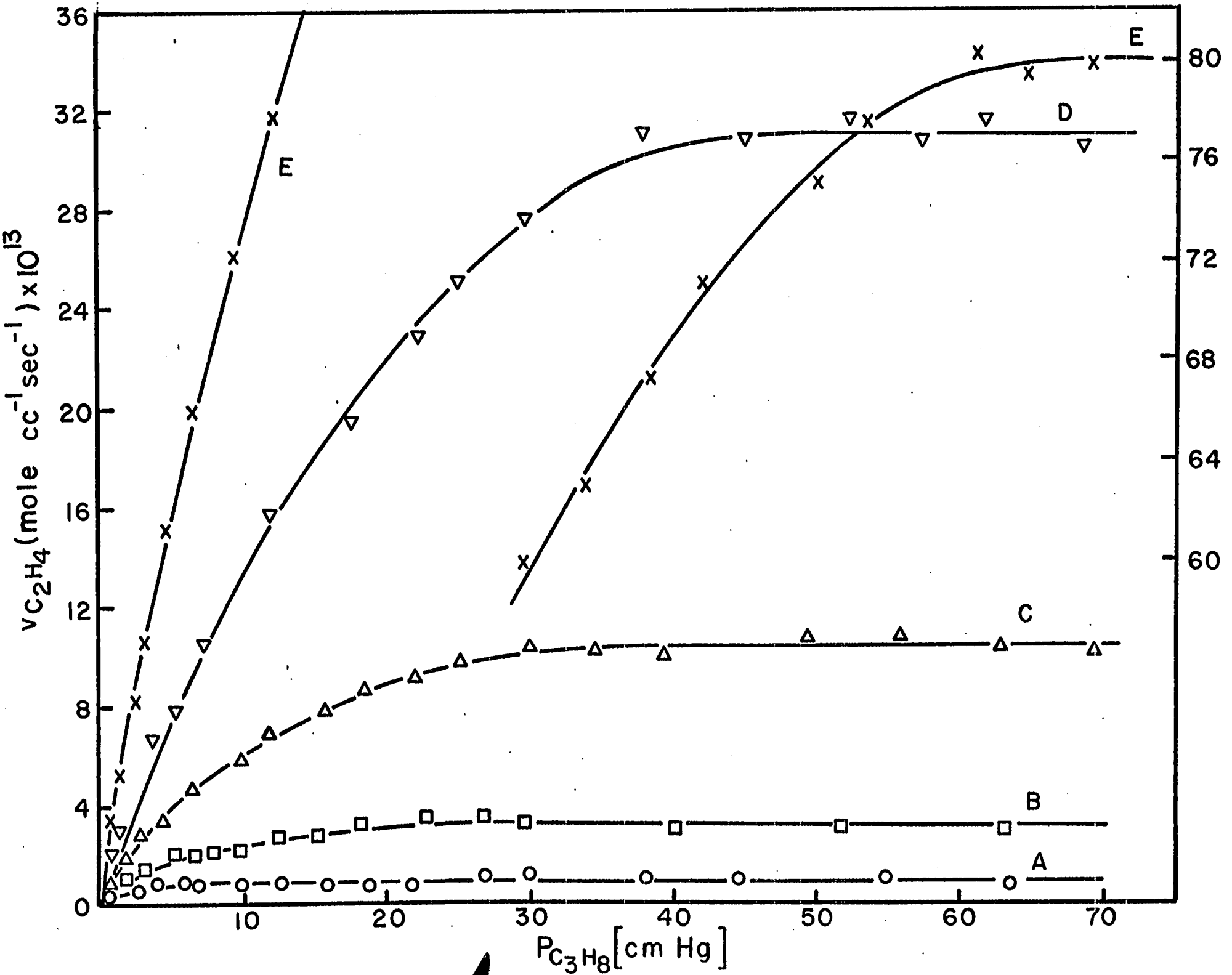
36
32
28
24
20
16
12
8
4
0
80
76
72
68
64
60
10
20
30
40
50
60
70
E
D
C
B
A
$v_{C_2H_4}$ (mole $cc^{-1}sec^{-1}$) x 10^{13}
$P_{C_3H_8}$ [cm Hg]

FIGURE 7

Plots of the rates of ethane production as a function of propane pressure at five different temperatures

A	252°C
B	276°C
C	301°C
D	325°C
E	350°C

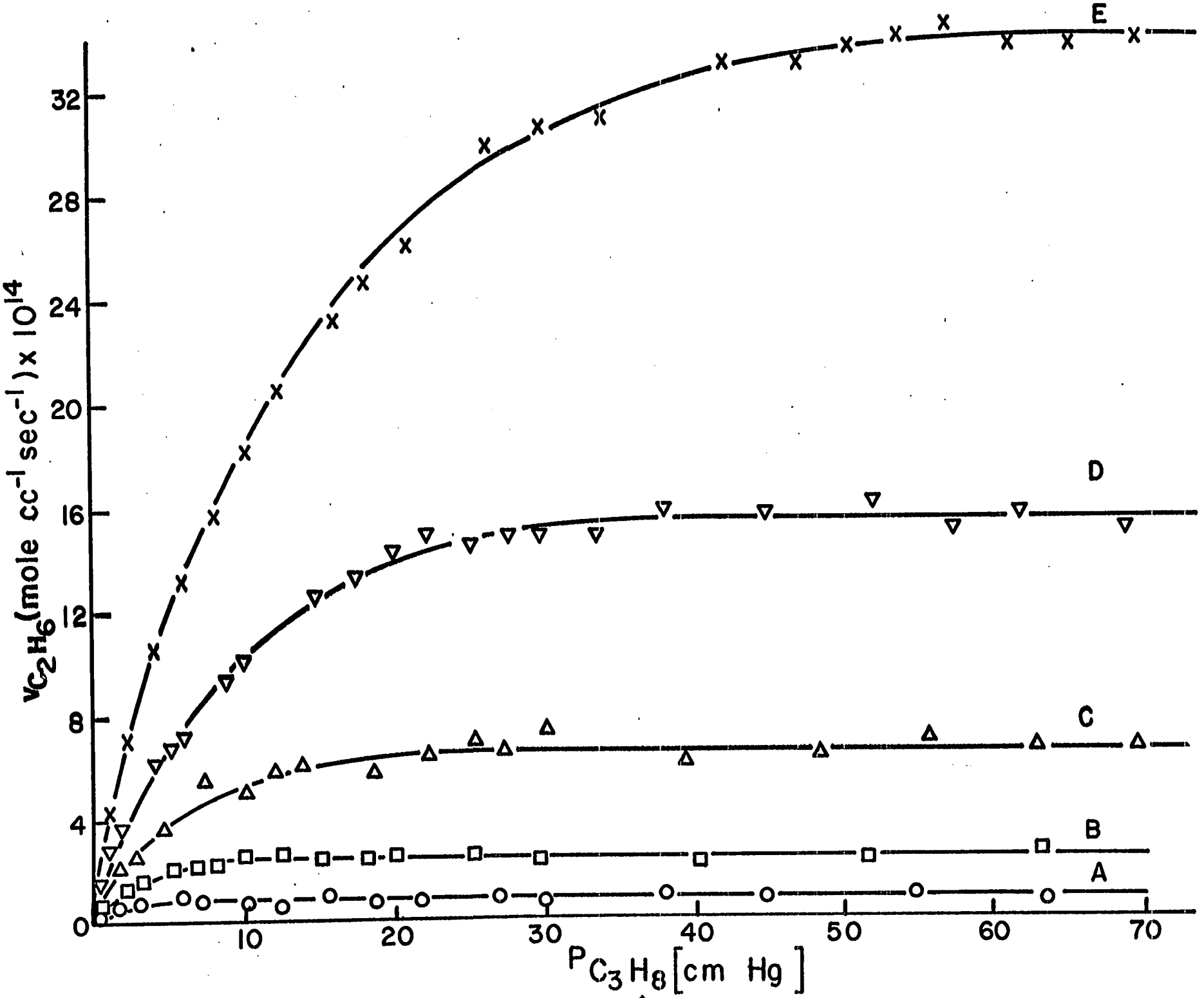
E
D
C
B
A
32
28
24
20
16
12
8
4
0
10
20
30
40
50
60
70
$v_{C_2H_6}$ (mole cc^{-1} sec^{-1}) x 10^{14}
$P_{C_3H_8}$ [cm Hg]

FIGURE 8

Plot of the rates of 2, 3-dimethylbutane production as a function of propane pressure at five different temperatures. The rate of 2, 3-dimethylbutane production does not depend on temperature

O	252°C
□	276°C
△	301°C
▽	325°C
X	350°C

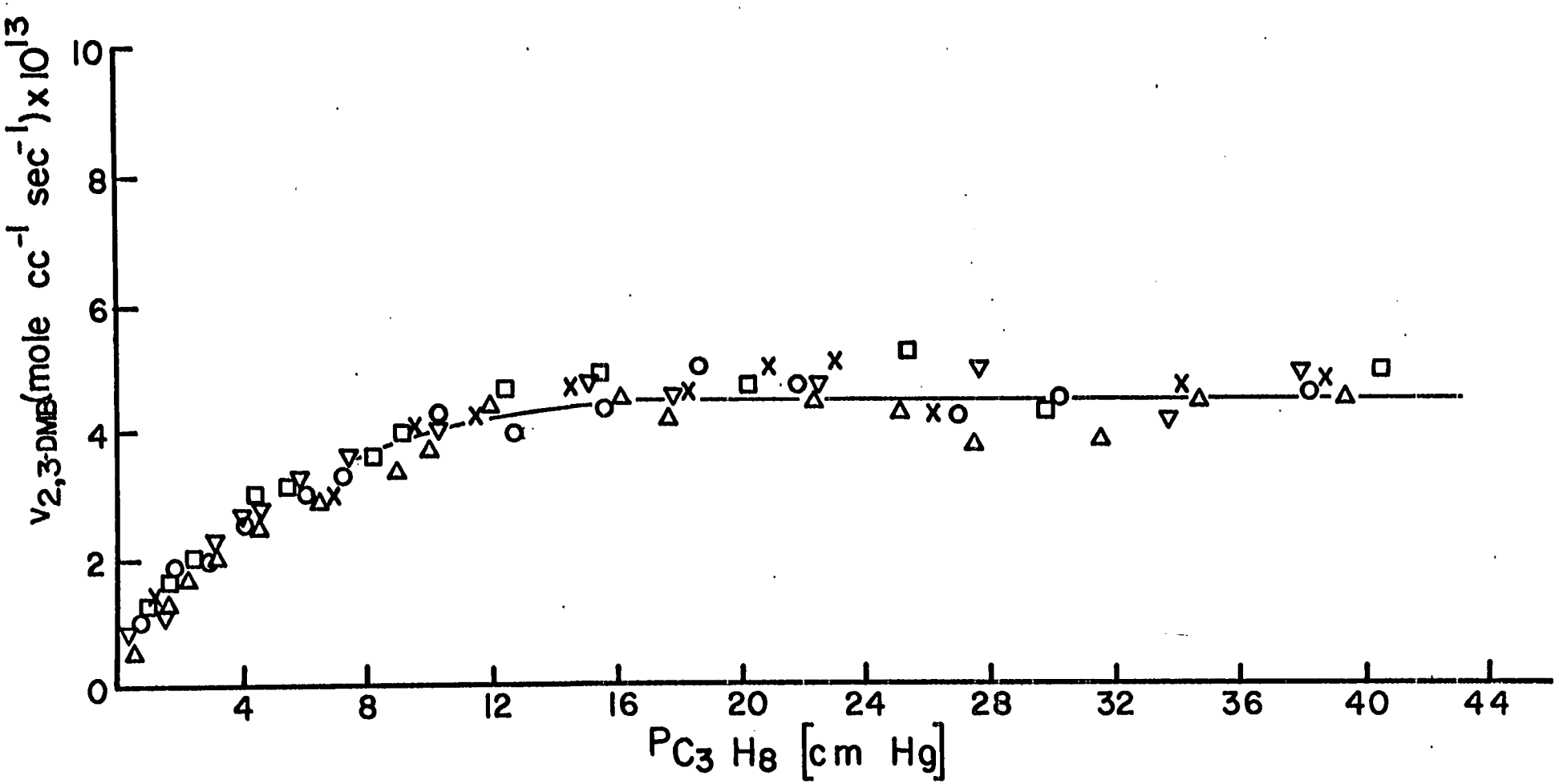
$v_{2,3\text{-DMB}}$ (mole cc^{-1} sec^{-1}) x 10^{13}
0
2
4
6
8
10
4
8
12
16
20
24
28
32
36
40
44
$P_{C_3H_8}$ [cm Hg]

FIGURE 9

Plots of the rates of 2-methylpentane production as a function of propane pressure at five different temperatures

A	252°C
B	276°C
C	301°C
D	325°C
E	350°C

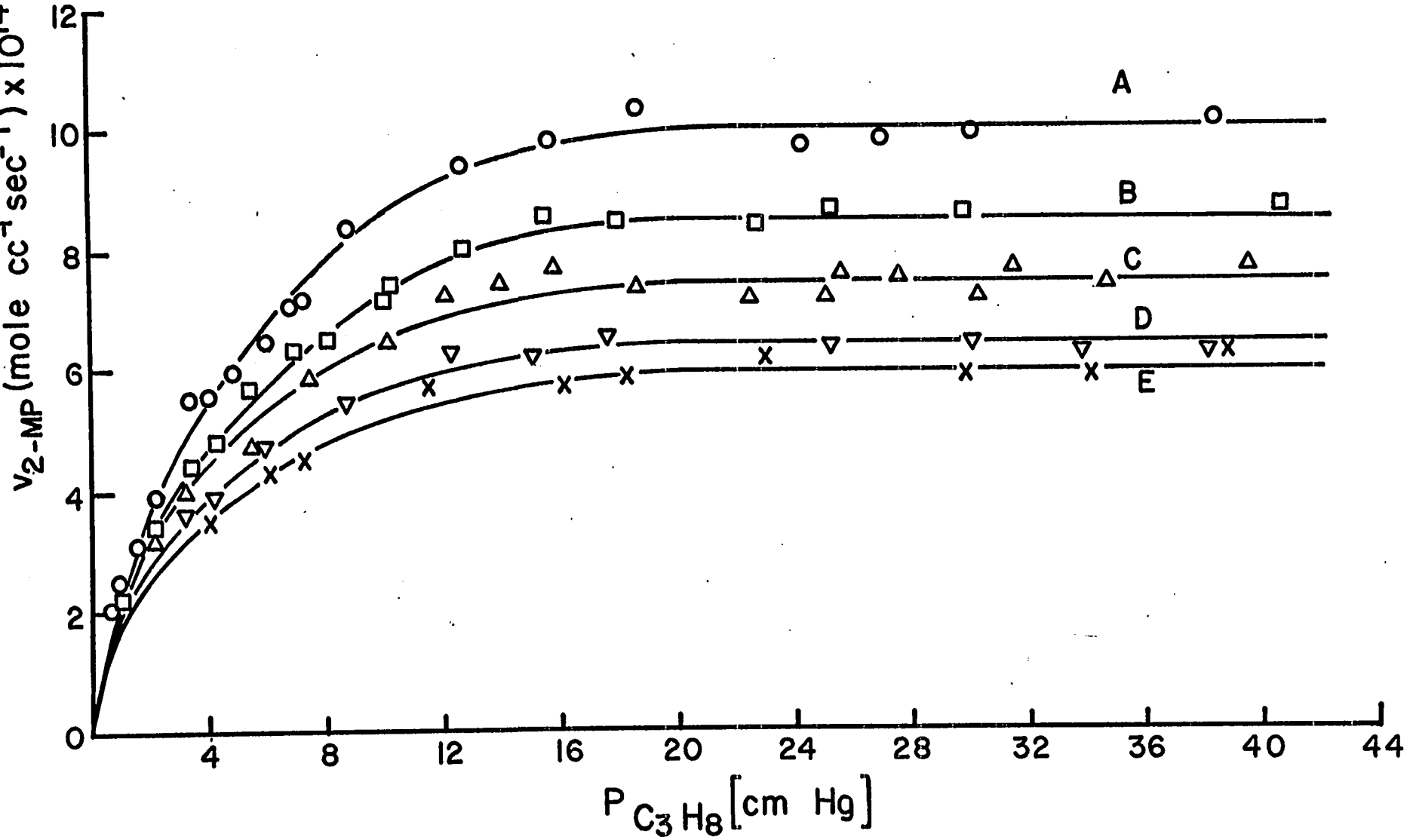
$v_{2\text{-MP}}$ (mole cc^{-1} sec^{-1}) x 10^{14}
0
2
4
6
8
10
12
4
8
12
16
20
24
28
32
36
40
44
$P_{C_3H_8}$ [cm Hg]
A
B
C
D
E

FIGURE 10

Plots of the rates of n-hexane production as a function of propane pressure at five different temperatures

A	252°C
B	276°C
C	301°C
D	325°C
E	350°C

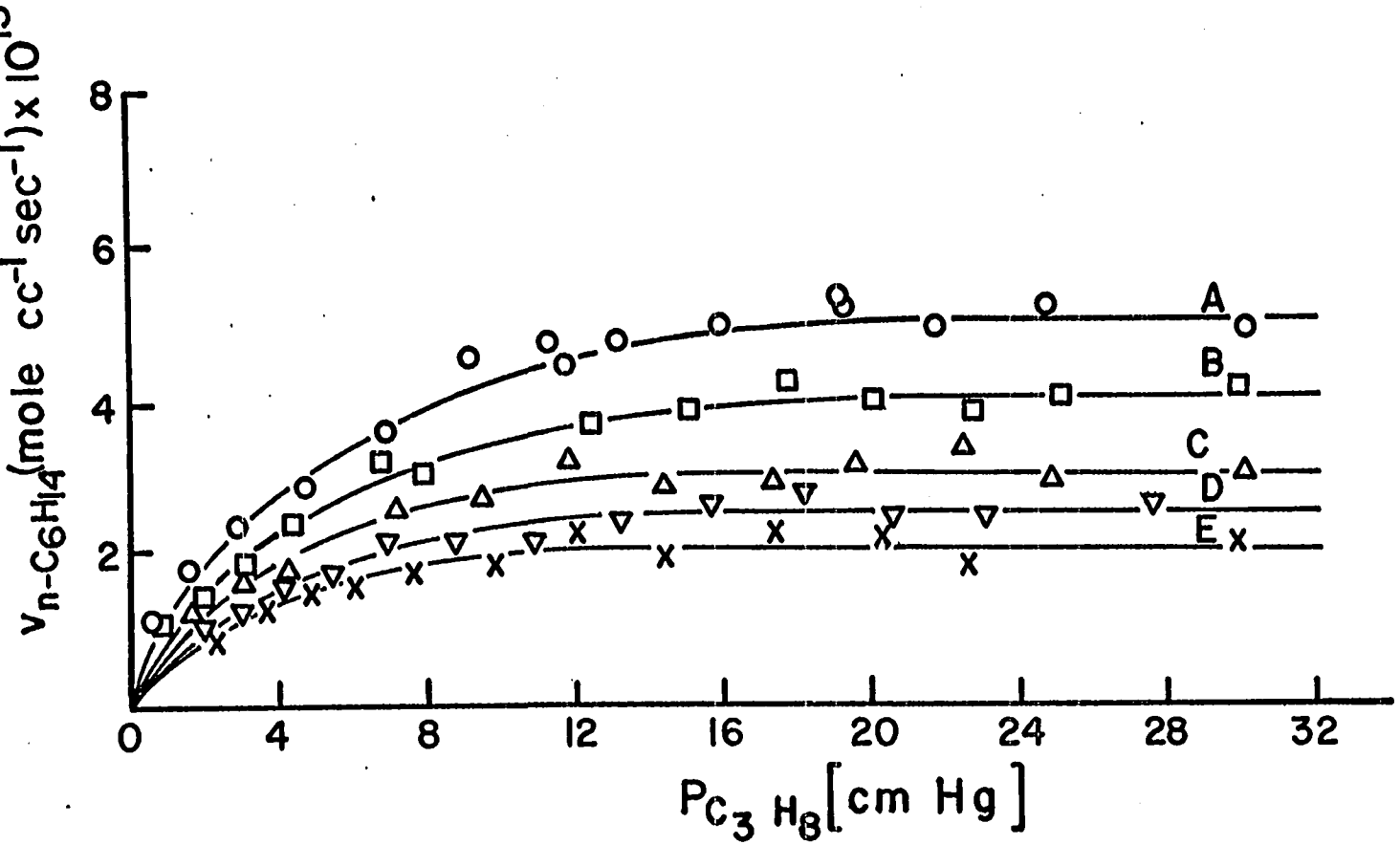
$v_{n\text{-}C_6H_{14}}$(mole cc^{-1} sec^{-1}) x 10^{15}
8
6
4
2
0
4
8
12
16
20
24
28
32
$P_{C_3H_8}$[cm Hg]
A
B
C
D
E

concentration does not affect the rate of the H atom and C_3H_7 radical production in the first elementary act. The propyl radical produced may undergo decomposition yielding methyl radicals and additional hydrogen atoms. Hydrogen atoms react with the parent propane much faster [$k = 6.3 \times 10^{13} \exp(-8.0/RT)$ cc mole^{-1}sec^{-1}] than do the methyl radicals [$k = 8.1 \times 10^{11} \exp(-10.3/RT)$ cc mole^{-1} sec^{-1}] (37). Consequently, the rate of hydrogen production becomes pressure independent at lower propane pressures and the rate of methane production at higher propane pressures. A more detailed discussion of the dependence of the rates of hydrogen and methane production on the propane pressure will be given later in Chapter 4.

At low temperatures (252° and 276°C), where presumably there is no decomposition of the propyl radical into H atom and propene, the rate of hydrogen production is independent of temperature and is greater than the rate of production of any other product. This region is referred to as a low-temperature region. At high temperatures (301°C, 325°C and 350°C) propyl radicals decompose to a considerable extent. The rate of hydrogen production becomes dependent on temperature and the rate of methane production becomes considerably greater than the rate of hydrogen production. This region is referred to as a high-temperature region.

3.2 Production of Hydrogen

It is well known that hydrogen is one of the major products in the mercury-photosensitized decomposition of propane. In the present investigation, at very low conversions the yield of hydrogen was found to be a linear function of time in the time interval up to 5000 sec. Typical hydrogen-production plots at different temperatures and pressures are shown in Figure 11. The independence of the rate of hydrogen production on time indicates that true initial yields were measured and that there was negligible addition of H-atoms to the olefins produced in the reaction. The initial rates were obtained from the slopes of the straight lines or by dividing the yields by time and taking the average values.

A double logarithmic plot of the initial rates of hydrogen production against propane pressure is shown in Figure 12. The order with respect to propane changes continuously from unity at low pressures to zero at high pressures of propane. Strictly speaking one should plot the logarithm of the velocity against the logarithm of the propane concentration, since $v = k\, c^n$ [moles $cc^{-1} sec^{-1}$]. This can be written as $v = k(P/RT)^n$ and for constant n, $v = k' P^n$. Consequently, for low and high propane pressures, which are of primary interest, one can plot pressure instead of concentration.

The rates of hydrogen production as functions of propane pressure at five different temperatures are listed in Table 2. The values are obtained from the diagrams in Figure 4. In the low-temperature region the rate of hydrogen production is independent of temperature. In the high-temperature region the rate of hydrogen production increases rapidly with increasing temperature. By subtraction of

TABLE 2

Rates of hydrogen production as a function of temperature and propane pressure*

T[°C]	252		276		301		325		350		
$P_{C_3H_8}$[mm Hg]	v_{H_2}	v_{H_2} (chain)	v_{H_2}	v_{H_2} (chain)	v_{H_2}	v_{H_2} (chain)	v_{H_2}	v_{H_2} (chain)	v_{H_2}	v_{H_2} (chain)	E_a(chain) kcal/mole
10	1.50	0.00	1.50	0.00	1.75	0.25	2.50	1.00	5.25	3.75	39.1
20	3.10	0.00	3.10	0.00	3.45	0.35	4.60	1.50	8.60	5.50	38.7
30	4.40	0.00	4.40	0.00	4.82	0.42	6.07	1.67	10.00	5.60	38.0
40	5.05	0.00	5.05	0.00	5.45	0.40	6.76	1.71	11.58	6.53	40.5
60	5.60	0.00	5.60	0.00	5.97	0.37	7.29	1.69	12.09	6.49	40.5
80	5.80	0.00	5.80	0.00	6.22	0.42	7.60	1.80	12.38	6.58	39.8
100	5.88	0.00	5.88	0.00	6.35	0.47	7.70	1.82	12.56	6.68	39.1
150	5.90	0.00	5.90	0.00	6.40	0.50	7.80	1.90	12.70	6.80	38.7
200	5.90	0.00	5.90	0.00	6.40	0.50	7.80	1.90	12.70	6.80	38.7
250	5.90	0.00	5.90	0.00	6.40	0.50	7.80	1.90	12.70	6.80	38.7
300	5.90	0.00	5.90	0.00	6.40	0.50	7.80	1.90	12.70	6.80	38.7
350	5.90	0.00	5.90	0.00	6.40	0.50	7.80	1.90	12.70	6.80	38.7

* All rates are quoted in mole cc^{-1} sec^{-1} x 10^{13}

FIGURE 11

Typical hydrogen yield-time plots at different temperatures and propane pressures

A	252°C and 10 mm Hg
B	252°C and 382 mm Hg
C	301°C and 11 mm Hg
D	301°C and 394 mm Hg
E	350°C and 8 mm Hg
F	350°C and 386 mm Hg

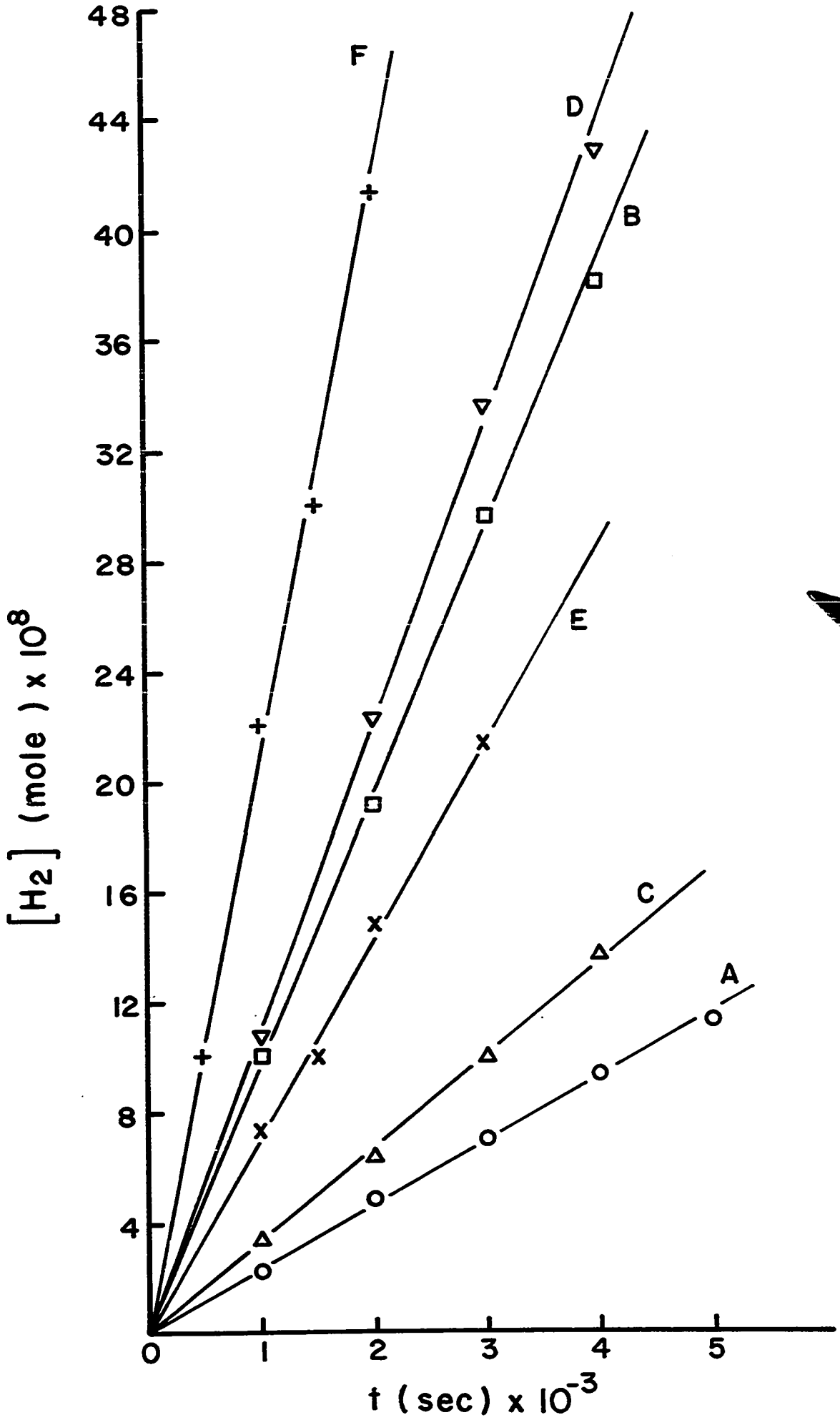
48
44
40
36
32
28
24
20
16
12
8
4
0
1
2
3
4
5
F
D
B
E
C
A
[H2] (mole) x 10^8
t (sec) x 10^-3

FIGURE 12

Order plots for hydrogen production at five different temperatures

A	252°C
B	276°C
C	301°C
D	325°C
E	350°C

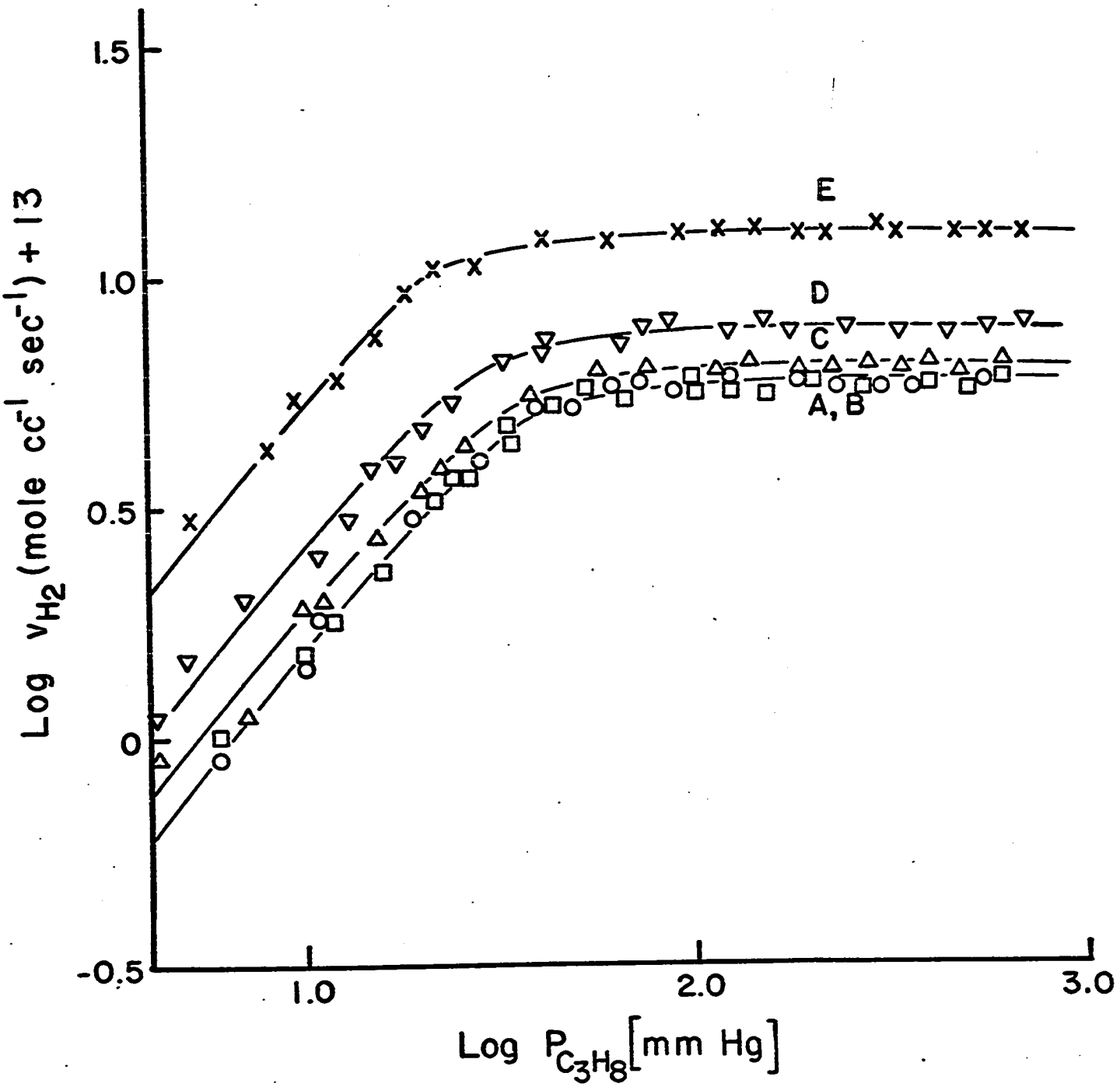
1.5
1.0
0.5
0
-0.5
1.0
2.0
3.0
Log v_{H_2} (mole cc^{-1} sec^{-1}) + 13
Log $P_{C_3H_8}$ [mm Hg]
E
D
C
A, B

the low-temperature rate of hydrogen production from the total rate of hydrogen production, the rate of hydrogen production by the chain mechanism is obtained. A more detailed discussion of the mechanism of hydrogen production will be given later in Chapter 4. The plots of the logarithms of the rates of the total and the chain-hydrogen production against reciprocal temperature are shown in Figure 13 for a propane pressure of 300 mm Hg. From the plot an activation energy of 38.7 kcal.mole^{-1} was obtained for the chain-hydrogen production. In the same way the activation energies for the chain-hydrogen production were obtained at other propane pressures. The values obtained are listed in Table 2 in column 12, and are plotted in Figure 14.

3.3 Production of Methane

Typical methane yield-time plots at different temperatures and pressures are shown in Figure 15. The yields are found to be a linear function of time, which indicates that true initial yields were measured. The initial rates were obtained from the slopes of the straight lines or by dividing the yields by reaction time and taking the average values.

A double logarithmic plot of the initial rates of methane production against pressure of propane is shown in Figure 16. The order with respect to propane changes continuously from 0.8 at low pressures to zero at high pressures of propane.

The rates of methane production as a function of pressure of propane at five different temperatures are listed in Table 3. The values are obtained from the diagrams in Figure 5.

TABLE 3

Rates of methane production as a function of temperature and propane pressure*

T[°C]	252	276	301	325	350	E_a
$P_{C_3H_8}$[mm Hg]	v_{CH_4}	v_{CH_4}	v_{CH_4}	v_{CH_4}	v_{CH_4}	kcal/mole
10	0.34	0.70	1.30	2.30	4.00	16.2
20	0.53	1.13	2.08	3.89	6.80	16.8
30	0.63	1.44	2.75	5.20	9.30	17.8
40	0.68	1.68	3.34	6.45	11.5	18.6
60	0.70	2.00	4.33	8.48	15.4	20.8
80	0.70	2.20	5.15	10.2	19.0	22.3
100	0.70	2.34	5.75	11.7	22.3	23.3
150	0.70	2.47	6.85	15.1	29.5	25.4
200	0.70	2.48	7.47	17.9	35.6	26.4
250	0.70	2.50	7.86	19.7	40.9	27.2
300	0.70	2.50	7.97	20.8	45.7	27.9
350	0.70	2.50	8.00	21.4	50.2	28.2
400	0.70	2.50	8.00	21.8	54.0	28.9
450	0.70	2.50	8.00	22.0	57.0	29.1
500	0.70	2.50	8.00	22.0	59.1	29.5
550	0.70	2.50	8.00	22.0	60.3	29.5
600	0.70	2.50	8.00	22.0	60.8	29.5
650	0.70	2.50	8.00	22.0	60.9	29.5
700	0.70	2.50	8.00	22.0	60.9	29.5

*All rates are quoted in mole cc^{-1} sec^{-1} x 10^{13}

FIGURE 13

Plots of the logarithm of the rates of the total hydrogen and the chain-hydrogen production at a propane pressure of 300 mm Hg, against reciprocal temperature

A total hydrogen

B chain hydrogen

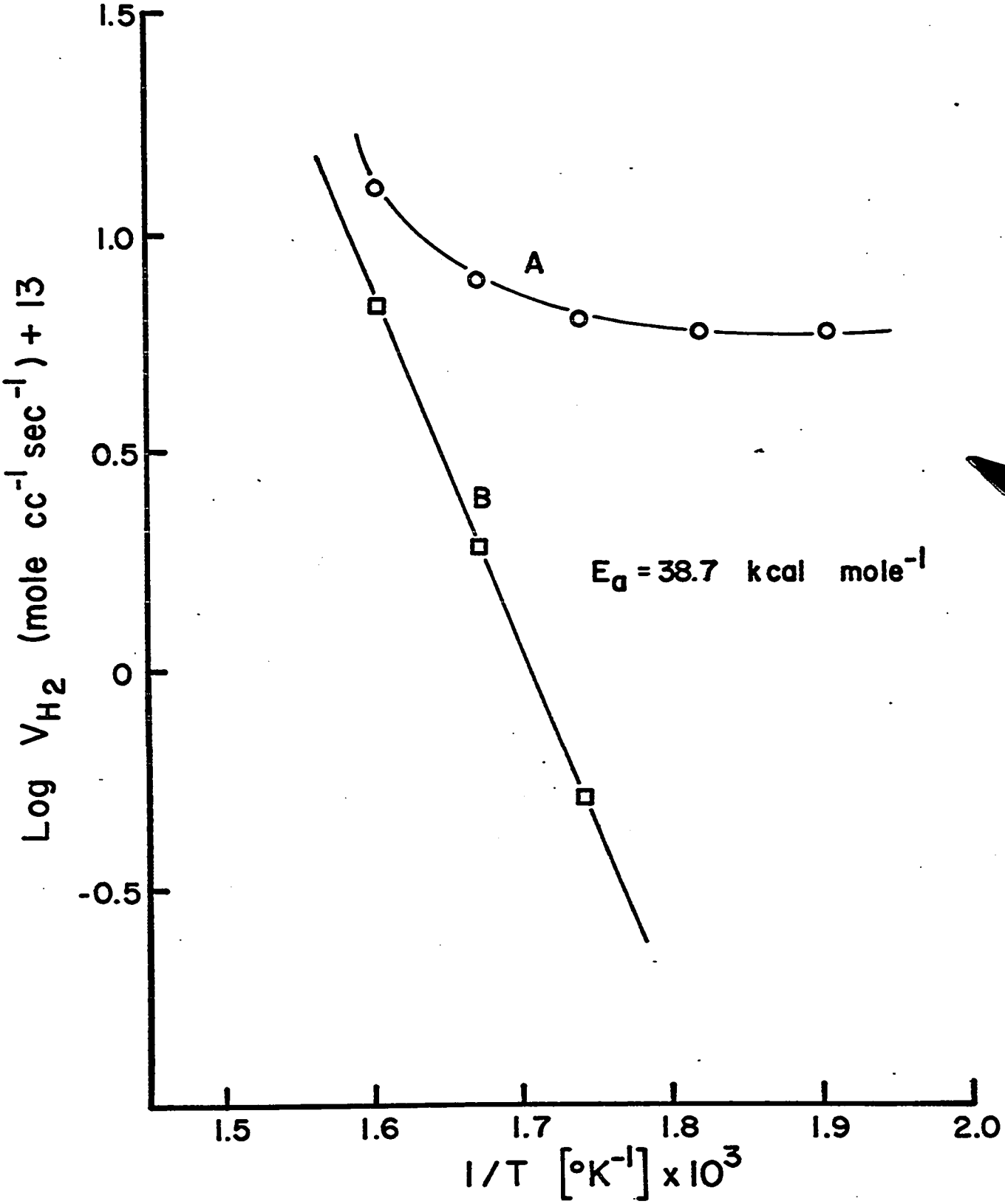
1.5
1.0
0.5
0
-0.5
Log V_{H2} (mole cc^{-1} sec^{-1}) + 13
A
B
E_a = 38.7 kcal mole^{-1}
1.5
1.6
1.7
1.8
1.9
2.0
1/T [°K^{-1}] x 10^3

FIGURE 14

Plot of the energy of activation for the chain-hydrogen production against the pressure of propane

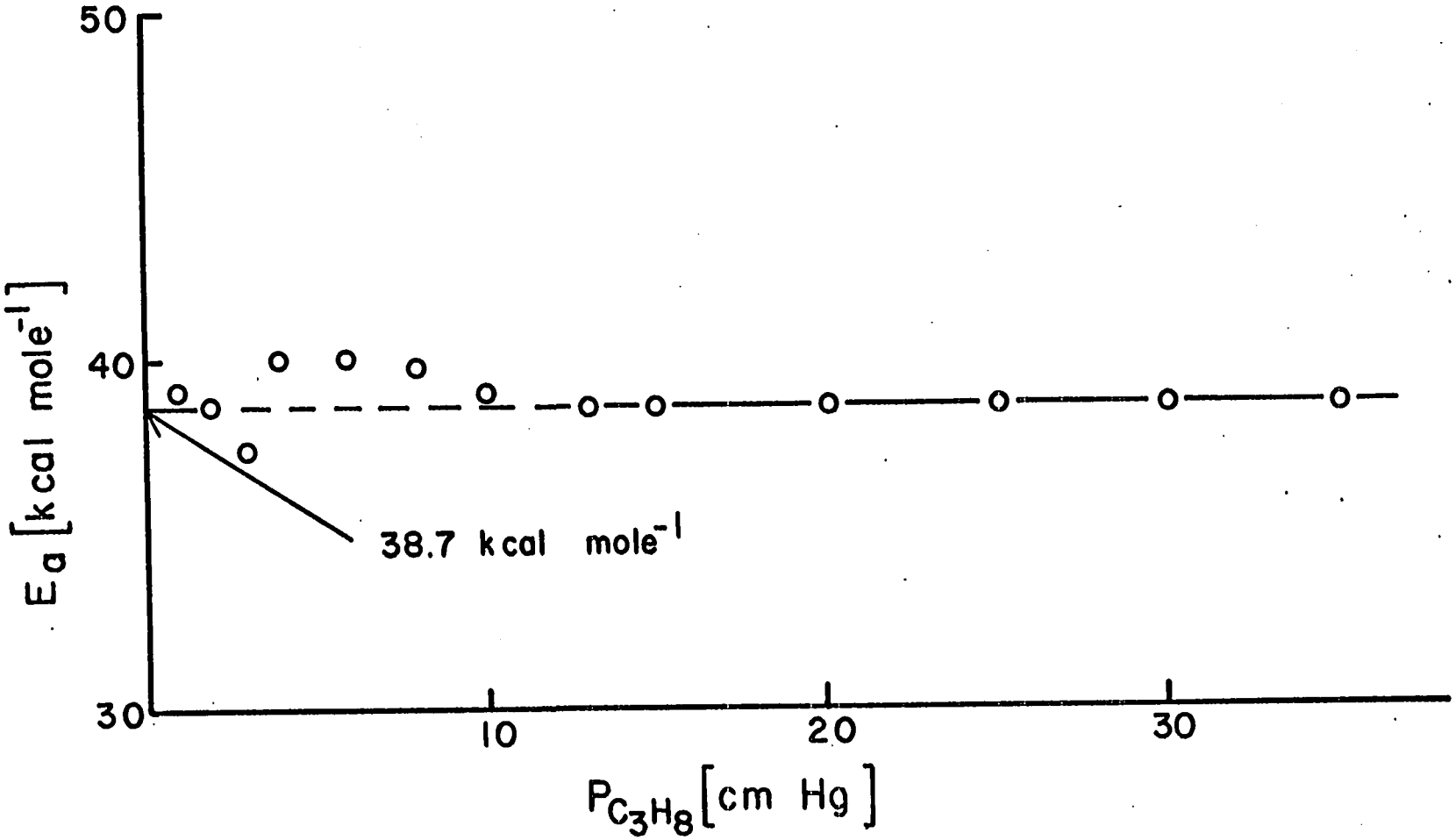
50
40
30
10
20
30
E_a [kcal mole^{-1}]
38.7 kcal mole^{-1}
$P_{C_3H_8}$ [cm Hg]

FIGURE 15

Typical methane yield-time plots at different temperatures and propane pressures

A	252°C and 10 mm Hg
B	252°C and 382 mm Hg
C	301°C and 11 mm Hg
D	301°C and 394 mm Hg
E	350°C and 8 mm Hg
F	350°C and 386 mm Hg

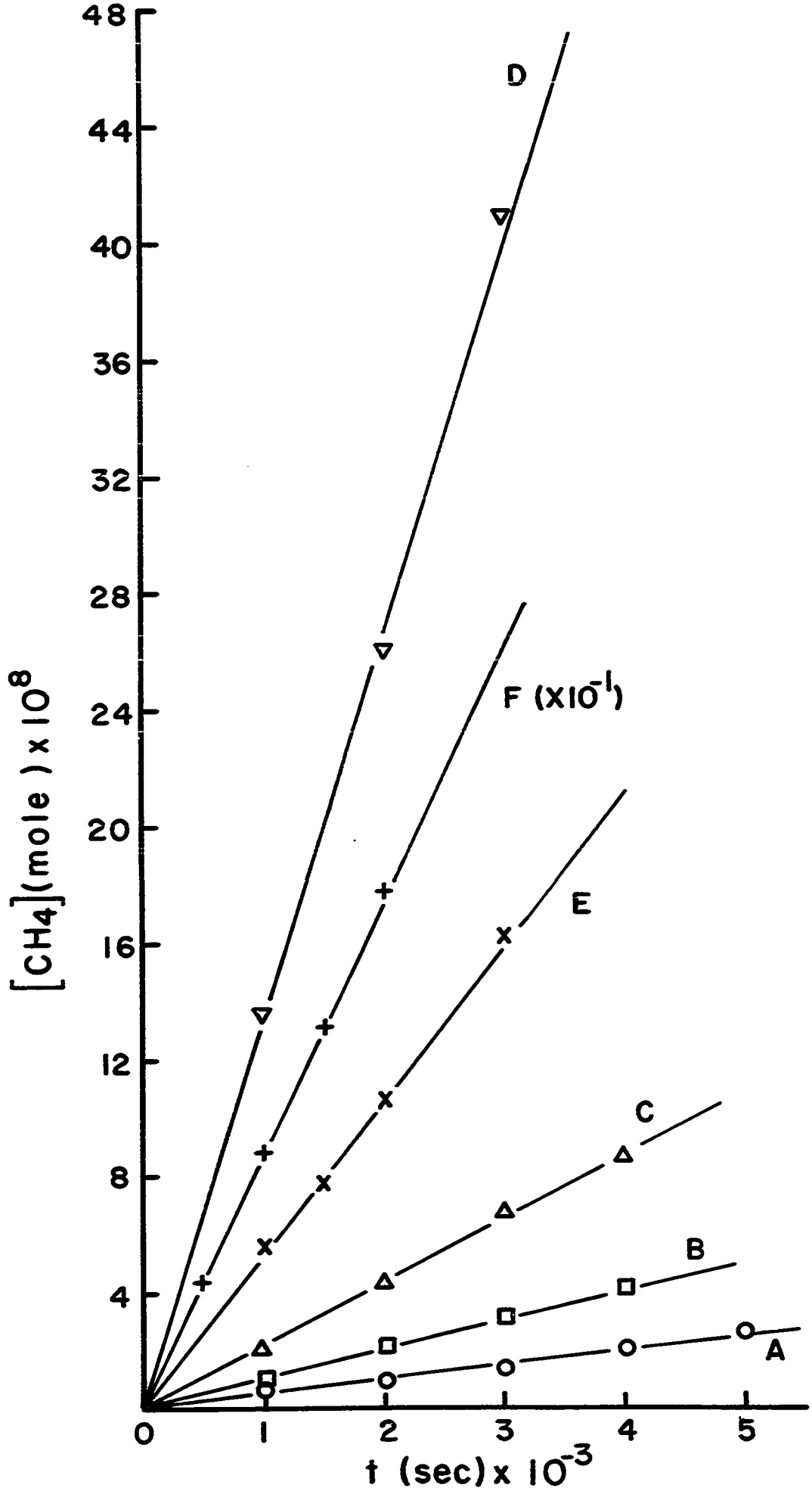
48
44
40
36
32
28
24
20
16
12
8
4
0
1
2
3
4
5
D
F (X10⁻¹)
E
C
B
A
[CH4](mole) x 10⁸
t (sec) x 10⁻³

FIGURE 16

Order plots for methane production of five different temperatures

A	252°C
B	276°C
C	301°C
D	325°C
E	350°C

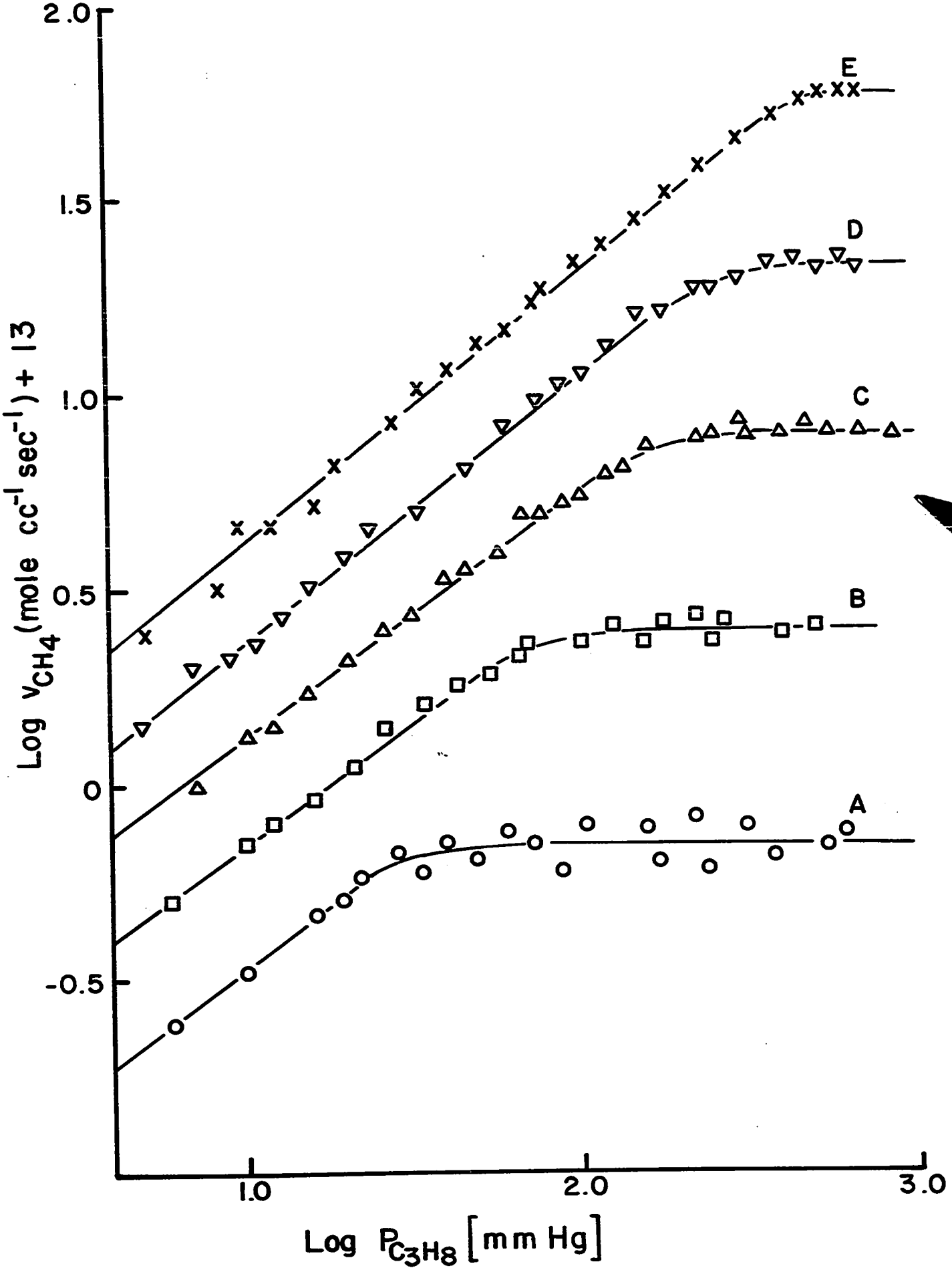
2.0
1.5
1.0
0.5
0
-0.5
Log v_{CH_4} (mole cc^{-1} sec^{-1}) + 13
E
D
C
B
A
1.0
2.0
3.0
Log $P_{C_3H_8}$ [mm Hg]

The rate of methane production is strongly dependent on temperature and increases rapidly with increasing temperature. A more detailed discussion of the mechanism of methane production will be given later in Chapter 4. The plot of the logarithm of the rate of methane production against reciprocal temperature is shown in Figure 17 for a propane pressure of 700 mm Hg. From the plot an activation energy of 29.5 kcal $mole^{-1}$ was obtained for the methane production at 700 mm Hg propane pressure. In the same way the activation energies for the methane production at other propane pressures were obtained. The obtained values are listed in Table 3 in column 7, and are plotted in Figure 18. The activation energy increases from an extrapolated value of 15 kcal $mole^{-1}$ at zero propane pressure to a constant value of 29.5 kcal $mole^{-1}$ at high pressures of propane. The difference amounts to 14.5 kcal $mole^{-1}$.

3.4 Production of Ethene

Typical ethene yield-time plots at different temperatures and propane pressures are shown in Figure 19. The yields are found to be a linear function of time, which indicates that primary initial yields were measured. The initial rates were obtained from the slopes of the straight lines or by dividing the yields by reaction time and taking the average values.

Double logarithmic plot of the initial rates of ethene production against pressure of propane is shown in Figure 20. The order with respect to propane changes continuously from 0.8 at low pressures to zero at high pressures of propane.

The rates of ethene production as a function of pressure of propane at five different temperatures are listed in Table 4. The values are obtained from the diagrams in Figure 6.

TABLE 4

Rates of ethene production as a function of temperature and propane pressure *

T[°C]	252	276	301	325	350	E_a
$P_{C_3H_8}$[mm Hg]	$v_{C_2H_4}$	$v_{C_2H_4}$	$v_{C_2H_4}$	$v_{C_2H_4}$	$v_{C_2H_4}$	kcal/mole
10	0.30	0.60	1.10	2.00	3.50	16.1
20	0.50	1.00	2.00	3.60	6.40	16.7
30	0.61	1.30	2.70	5.10	9.60	18.0
40	0.67	1.59	3.30	6.30	12.5	18.4
60	0.74	1.98	4.37	8.60	17.8	19.9
80	0.79	2.25	5.30	10.8	22.6	21.3
100	0.83	2.47	6.16	12.8	27.0	22.9
150	0.88	2.89	7.70	17.4	37.0	25.5
200	0.90	3.12	8.85	21.5	45.6	26.9
250	0.90	3.18	9.70	25.0	53.1	27.7
300	0.90	3.20	10.2	28.0	59.4	28.6
350	0.90	3.20	10.5	30.2	64.6	29.1
400	0.90	3.20	10.5	30.9	69.0	29.1
450	0.90	3.20	10.5	31.0	72.6	29.3
500	0.90	3.20	10.5	31.0	75.6	29.5
550	0.90	3.20	10.5	31.0	78.1	29.7
600	0.90	3.20	10.5	31.0	79.7	29.7
650	0.90	3.20	10.5	31.0	80.0	29.7
700	0.90	3.20	10.5	31.0	80.0	29.7

* All rates are quoted in mole cc^{-1} sec^{-1} x 10^{13}

FIGURE 17

Plot of the logarithm of the rate of methane production at a propane pressure of 700 mm Hg, against reciprocal temperature

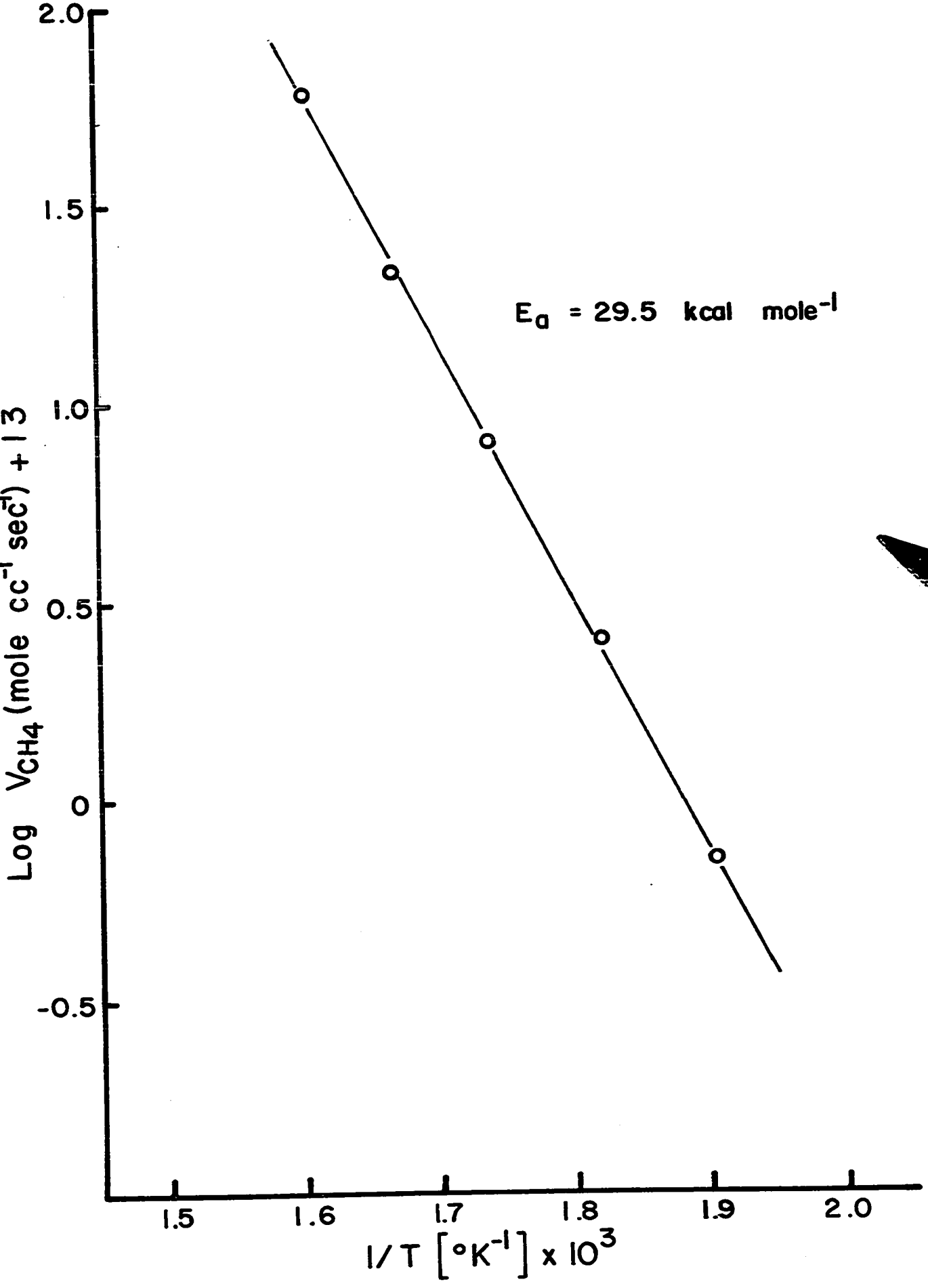
2.0
1.5
1.0
0.5
0
-0.5
Log V_{CH_4} (mole cc^{-1} sec^{-1}) + 13
E_a = 29.5 kcal mole^{-1}
1.5
1.6
1.7
1.8
1.9
2.0
1/T [°K^{-1}] x 10^3

FIGURE 18

Plot of the energy of activation for the methane production against the pressure of propane

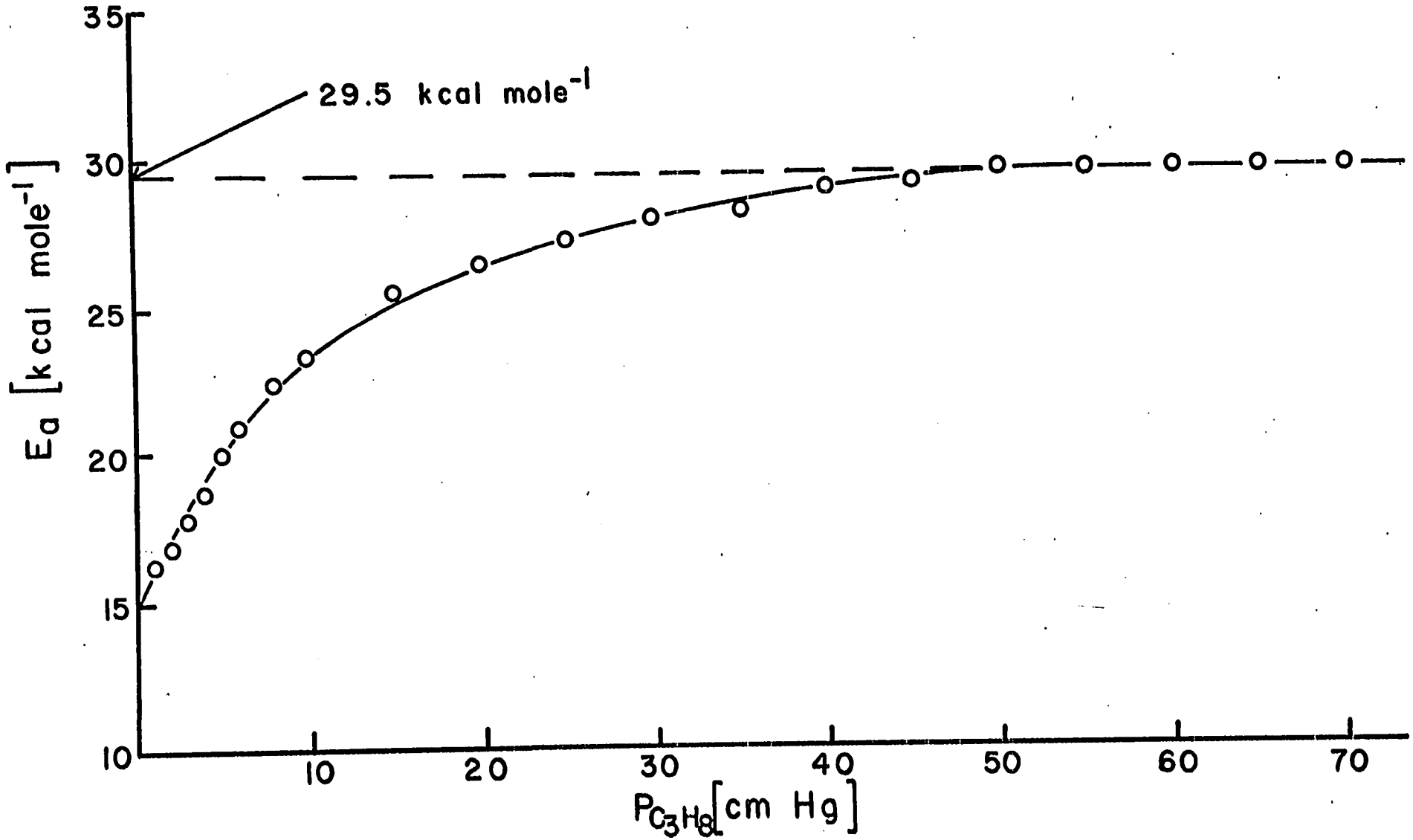
35
30
25
20
15
10
29.5 kcal mole⁻¹
Ea [kcal mole⁻¹]
10
20
30
40
50
60
70
P C3H8 [cm Hg]

FIGURE 19

Typical ethene yield-time plots at different temperatures and propane pressures

A	252°C and 10 mm Hg
B	252°C and 382 mm Hg
C	301°C and 11 mm Hg
D	301°C and 394 mm Hg
E	350°C and 8 mm Hg
F	350°C and 386 mm Hg

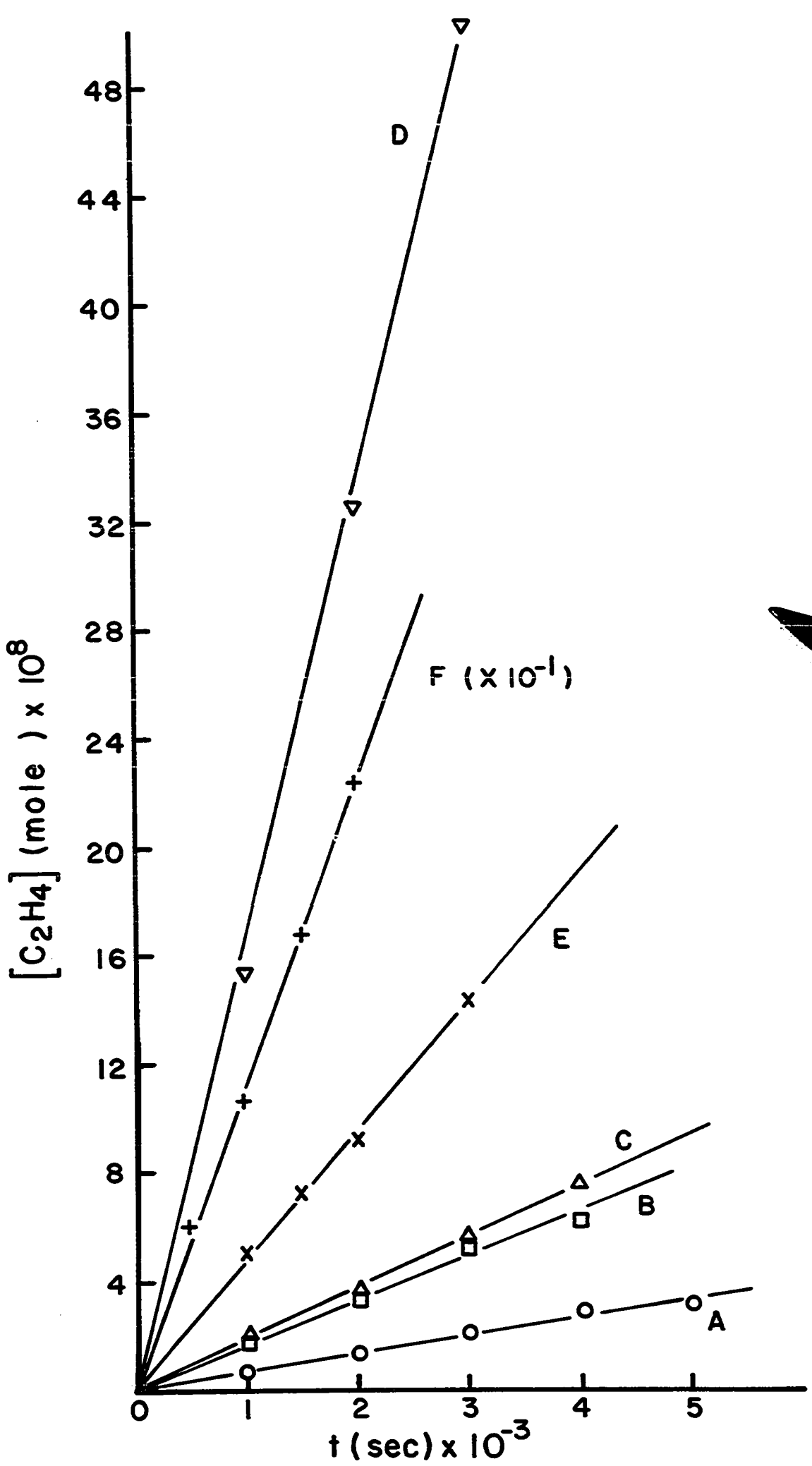
48
44
40
36
32
28
24
20
16
12
8
4
0
1
2
3
4
5
D
F (X 10⁻¹)
E
C
B
A
[C2H4] (mole) x 10⁸
t (sec) x 10⁻³

FIGURE 20

Order plots for ethene production at five different temperatures

A	252°C
B	276°C
C	301°C
D	325°C
E	350°C

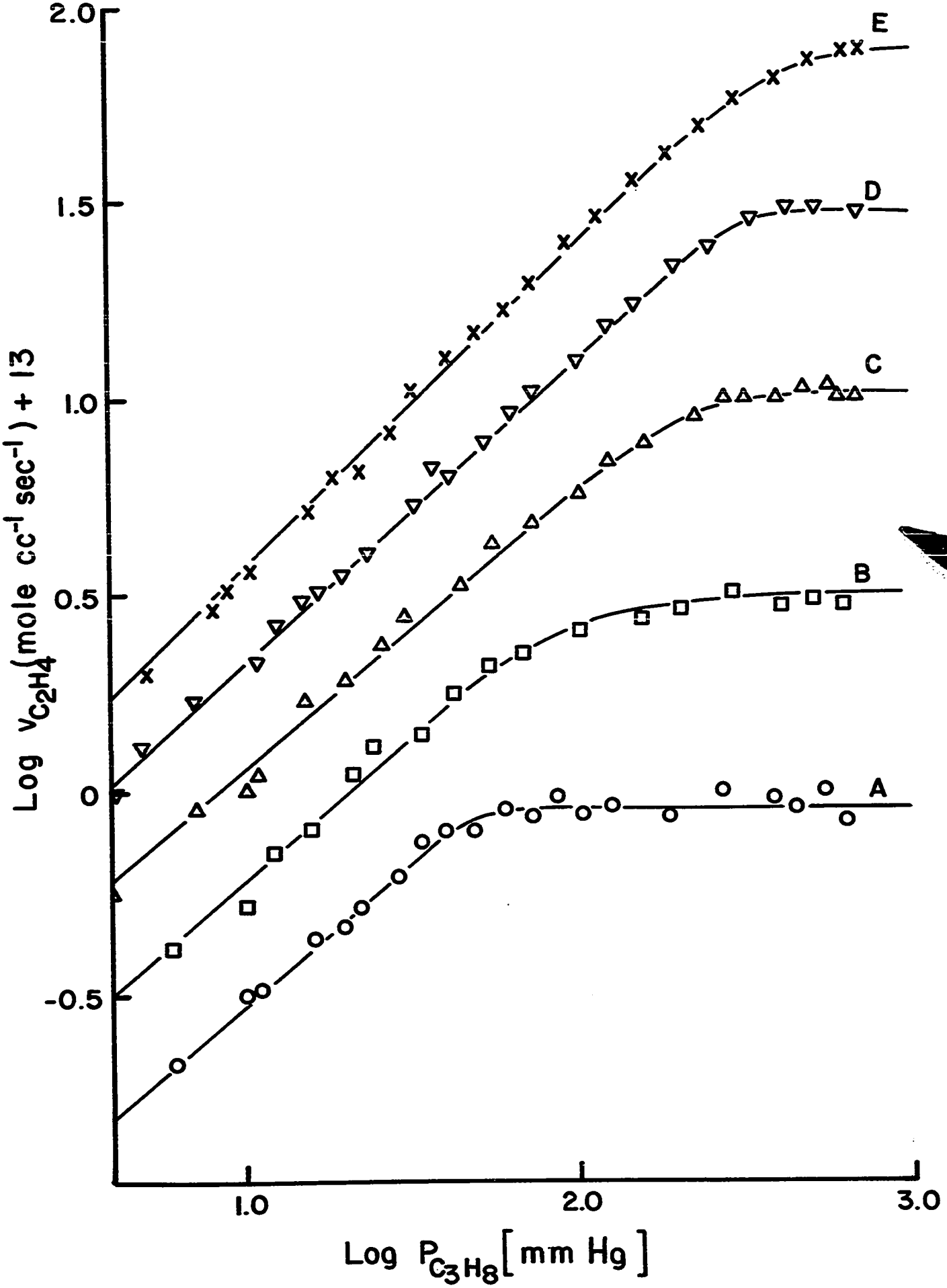
2.0
1.5
1.0
0.5
0
-0.5
Log $v_{C_2H_4}$(mole cc^{-1} sec^{-1}) + 13
E
D
C
B
A
1.0
2.0
3.0
Log $P_{C_3H_8}$[mm Hg]

The rate of ethene production is strongly dependent on temperature and increases rapidly with increasing temperature. A more detailed discussion on the mechanism of ethene production will be given later in Chapter 4. The plot of the logarithm of the rate of ethene production against reciprocal temperature is shown in Figure 21 for a propane pressure of 700 mm Hg. From the plot an activation energy of 29.7 kcal $mole^{-1}$ was obtained for the ethene production at 700 mm Hg propane pressure. Similarly, the activation energies for the ethene production at other propane pressures were obtained. The obtained values are listed in Table 4 in column 7, and are plotted in Figure 22. The activation energy increases from an extrapolated value of 15 kcal $mole^{-1}$ at zero propane pressure to a constant value of 29.7 kcal $mole^{-1}$ at high pressures of propane. The difference amounts to 14.7 kcal $mole^{-1}$.

3.5 Production of Ethane

Typical ethane yield-time plots at different temperatures and propane pressures are shown in Figure 23. The yields are found to be a linear function of time, which indicates that primary initial yields were measured. The initial rates were obtained from the slopes of the straight lines or by dividing the yields by reaction times and taking the average values.

A double logarithmic plot of the initial rates of ethane production against the pressure of propane is shown in Figure 24. The order with respect to propane changes continuously from 0.8 at low pressures to zero at high pressures of propane.

FIGURE 21

Plot of the logarithm of the rate of ethene production at a propane pressure of 700 mm Hg, against reciprocal temperature

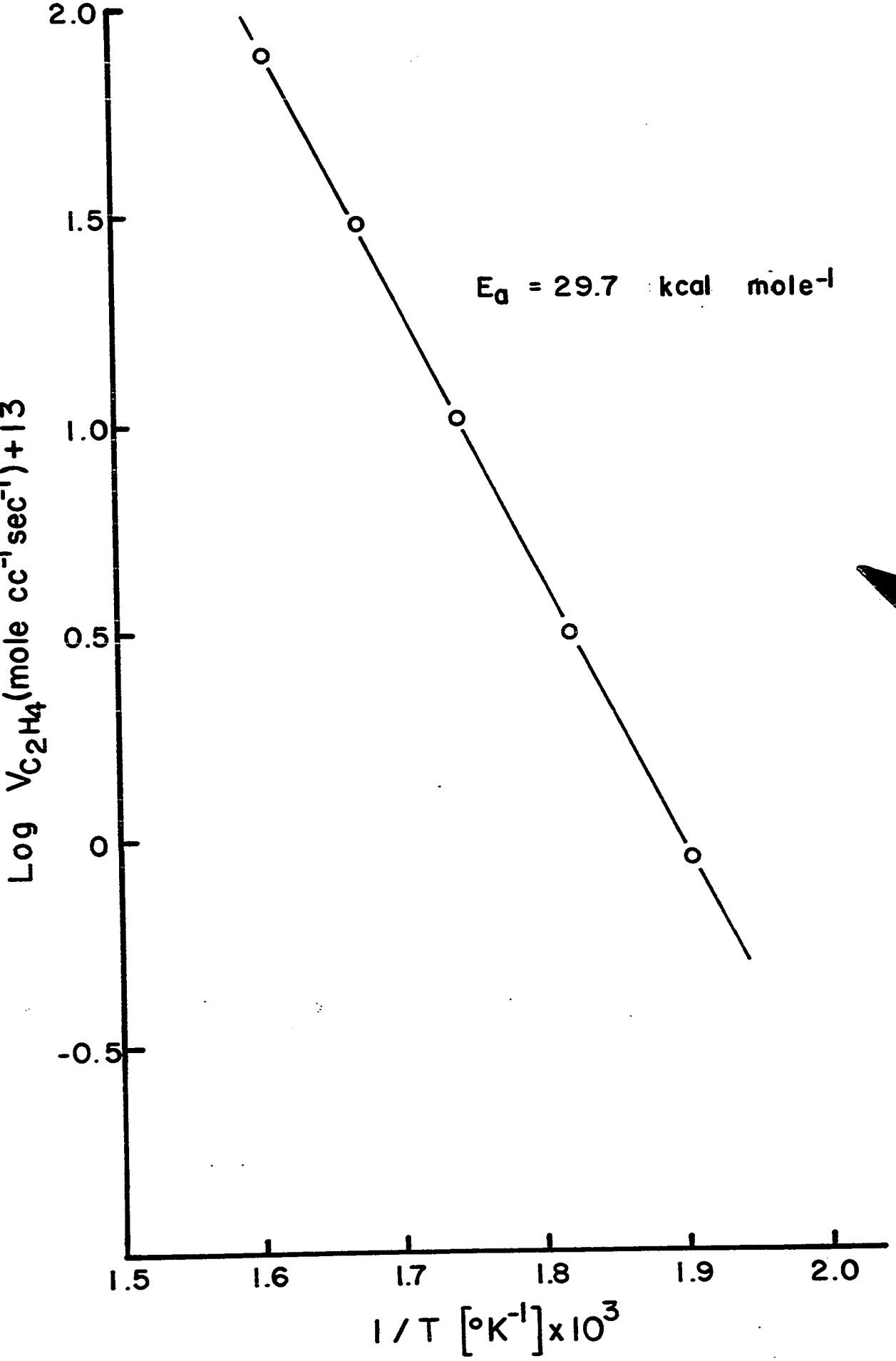
2.0
1.5
1.0
0.5
0
-0.5
Log $V_{C_2H_4}$(mole $cc^{-1}sec^{-1}$)+13
E_a = 29.7 kcal mole^{-1}
1.5
1.6
1.7
1.8
1.9
2.0
1 / T [°K^{-1}] x 10^3

FIGURE 22

Plot of the energy of activation for the ethene production against the pressure of propane

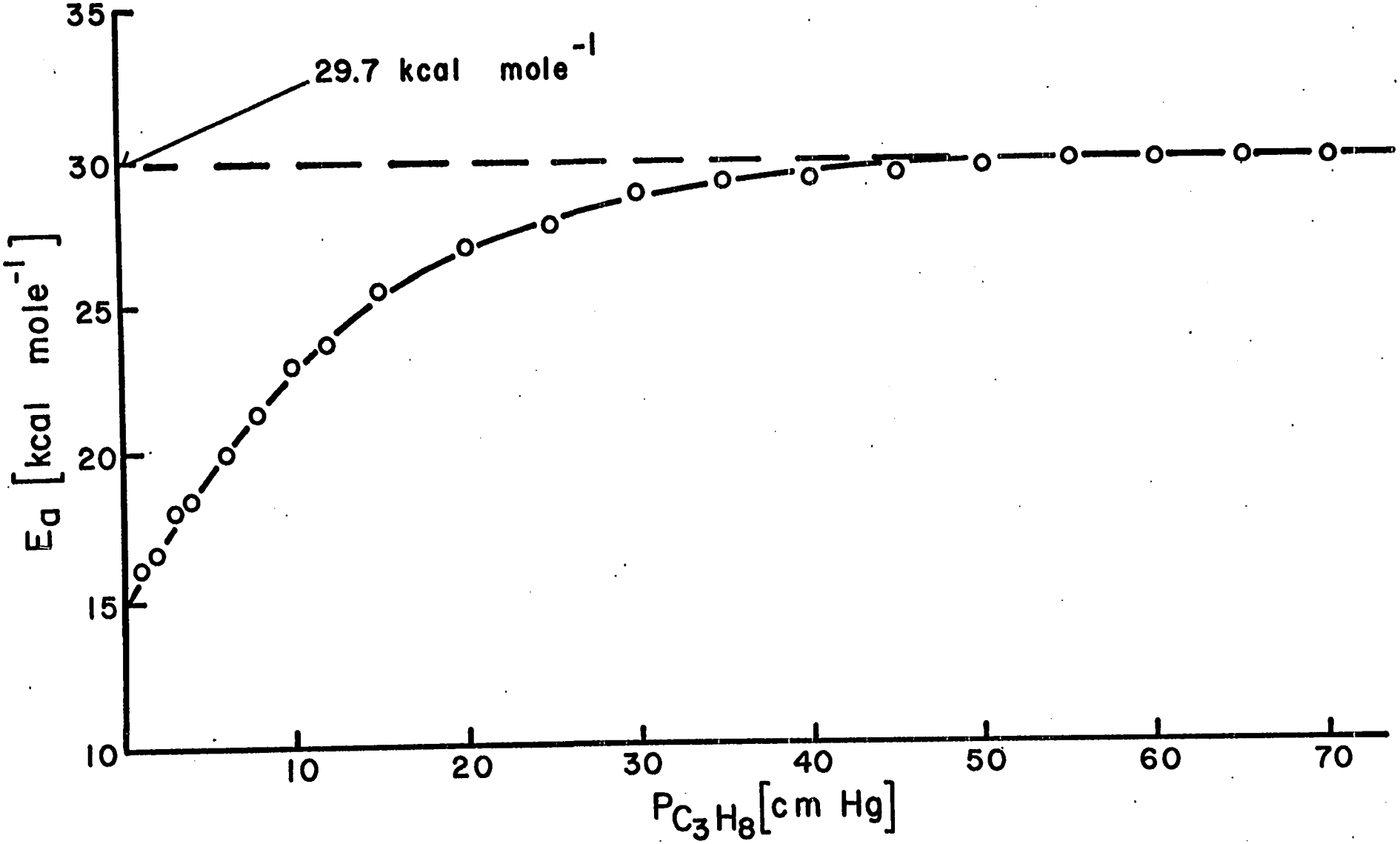
35
30
25
20
15
10
29.7 kcal mole-1
Ea [kcal mole-1]
10
20
30
40
50
60
70
PC3H8[cm Hg]

FIGURE 23

Typical ethane yield-time plots at different temperatures and propane pressures

A	252°C and 10 mm Hg
B	252°C and 382 mm Hg
C	301°C and 11 mm Hg
D	301°C and 394 mm Hg
E	350°C and 8 mm Hg
F	350°C and 386 mm Hg

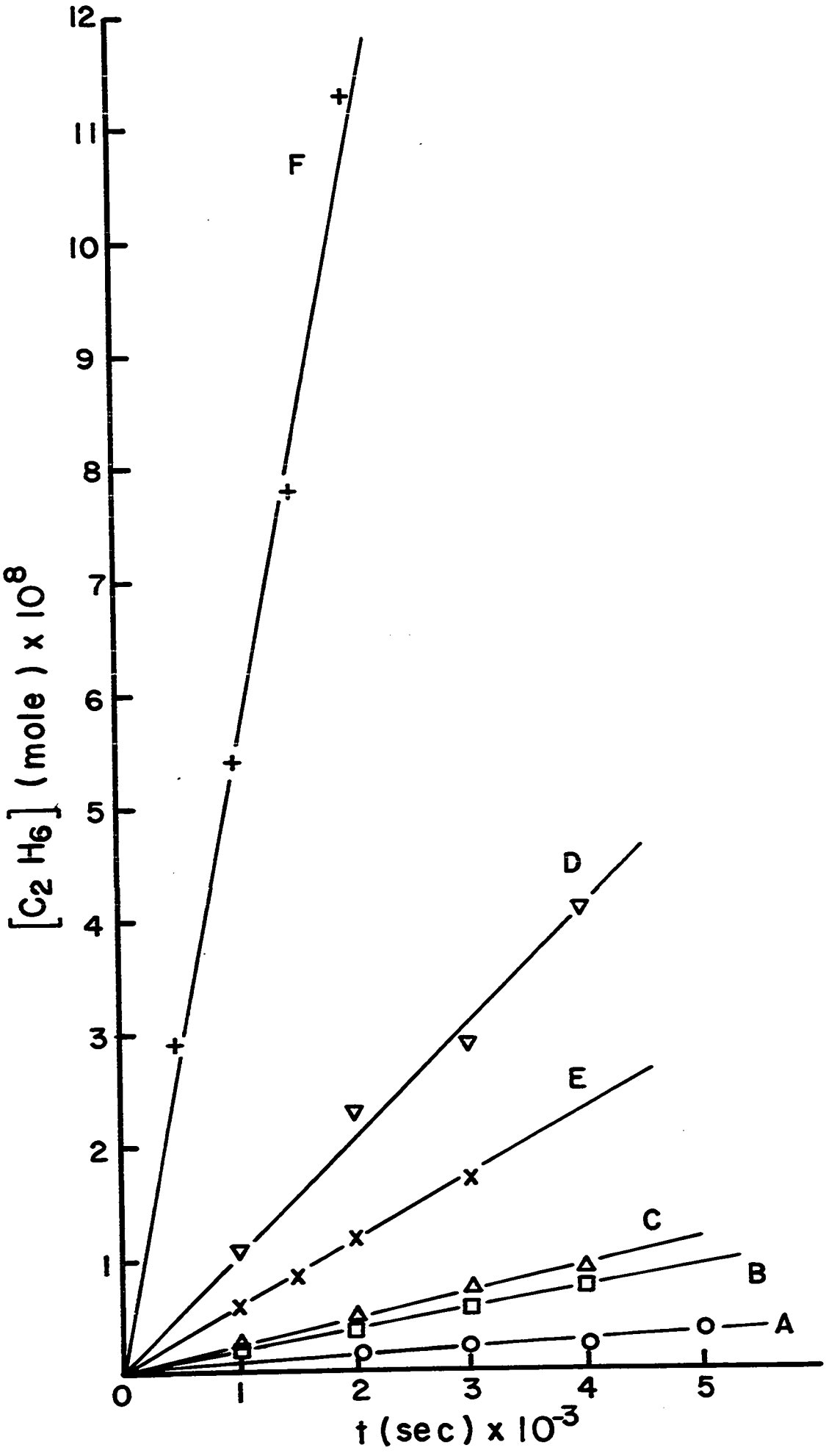
12
11
10
9
8
7
6
5
4
3
2
1
0
1
2
3
4
5
F
D
E
C
B
A
[C2 H6] (mole) x 10^8
t (sec) x 10^-3

FIGURE 24

Order plots for ethane production at five different temperatures

A	252°C
B	276°C
C	301°C
D	325°C
E	350°C

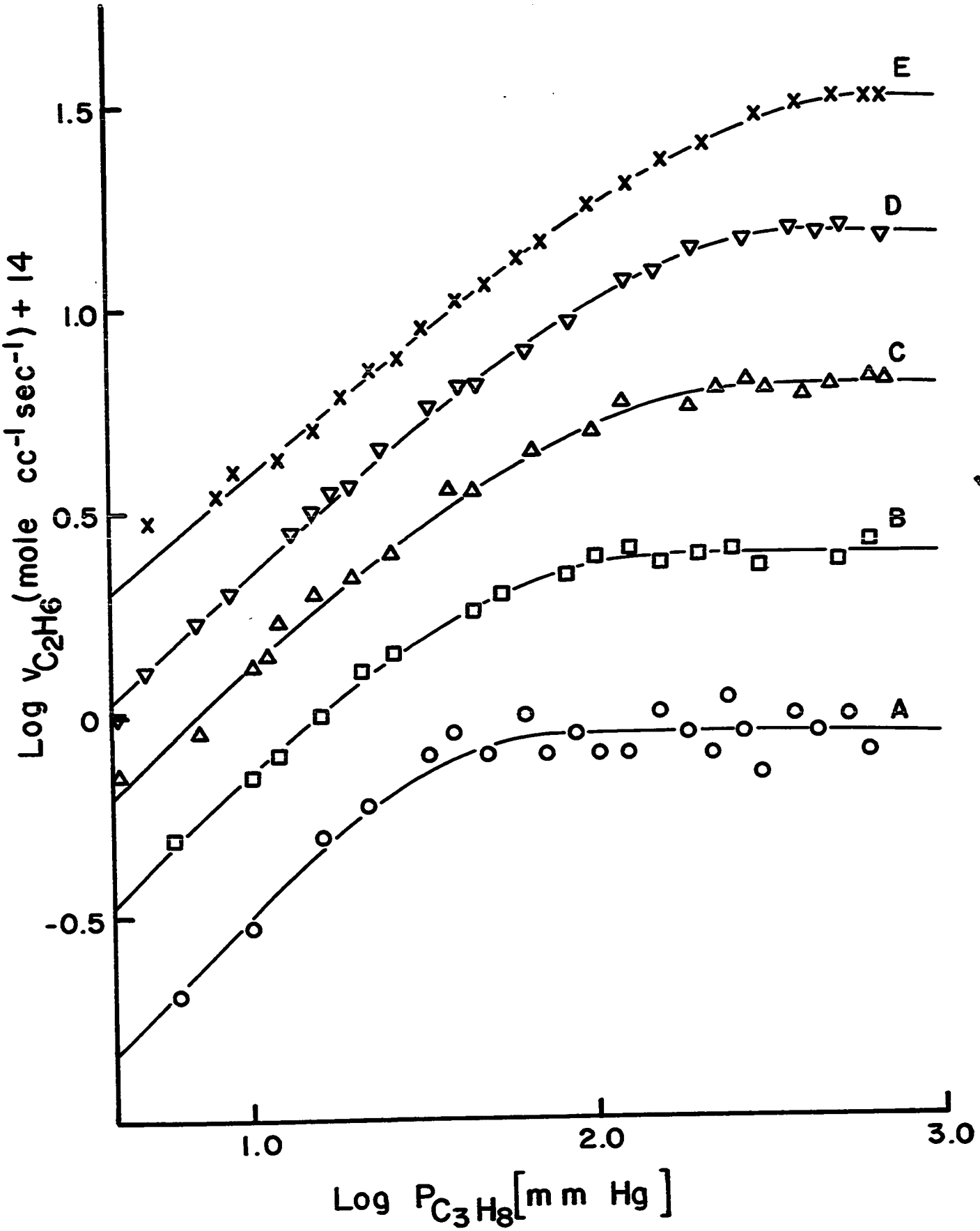
E
D
C
B
A
1.5
1.0
0.5
0
-0.5
1.0
2.0
3.0
Log $v_{C_2H_6}$(mole cc^{-1} sec^{-1}) + 14
Log $P_{C_3H_8}$[mm Hg]

The rates of ethane production as a function of the pressure of propane at five different temperatures are listed in Table 5. The values are obtained from the diagrams in Figure 7. The rate of ethane production is dependent on temperature and increases with increasing temperature.

The plot of the logarithm of the rate of ethane production against reciprocal temperature is shown in Figure 25 for a propane pressure of 700 mm Hg. From the plot an activation energy of 24.0 kcal $mole^{-1}$ was obtained for the ethane production at 700 mm Hg propane pressure. Similarly, the activation energies for the ethane production at other propane pressures were obtained. The values obtained are listed in Table 5 in column 7 and are plotted in Figure 26. The activation energy increases from an extrapolated value of 15 kcal $mole^{-1}$ at zero propane pressure to a constant value of 24.0 kcal $mole^{-1}$ at high pressures of propane. The difference amounts to 9 kcal $mole^{-1}$. Actually, at low propane pressures up to about 30 mm Hg the activation energy of ethane production does not change with propane pressure and attains a constant value of about 16 kcal $mole^{-1}$. The mechanism of the ethane production will be discussed in more detail in Chapter 4.

3.6 Production of 2,3-Dimethylbutane

Typical 2,3-DMB yield-time plots at different temperatures and propane pressures are shown in Figure 27. The yields are found to be a linear function of time, which indicates that primary initial yields were measured. The initial rates were obtained from the slopes of the straight lines or by division of the yields by reaction time, average values being taken.

TABLE 5

Rates of ethane production as a function of temperature and propane pressure *

T[°C]	252	276	301	325	350	E_a
$P_{C_3H_8}$[mm Hg]	$v_{C_2H_6}$	$v_{C_2H_6}$	$v_{C_2H_6}$	$v_{C_2H_6}$	$v_{C_2H_6}$	kcal/mole
10	0.35	0.70	1.40	2.40	4.00	16.2
20	0.60	1.20	2.30	3.85	6.50	16.0
30	0.80	1.50	3.00	5.10	8.50	16.0
40	0.85	1.70	3.50	6.10	10.3	16.5
60	0.90	2.05	4.35	7.65	13.4	17.5
80	0.90	2.30	4.90	8.95	16.0	19.5
100	0.90	2.40	5.40	10.1	18.2	20.1
150	0.90	2.50	6.10	12.4	22.5	21.8
200	0.90	2.50	6.50	14.0	26.0	22.9
250	0.90	2.50	6.60	14.9	28.7	23.4
300	0.90	2.50	6.60	15.3	30.5	23.7
350	0.90	2.50	6.60	15.5	31.7	23.9
400	0.90	2.50	6.60	15.5	32.5	23.9
450	0.90	2.50	6.60	15.5	33.1	24.0
500	0.90	2.50	6.60	15.5	33.5	24.0
550	0.90	2.50	6.60	15.5	33.8	24.0
600	0.90	2.50	6.60	15.5	34.0	24.0
650	0.90	2.50	6.60	15.5	34.0	24.0
700	0.90	2.50	6.60	15.5	34.0	24.0

* All rates are quoted in mole cc^{-1} sec^{-1} x 10^{14}

FIGURE 25

Plot of the logarithm of the rate of ethane production at a propane pressure of 700 mm Hg, against reciprocal temperature.

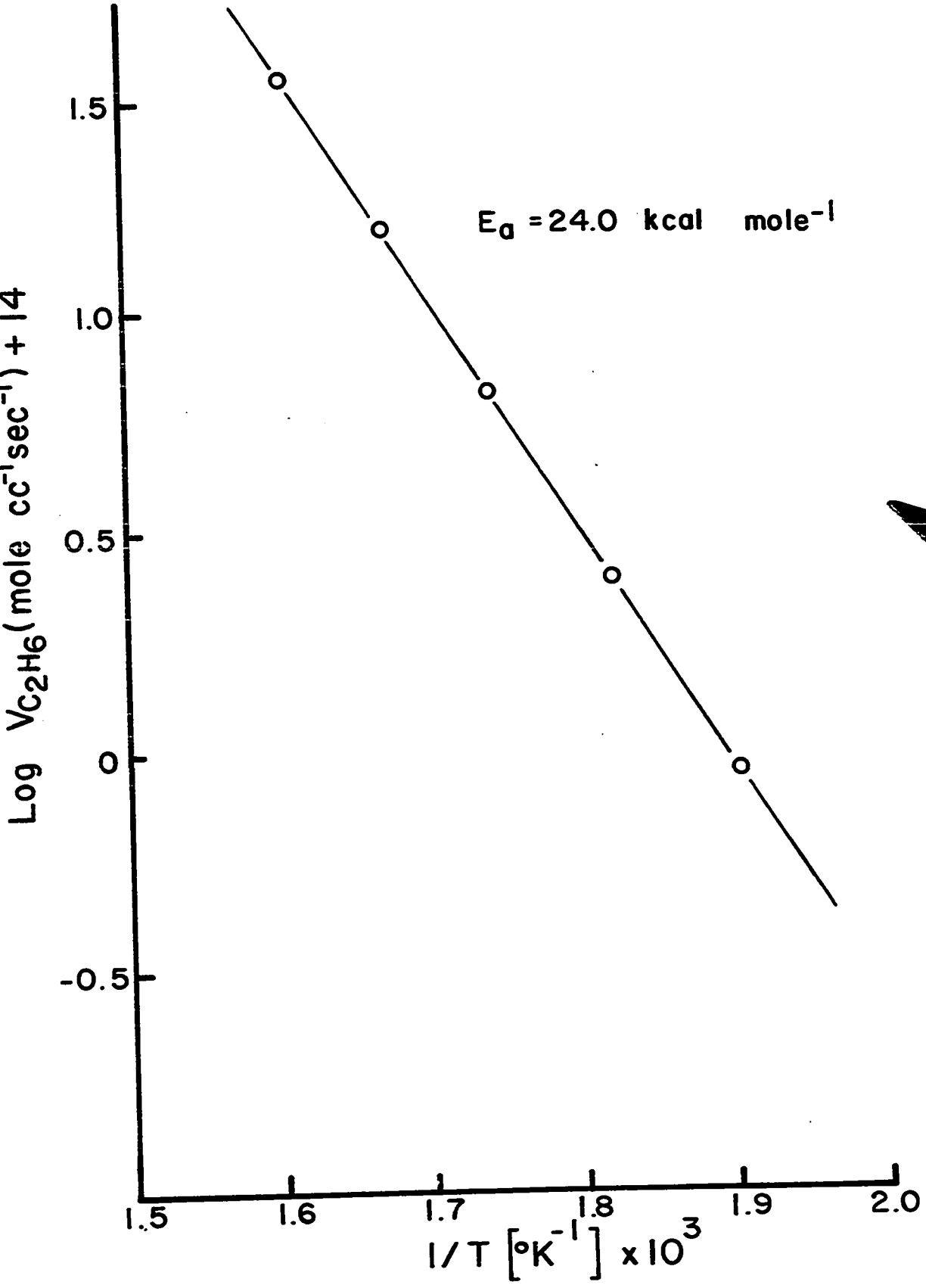
E_a = 24.0 kcal mole^{-1}
Log $V_{C_2H_6}$(mole cc^{-1}sec^{-1}) + 14
1.5
1.0
0.5
0
-0.5
1.5
1.6
1.7
1.8
1.9
2.0
1/T [°K^{-1}] x10^3

FIGURE 26

Plot of the energy of activation for ethane production against the pressure of propane

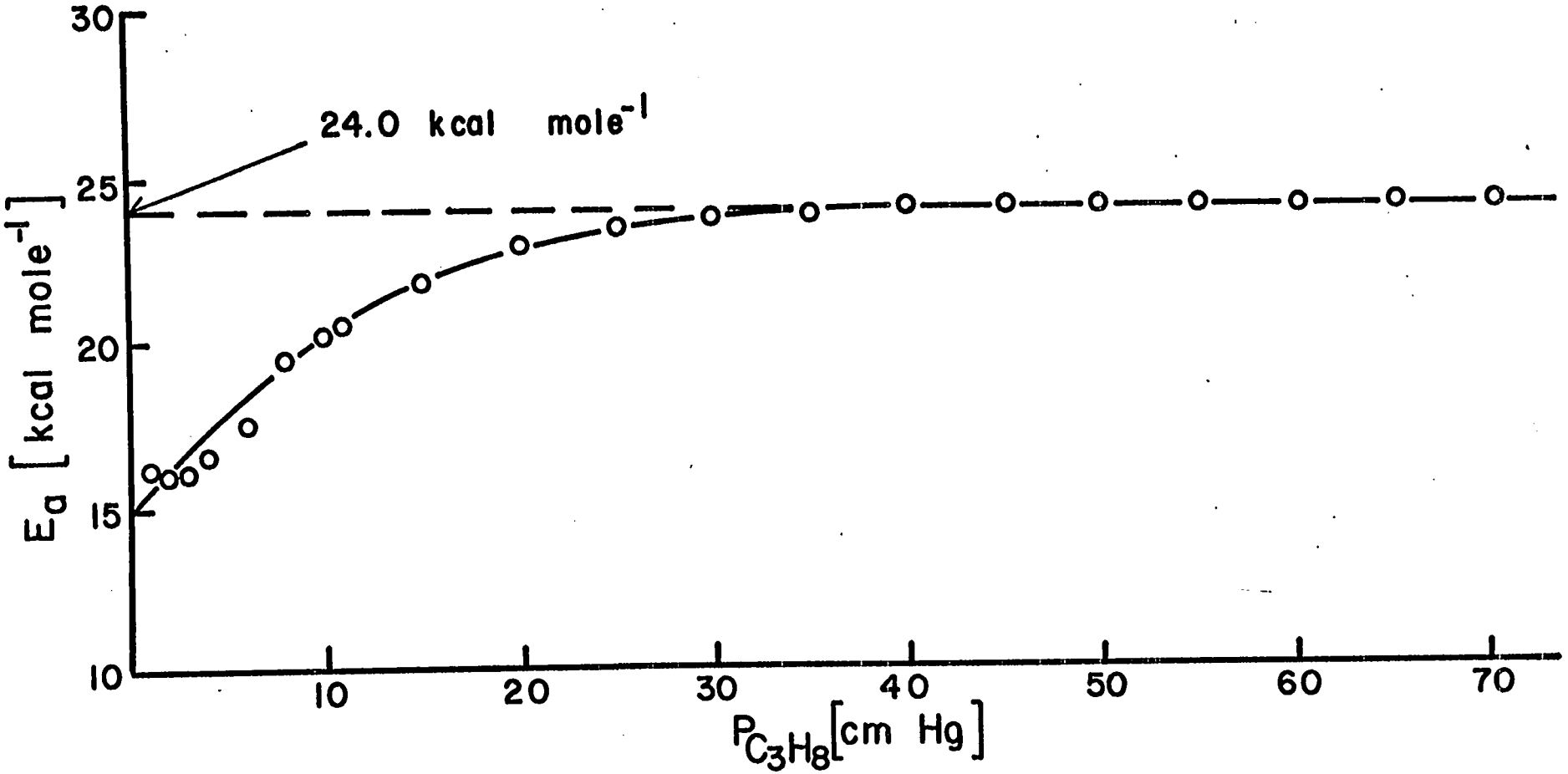
30
25
20
15
10
24.0 kcal mole^{-1}
E_a [kcal mole^{-1}]
10
20
30
40
50
60
70
$P_{C_3H_8}$[cm Hg]

FIGURE 27

Typical 2, 3-dimethylbutane yield-time plots at different temperatures and propane pressures

A	252°C and 10mm Hg
B	252°C and 382 mm Hg
C	301°C and 11 mm Hg
D	301°C and 394 mm Hg
E	350°C and 8 mm Hg
F	350°C and 386 mm Hg

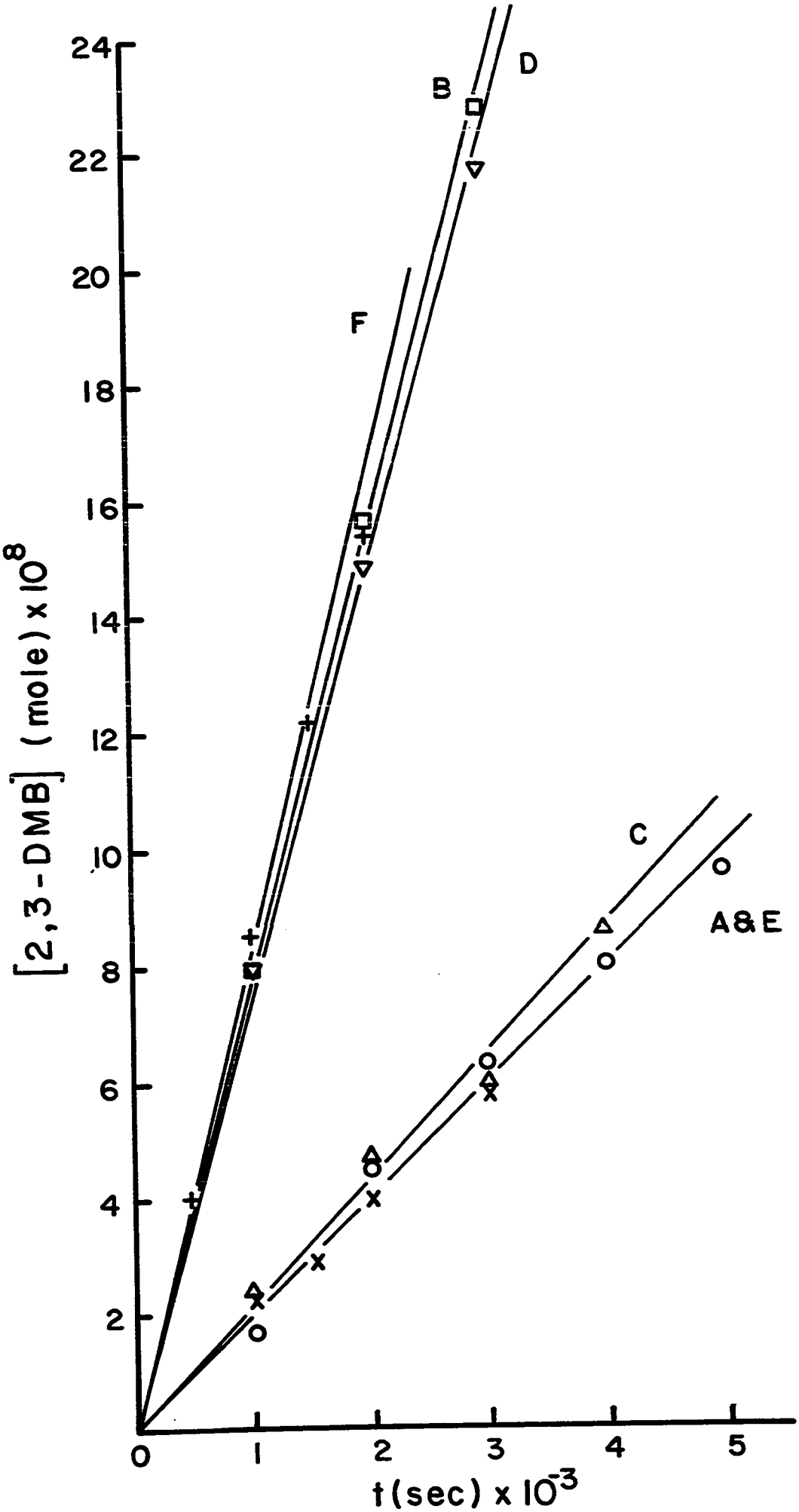
24
22
20
18
16
14
12
10
8
6
4
2
0
1
2
3
4
5
[2,3-DMB] (mole) x 10^8
t(sec) x 10^-3
B
D
F
C
A&E

A double logarithmic plot of the initial rates of 2,3-DMB production against pressure of propane is shown in Figure 28. The order with respect to propane changes continuously from 0.5 at about 10 to 50 mm Hg pressure to zero at high pressures of propane. It should be pointed out that the order of 2,3-DMB production with respect to propane changes considerably at low pressures of propane, up to 5 mm Hg (see Figure 8), and it may be expected that the order of 2,3-DMB production with respect to propane at low propane pressures is considerably higher than 0.5.

The rates of 2,3-DMB production as a function of pressure of propane are listed in Table 6. The values are obtained from the diagrams in Figure 8. Within the experimental error the rate of 2,3-DMB production was found to be independent of temperature in the temperature interval from 250°C to 350°C. Consequently, the activation energy for 2,3-DMB production is zero. A more detailed discussion of the mechanism of 2,3-DMB production will be given later in Chapter 4.

3.7 Production of 2-Methylpentane

Typical 2-MP yield-time plots at different temperatures and propane pressures are shown in Figure 29. The yields are found to be a linear function of time, which indicates that primary initial yields were measured. The initial rates were obtained from the slopes of the straight lines or by dividing the yields by reaction times and taking the average values.

A double logarithmic plot of the initial rates of 2-MP production against the pressure of propane is shown in Figure 30. For clarity the rates are given at only three different temperatures. The order with respect to propane changes continuously from 0.5 at about 10 to 50 mm Hg pressure to zero at high pressures of propane.

TABLE 6

Rates of 2, 3-dimethylbutane production as a function of propane pressure*

$P_{C_3H_8}$ [mm Hg]	10	20	30	40	60	80	100	150	200	250	300
$v_{2,3\text{-DMB}}$	1.10	1.73	2.15	2.50	3.10	3.58	3.97	4.48	4.50	4.50	4.50

* All rates are quoted in mole cc^{-1} sec^{-1} x 10^{13}. The rate of 2, 3-DMB production does not depend on temperature.

FIGURE 28

Order plots for 2, 3-dimethylbutane production at five different temperatures. There is one curve for all temperatures.

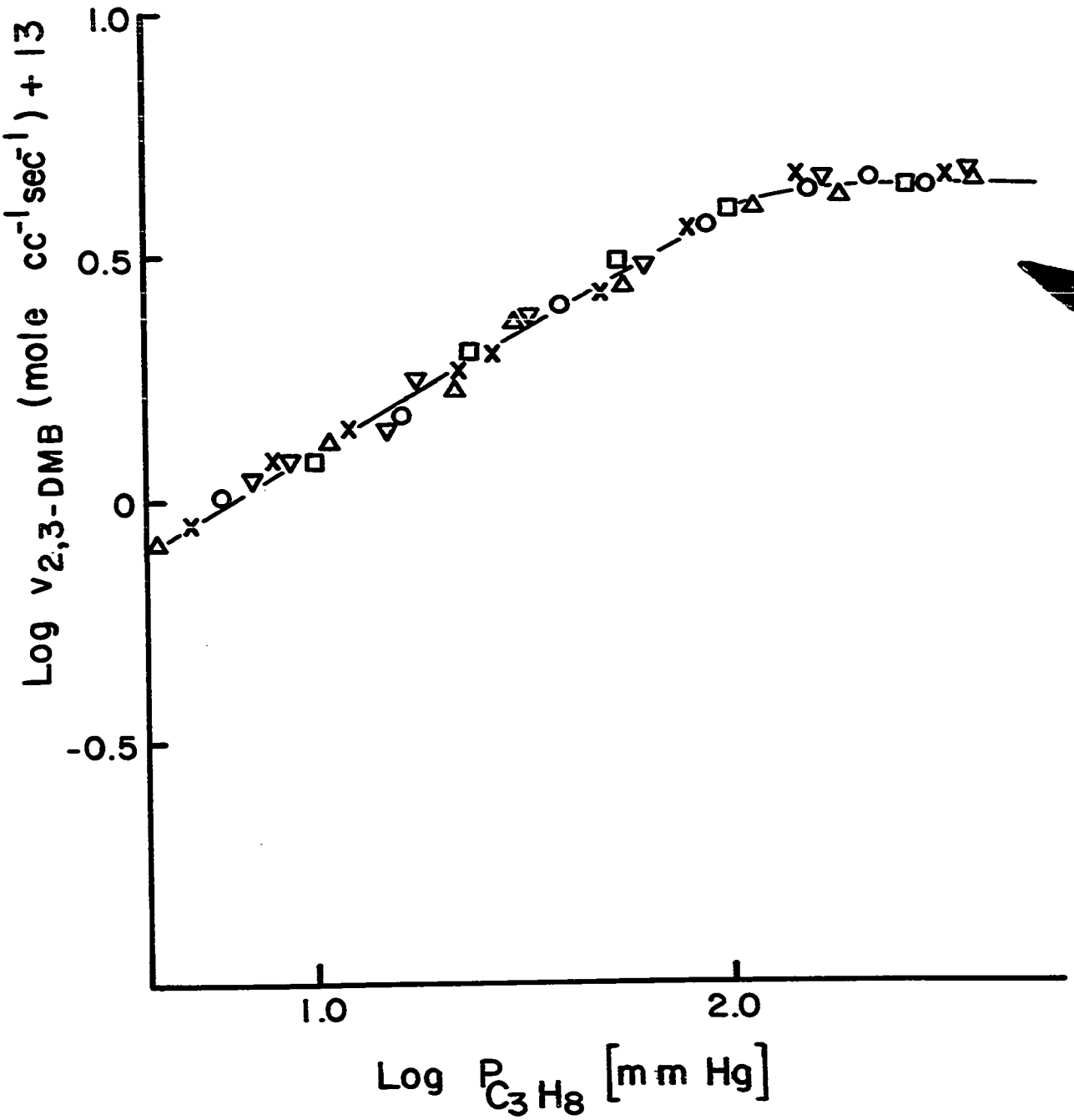
1.0
0.5
0
-0.5
Log $v_{2,3\text{-DMB}}$ (mole $cc^{-1}sec^{-1}$) + 13
1.0
2.0
Log $P_{C_3H_8}$ [mm Hg]

FIGURE 29

Typical 2-methylpentane yield-time plots at different temperatures and propane pressures

A	252°C and 10 mm Hg
B	252°C and 382 mm Hg
C	301°C and 11 mm Hg
D	301°C and 394 mm Hg
E	350°C and 8 mm Hg
F	350°C and 386 mm Hg

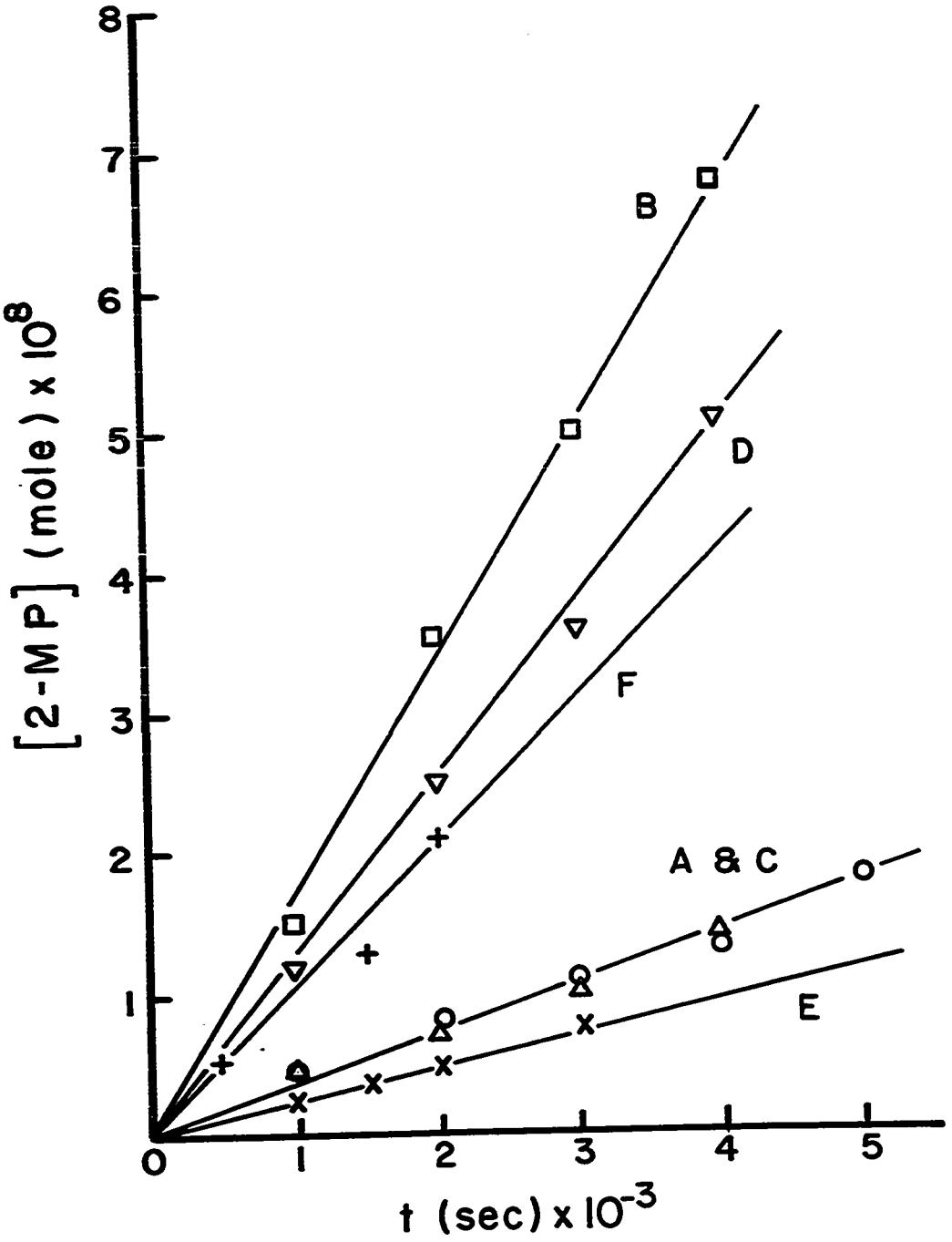
[2-MP] (mole) x 10^8
t (sec) x 10^-3
0
1
2
3
4
5
6
7
8
B
D
F
A & C
E

FIGURE 30

Order plots for 2-methylpentane production at three different temperatures

A 252°C

B 276°C

D 325°C

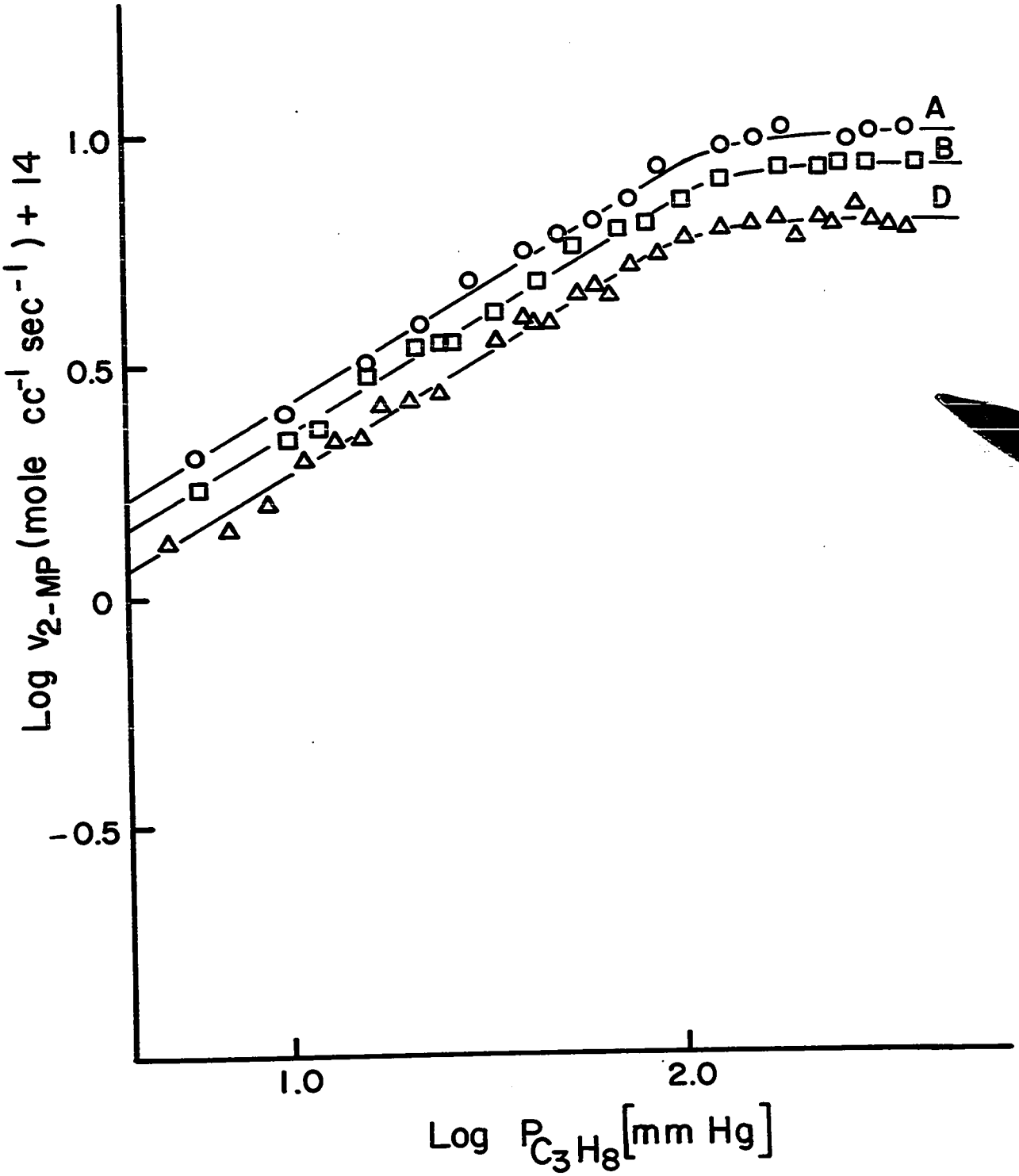
1.0
0.5
0
-0.5
Log $v_{2\text{-MP}}$ (mole cc^{-1} sec^{-1}) + 14
A
B
D
1.0
2.0
Log $P_{C_3H_8}$ [mm Hg]

Again, it should be pointed out that the order of 2-MP production with respect to propane changes considerably at low pressures of propane up to 5 mm Hg (see Figure 9), and it may be expected that the order of 2-MP production with respect to propane at low propane pressures is considerably higher than 0.5.

The rates of 2-MP production as a function of the pressure of propane at five different temperatures are listed in Table 7. The values are obtained from the diagrams in Figure 9.

The rate of 2-MP production is dependent on temperature and decreases with increasing temperature. A more detailed discussion of the mechanism of 2-MP productinn will be given later in Chapter 4. The plot of the logarithm of the rate of 2-MP production against reciprocal temperature is shown in Figure 31 for a propane pressure of 300 mm Hg. From the plot an apparent activation energy of -3.4 kcal $mole^{-1}$ was obtained for the 2-MP production at 300 mm Hg propane pressure. In the same way the activation energies for the 2-MP production at other propane pressures were obtained. The values obtained are listed in column 7 of Table 7 and are plotted in Figure 32.

3.8 Production of n-Hexane

Typical n-hexane yield-time plots at different temperatures and propane pressures are shown in Figure 33. The yields are found to be a linear function of time, which indicates that primary initial yields were measured. The initial rates were obtained from the slopes of the straight lines or by division of the yields by reaction times and taking the average values.

TABLE 7

Rates of 2-methylpentane production as a function of temperature and propane pressure *

T[°C]	252	276	301	325	350	E_a
$P_{C_3H_8}$[mm Hg]	$v_{2\text{-MP}}$	$v_{2\text{-MP}}$	$v_{2\text{-MP}}$	$v_{2\text{-MP}}$	$v_{2\text{-MP}}$	kcal/mole
10	2.5	2.1	2.0	1.8	1.7	-2.5
20	3.7	3.3	3.0	2.7	2.6	-2.4
30	4.7	4.1	3.8	3.3	3.1	-2.6
40	5.5	4.7	4.4	3.9	3.6	-2.6
60	6.8	5.8	5.3	4.7	4.3	-2.8
80	7.8	6.7	6.0	5.3	4.8	-3.0
100	8.6	7.4	6.5	5.7	5.2	-3.0
150	9.7	8.3	7.2	6.3	5.8	-3.5
200	10.0	8.5	7.5	6.5	6.0	-3.4
250	10.0	8.5	7.5	6.5	6.0	-3.4
300	10.0	8.5	7.5	6.5	6.0	-3.4

* All rates are quoted in mole cc^{-1} sec^{-1} x 10^{14}

FIGURE 31

Plot of the logarithm of the rate of 2-methylpentane production at propane pressure of 300 mm Hg, against reciprocal temperature

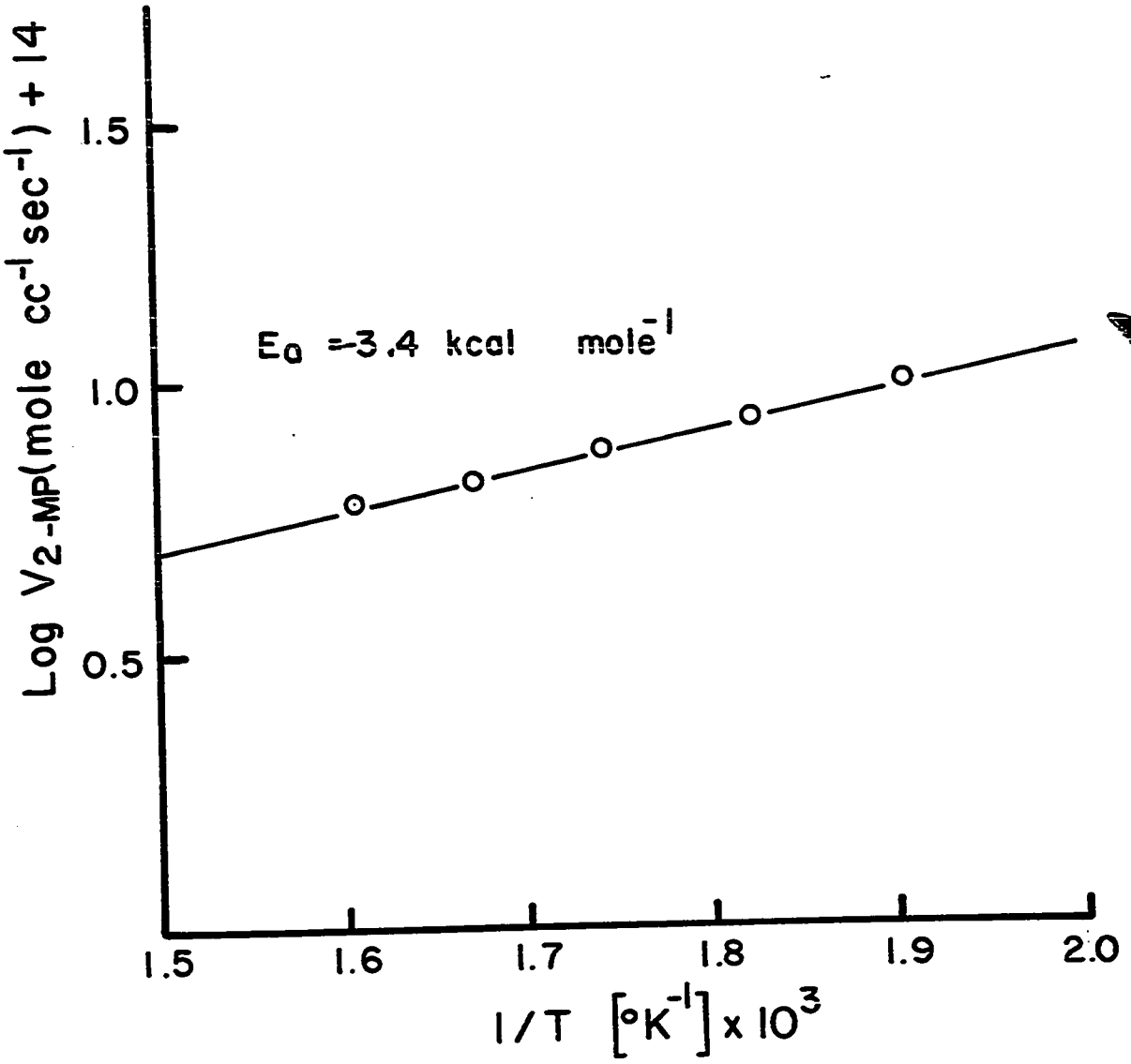
Log $V_{2\text{-MP}}$(mole cc^{-1} sec^{-1}) + 14
1.5
1.0
0.5
E_a = -3.4 kcal mole^{-1}
1.5
1.6
1.7
1.8
1.9
2.0
1/T [°K^{-1}] x 10^3

FIGURE 32

Plot of the apparent energy of activation for the 2-methylpentane production against the pressure of propane

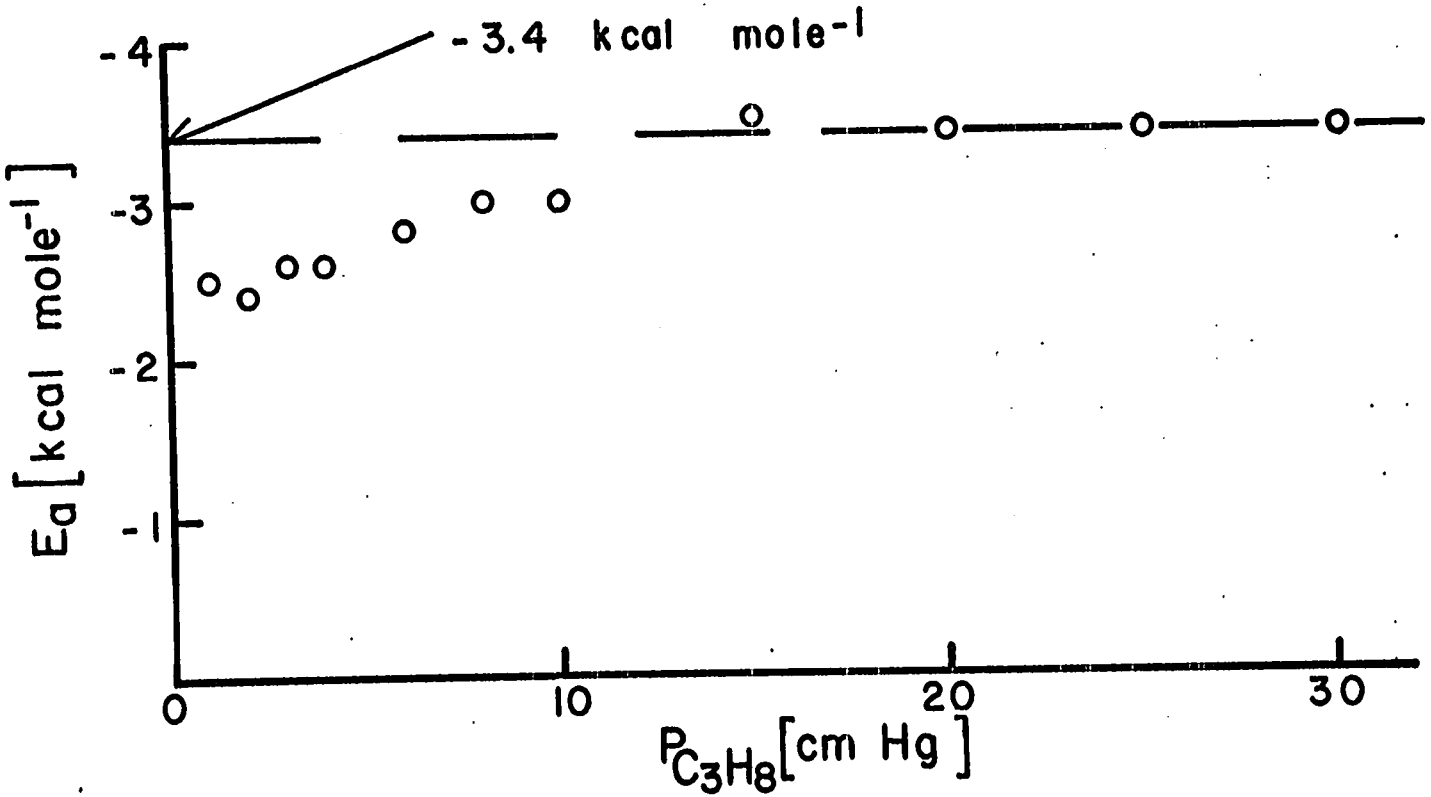
-3.4 kcal mole-1
-4
-3
-2
-1
Ea [kcal mole-1]
0
10
20
30
PC3H8 [cm Hg]

FIGURE 33

Typical n-hexane yield-time plots at different temperatures and propane pressures

A	252°C and 16 mm Hg
B	252°C and 300 mm Hg
C	301°C and 18 mm Hg
D	301°C and 301 mm Hg
E	350°C and 22 mm Hg
F	350°C and 299 mm Hg

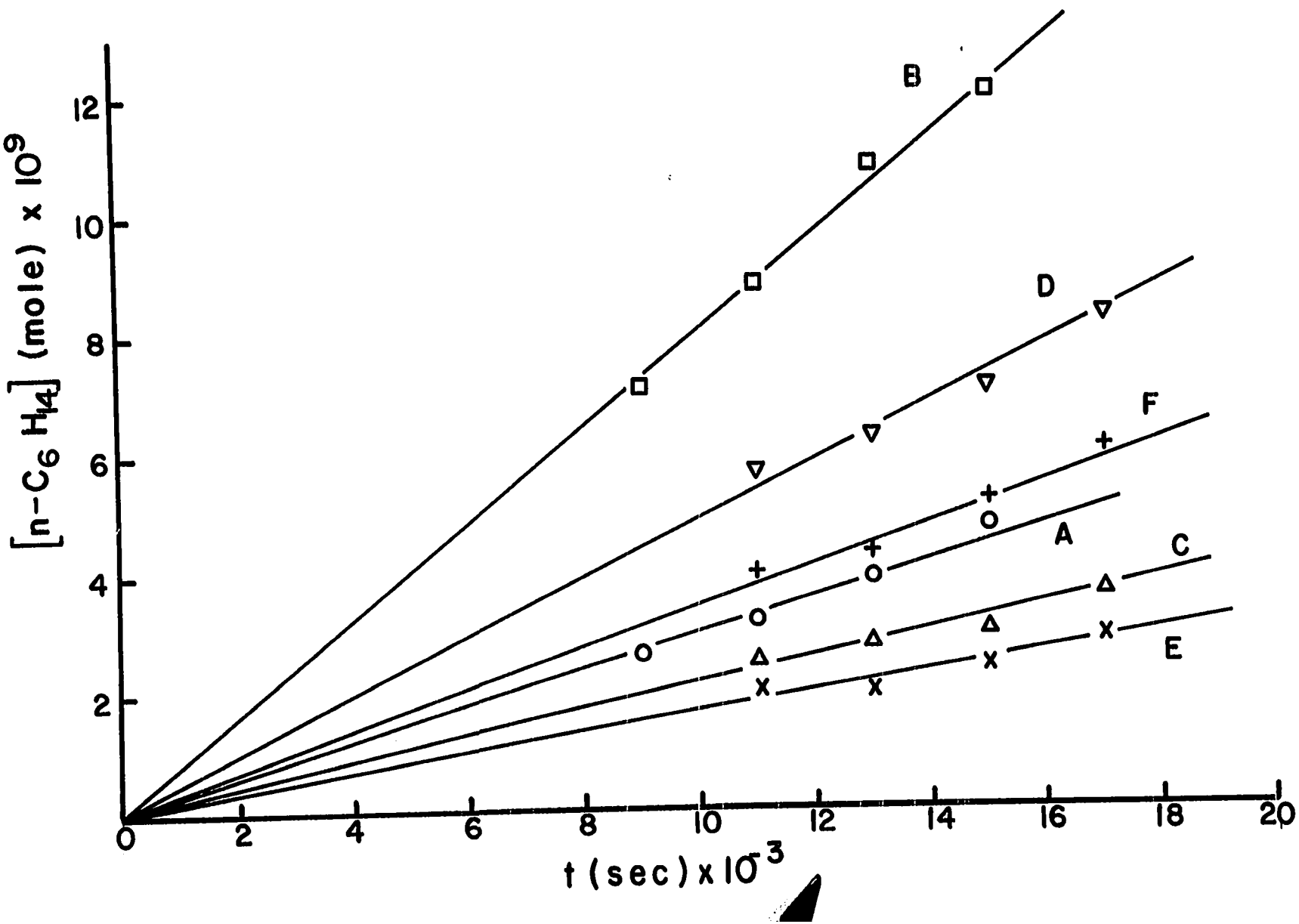
[n-C6 H14] (mole) x 10^9
12
10
8
6
4
2
0
2
4
6
8
10
12
14
16
18
20
t (sec) x 10^3
B
D
F
A
C
E

A double logarithmic plot of the initial rates of n-hexane production against the pressure of propane is shown in Figure 34. The order with respect to propane changes continuously from 0.5 at about 10 to 50 mm Hg pressure to zero at high pressures of propane. As with 2, 3-DMB and 2-MP the order of n-hexane production with respect to propane changes considerably at low pressures of propane up to 5 mm Hg (see Figure 10) and it may be expected that the order of n-hexane production with respect to propane at low propane pressures is considerably higher than 0.5.

The rates of n-hexane production as a function of pressure of propane at five different temperatures are listed in Table 8. The values are obtained from the diagrams in Figure 10.

The rate of n-hexane production is dependent on temperature and decreases with increasing temperature. A more detailed discussion of the mechanism of n-hexane production will be given later in Chapter 4. The plot of the logarithm of the rate of n-hexane production against reciprocal temperature is shown in Figure 35 for a propane pressure of 300 mm Hg. From the plot an apparent activation energy of -6.0 kcal $mole^{-1}$ was obtained for the n-hexane production at 300 mm Hg propane pressure. Similarly, the activation energies for the n-hexane production at other propane pressures were obtained. The values obtained are listed in Table 8, column 7, and are plotted in Figure 36.

TABLE 8

Rates of n-hexane production as a function of temperature and propane pressure*

T[°C]	252	276	301	325	350	E_a
$P_{C_3H_8}$[mm Hg]	$v_{n\text{-}C_6H_{14}}$	$v_{n\text{-}C_6H_{14}}$	$v_{n\text{-}C_6H_{14}}$	$v_{n\text{-}C_6H_{14}}$	$v_{n\text{-}C_6H_{14}}$	kcal/mole
10	1.25	0.95	0.75	0.60	0.55	-5.8
20	1.88	1.40	1.20	1.00	0.82	-5.5
30	2.30	1.82	1.55	1.26	1.02	-5.7
40	2.72	2.17	1.83	1.51	1.25	-5.7
60	3.35	2.71	2.29	1.90	1.60	-5.3
80	3.85	3.13	2.60	2.18	1.81	-5.3
100	4.22	3.42	2.80	2.35	1.95	-5.4
150	4.90	3.85	3.00	2.50	2.00	-6.0
200	5.00	4.00	3.00	2.50	2.00	-6.0
250	5.00	4.00	3.00	2.50	2.00	-6.0
300	5.00	4.00	3.00	2.50	2.00	-6.0

* All rates are quoted in mole cc^{-1} sec^{-1} x 10^{15}

FIGURE 34

Order plots for n-hexane production at five different temperatures

A	252°C
B	276°C
C	301°C
D	325°C
E	350°C

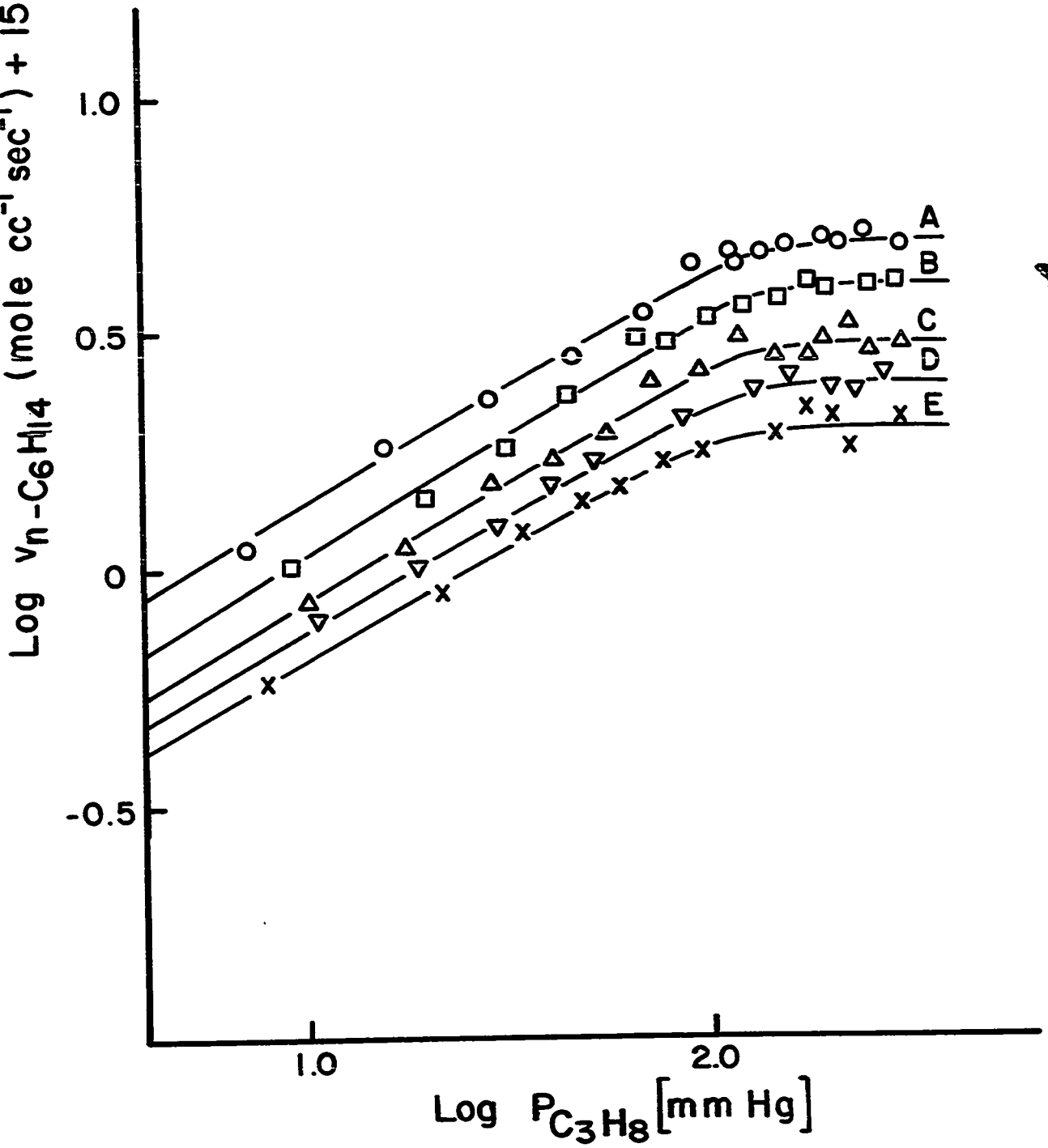
Log $v_{n-C_6H_{14}}$ (mole cc^{-1} sec^{-1}) + 15
1.0
0.5
0
-0.5
1.0
2.0
Log $P_{C_3H_8}$ [mm Hg]
A
B
C
D
E

FIGURE 35

Plot of the logarithm of the rate of n-hexane production at a propane pressure of 300 mm Hg, against reciprocal temperature

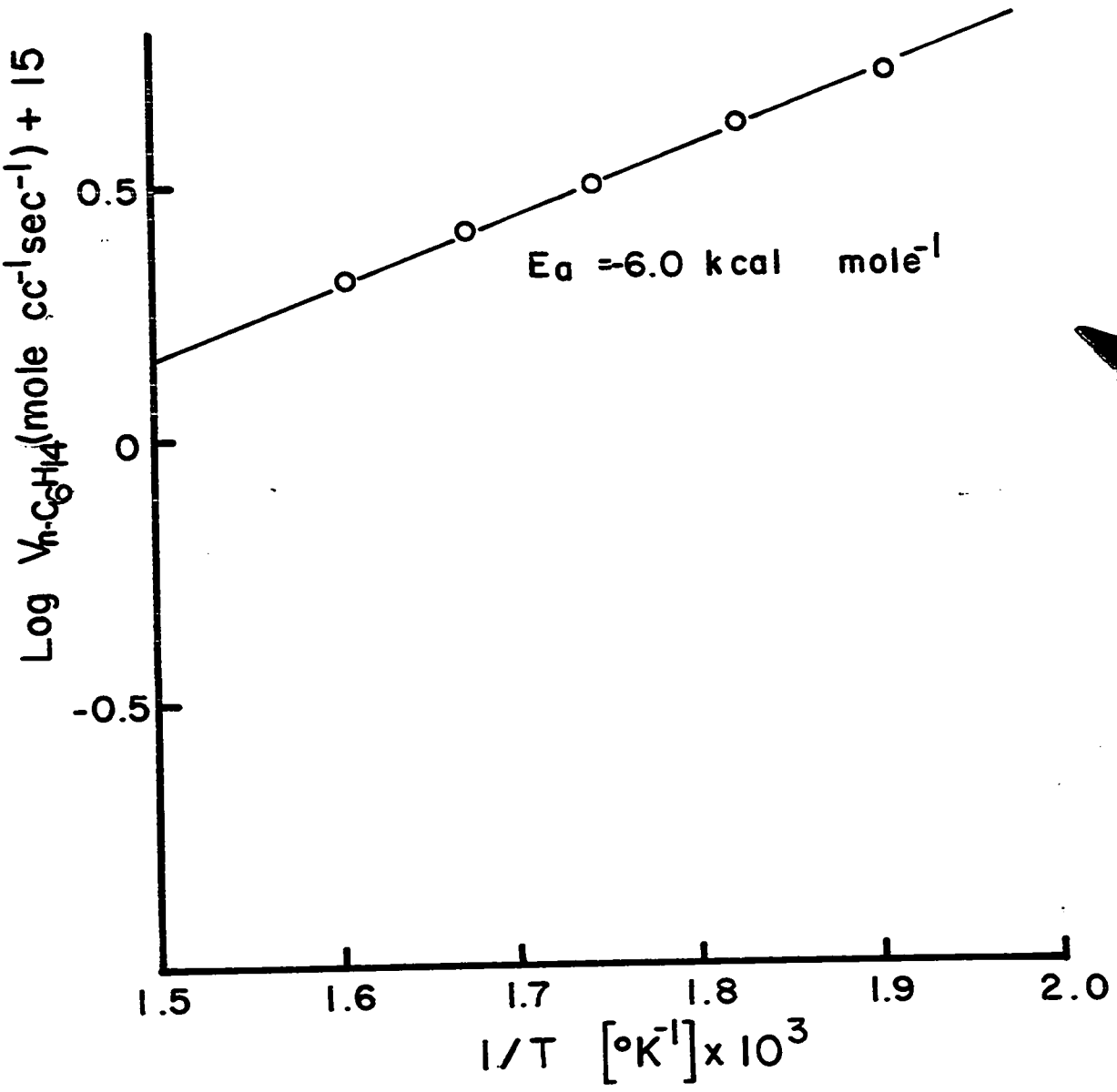
Log $V_{n\text{-}C_6H_{14}}$(mole $cc^{-1}sec^{-1}$) + 15
0.5
0
-0.5
Ea =-6.0 kcal mole^{-1}
1.5
1.6
1.7
1.8
1.9
2.0
1/T [$°K^{-1}$] x 10^3

FIGURE 36

Plot of the apparent energy of activation for n-hexane production against the pressure of propane

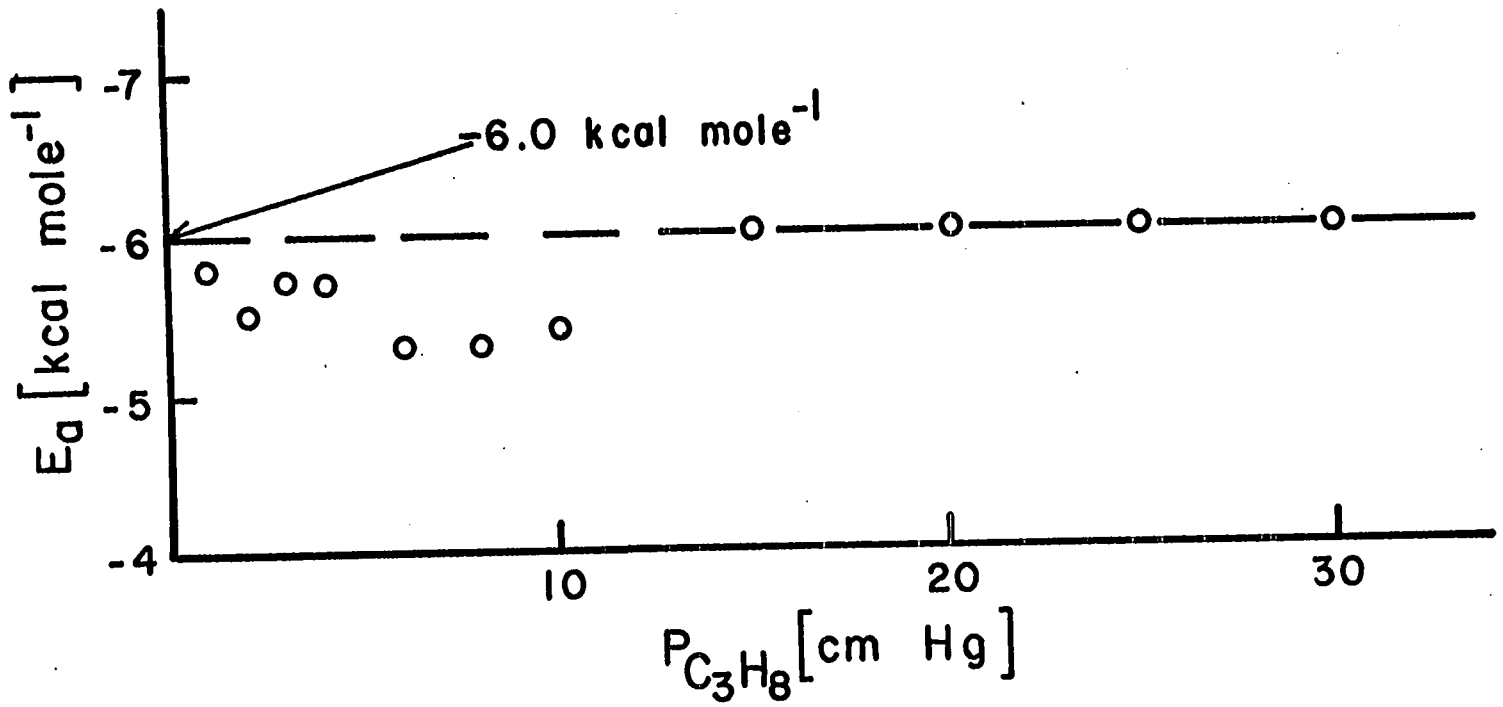
-7
-6
-5
-4
E_a [kcal mole^{-1}]
-6.0 kcal mole^{-1}
10
20
30
$P_{C_3H_8}$ [cm Hg]

3.9 Cross-combination of Propyl Radicals

The n-propyl and i-propyl radicals can combine and cross-combine giving rise to three isomeric hexanes. The ratios $v_{2\text{-MP}}/(v_{2,3\text{-DMB}} \times v_{n\text{-}C_6H_{14}})^{1/2}$ are listed in Table 9 at different temperatures and pressures of propane. In average the ratios are between 1.9 and 2.1. According to the simple collision theory of chemical kinetics this ratio should be 2 for reactions with no activation energy. This matter will be discussed further in Chapter 4.

3.10 Inert Gas Effect

The effect of inert gas on the rates of products formation was briefly examined at 301°C. Various amounts of carbon dioxide were added to propane at pressure of 15 mm Hg. The results are summarized in Table 10.

In one experiment helium was added instead of carbon dioxide. The effect was similar to that of carbon dioxide. The data obtained are plotted in Figure 37.

The rates of formation of all products decrease strongly with increasing pressure of added inert gas. At a carbon dioxide pressure of 90 mm Hg the rates fall off to approximately 20% of their values at zero pressure of inert gas.

TABLE 9

Cross-combination of propyl radicals *

T[°C]	252	276	301	325	350
$P_{C_3H_8}$[mm Hg]	$v_{ab}/(v_{aa}xv_{bb})^{1/2}$	$v_{ab}/(v_{aa}xv_{bb})^{1/2}$	$v_{ab}/(v_{aa}xv_{bb})^{1/2}$	$v_{ab}/(v_{aa}xv_{bb})^{1/2}$	$v_{ab}/(v_{aa}xv_{bb})^{1/2}$
10	2.1	2.1	2.1	2.2	2.2
20	2.1	2.1	2.1	2.1	2.2
30	2.1	2.0	2.1	2.0	2.1
40	2.1	2.0	2.1	2.0	2.0
60	2.1	2.0	2.0	1.9	1.9
80	2.1	2.0	2.0	1.9	1.9
100	2.1	2.0	2.0	1.9	1.9
150	2.1	2.0	2.0	1.9	1.9
200	2.1	2.0	2.0	1.9	2.0
250	2.1	2.0	2.0	1.9	2.0
300	2.1	2.0	2.0	1.9	2.0

* $v_{aa} = v_{2,3\text{-DMB}}$. $v_{bb} = v_{n\text{-}C_6H_{14}}$. $v_{ab} = v_{2\text{-MP}}$.

TABLE 10

The effect of CO_2 on the rates of formation of products

$T = 301^{\circ}C$, $P_{C_3H_8} = 15$ mm Hg, Hg-trap temperature = $-32^{\circ}C$

P_{CO_2} [mm Hg]	v(mole $cc^{-1}sec^{-1}$)x 10^{14}					
	H_2	CH_4	C_2H_4	C_2H_6	2,3-DMB	2-MP
0	26.5	17.0	15.5	1.9	14.8	2.5
5	22.0	10.0	9.0	1.3	8.7	2.2
9	18.6	8.0	7.5	0.8	7.0	2.0
16	15.0	6.2	5.6	0.5	5.2	1.5
28	10.0	4.6	4.5	0.4	3.5	1.2
45	7.0	4.0	4.0	0.4	3.5	0.9
65	6.0	3.9	3.9	0.3	2.9	0.8
90	5.8	4.0	4.0	0.4	2.5	0.8

FIGURE 37

Inert gas effect on the rates of products formation.

$T = 301^{\circ}C$, $P_{C_3H_8} = 15$ mm Hg, Hg-trap temperature = $-32^{\circ}C$

A v_{H_2}

B v_{CH_4}

C $v_{C_2H_4}$

D $v_{2,3\text{-DMB}}$

E $v_{2\text{-MP}}$

F $v_{C_2H_6}$

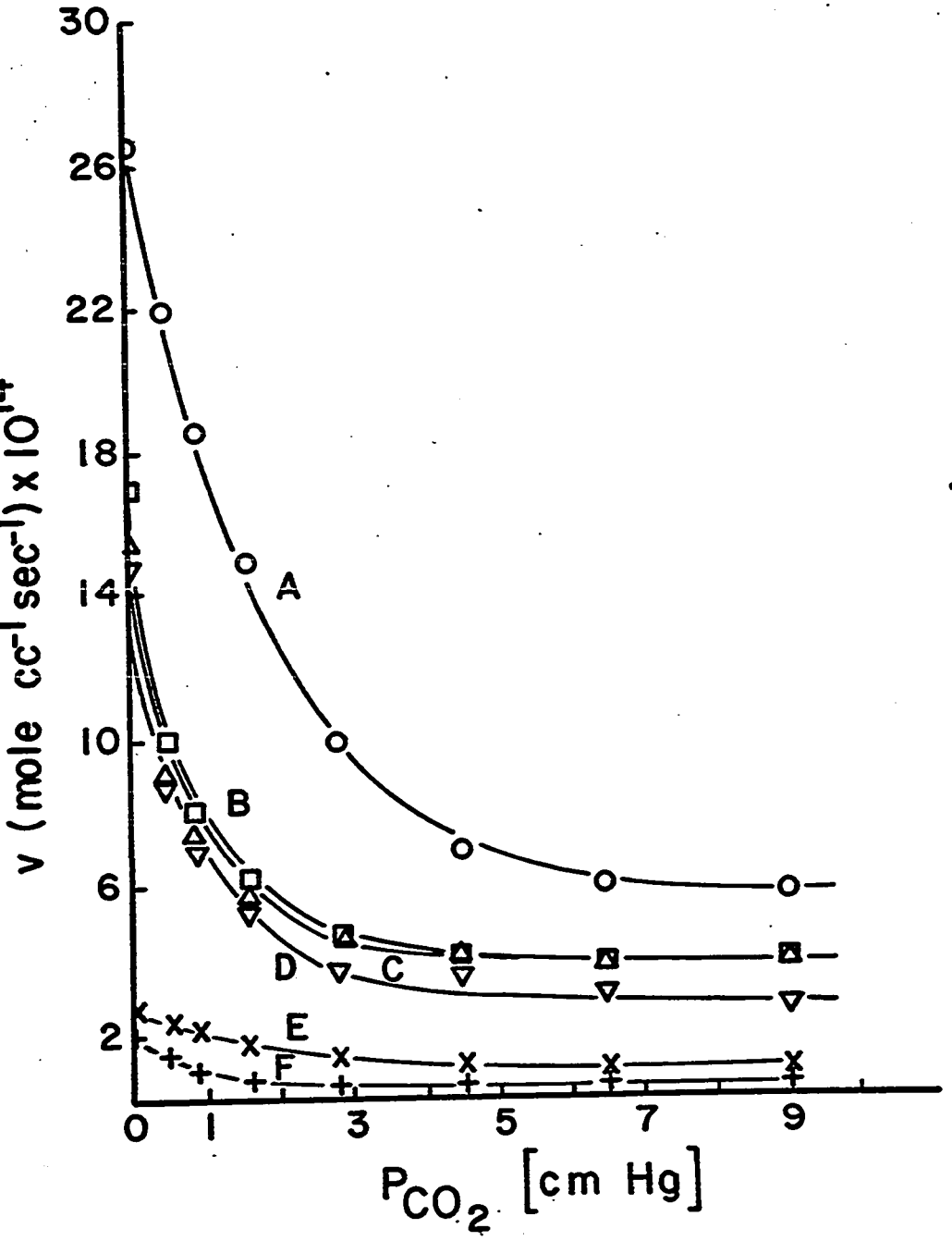
30
26
22
18
14
10
6
2
0
1
3
5
7
9
v (mole cc⁻¹ sec⁻¹) x 10¹⁴
P$_{CO_2}$ [cm Hg]
A
B
C
D
E
F

CHAPTER 4

DISCUSSION

4.1 Kinetics and Mechanism

The object of the present chapter is to consider a mechanism which can account for the primary reactions in the mercury-photosensitized decomposition of propane. A primary reaction is a reaction which occurs with a non-vanishing rate at zero reaction time. Photochemical reactions are initiated by the primary photochemical process, which comprises the series of events beginning with the absorption of a photon by a molecule, and ending either with the disappearance of that molecule or with its conversion to a state such that its reactivity is statistically not greater than that of similar molecules in thermal equilibrium with their surroundings (17).

It is well established that the primary initial act in the mercury-photosensitized decomposition of propane comprises the excitation of mercury atoms by absorption of light, their de-excitation by the quencher propane molecules, and a consequent C-H bond split in propane (1). At low temperatures, below about 300°C, the hydrogen atoms and propyl radicals produced undergo substitutions, combinations and disproportionations. At high temperatures, the decomposition of propyl radicals becomes predominant (10, 27, 28, 34). The subsequent discussion will be based on the following reaction scheme, in which P refers to the primary propyl radical, $CH_3CH_2CH_2$, and S to the secondary propyl radical, CH_3CHCH_3 :

[1]	$Hg + h\nu$	→	Hg^*
[2p]	$Hg^* + C_3H_8$	→	$Hg + H + P$
[2s]	$Hg^* + C_3H_8$	→	$Hg + H + S$
[3p]	$H + C_3H_8$	→	$H_2 + P$
[3s]	$H + C_3H_8$	→	$H_2 + S$
[4]	$2P$	→	$n\text{-}C_6H_{14}$
[5]	$2S$	→	2,3-DMB
[6]	$P + S$	→	2-MP
[7]	$2P$	→	$C_3H_8 + C_3H_6$
[8]	$2S$	→	$C_3H_8 + C_3H_6$
[9]	$P + S$	→	$C_3H_8 + C_3H_6$
[10a]	$H + P$	→	$CH_3 + C_2H_5$
[10b]	$H + S$	→	$CH_3 + C_2H_5$
[11]	$H + C_2H_5$	→	$2CH_3$
[12]	$H + CH_3$	→	CH_4
[13]	$H + C_2H_5$	→	C_2H_6
[14p]	$H + P$	→	C_3H_8
[14s]	$H + S$	→	C_3H_8
[15p]	$CH_3 + C_3H_8$	→	$CH_4 + P$
[15s]	$CH_3 + C_3H_8$	→	$CH_4 + S$
[16p]	$C_2H_5 + C_3H_8$	→	$C_2H_6 + P$
[16s]	$C_2H_5 + C_3H_8$	→	$C_2H_6 + S$
[17]	$CH_3 + P$	→	$n\text{-}C_4H_{10}$
[18]	$CH_3 + S$	→	$i\text{-}C_4H_{10}$
[19]	$2CH_3$	→	C_2H_6
[20a]	P	→	$H + C_3H_6$
[20b]	P	→	$CH_3 + C_2H_4$
[21a]	S	→	$H + C_3H_6$
[21b]	S	→	$CH_3 + C_2H_4$

The mercury-photosensitized decomposition of propane is initiated by reaction [1] which represents the absorption of a photon of wavelength 2537 A by the mercury atom. In this way mercury becomes excited by 112.2 kcal.mole^{-1} and is converted into the 6($^3P_1$) state. The rate of reaction [1] is equal to the intensity of absorbed light, i.e. $v_1 = I_a$. In the present investigation the light intensities were not measured.

Reactions [2] represent the process of quenching of the excited mercury atom to the ground state. The transfer of energy to the propane molecule results in cleavage of the C-H bond. In this way hydrogen atoms and n- or i-propyl radicals are formed. At low temperatures this is the only source of hydrogen. The rate of reaction [2] is equal to ϕI_a where ϕ represents the quantum yield. It is believed that the primary quantum yield of this process is close to unity (29, 32).

The hydrogen atoms produced abstract hydrogen atoms from the parent propane molecules and form hydrogen molecules and n- or i-propyl radicals. This process is represented by reactions [3].

Reactions [4], [5] and [6] are propyl-radical combinations. They yield three isomeric hexanes, the relative amounts of which indicate the ratio between n- and i-propyl radicals.

Reactions [7], [8] and [9] are propyl-radical disproportionations, all of them yielding propane and propene. Neither of these products could be directly measured by the methods of gas chromatography employed in the present investigation, because of the presence of large amounts of propane.

Reactions [10], and [11] are the atomic cracking reactions between hydrogen atoms and alkyl radicals. These reactions were introduced to explain the low-temperature methane and ethane production. Under the conditions of the present investigation, these reactions occur to a small extent.

Reactions [12], [13] and [14] are combinations between hydrogen atoms and alkyl radicals. There is a competition between atomic cracking reactions and these combinations reactions. The importance of reactions [12], [13] and [14] relative to reactions [10] and [11] increases with increasing pressure of propane.

Reactions [15] and [16] are the abstractions of hydrogen atoms from the parent propane molecules by methyl and ethyl radicals, yielding methane and n- or i-propyl radicals and ethane and n- or i-propyl radicals, respectively. These reactions are a logical consequence of reactions [10] and [11].

Reactions [17] and [18] are combinations of methyl and propyl radicals yielding n- and i-butane. These products could not be measured by the methods of gas chromatography employed in the present investigation. However, they seem reasonable and are necessary to account for the total disappearance of methyl radicals.

Reaction [19] is a combination of methyl radicals yielding ethane. Under the conditions of the present investigation it occurs to a very small extent.

Reactions [20] and [21] present the decompositions of n-propyl and i-propyl radicals. At low temperatures, these reactions are negligible. At high temperatures, however, the decomposition of propyl radicals becomes predominant and reactions [20] and [21] play an important role. A more detailed discussion on the decomposition of propyl radicals will be considered later in this chapter.

The Arrhenius parameters for these individual reactions are given in Table 11.

TABLE 11

Kinetic parameters for elementary reactions

Reaction	log k	Reference
$H + C_3H_8 \rightarrow H_2 + C_3H_7$	13.8 - 8.0/2.3 RT	(37)
$H + C_3H_7 \rightarrow CH_3 + C_2H_5$	≈15	(a)
$H + C_3H_7 \rightarrow C_3H_8$		
$H + C_2H_5 \rightarrow 2CH_3$	≈15	(a)
$H + C_2H_5 \rightarrow C_2H_6$		
$H + CH_3 \rightarrow CH_4$	≈15	(a)
$CH_3 + C_3H_8 \rightarrow CH_4 + C_3H_7$	11.9 - 10.3/2.3 RT	(37)
$CH_3 + P \rightarrow n - C_4H_{10}$	13.7	(39)
$CH_3 + S \rightarrow i\text{-}C_4H_{10}$		
$CH_3 + CH_3 \rightarrow C_2H_6$	13.6	(40)
$C_2H_5 + C_3H_8 \rightarrow C_2H_6 + C_3H_7$	11.3 - 10.4/2.3 RT	(41)
$P + P \rightarrow n\text{-}C_6H_{14}$	13.4	(37)
$S + S \rightarrow$ 2,3-DMB	13.4	(42)
$P + S \rightarrow$ 2-MP	13.7	(b)
$P + P \rightarrow C_3H_8 + C_3H_6$	12.6	(43)
$S + S \rightarrow C_3H_8 + C_3H_6$	13.2	(44)
$P + S \rightarrow C_3H_8 + C_3H_6$	13	(c)
$P \rightarrow H + C_3H_6$	14.1 - 37.0/2.3 RT	(45)
$P \rightarrow CH_3 + C_2H_4$	14.4 - 32.6/2.3 RT	(d)
$S \rightarrow H + C_3H_6$	14.3 - 38.7/2.3 RT	(d)
$S \rightarrow CH_3 + C_2H_4$	12.0 - 34.5/2.3 RT	(46)

P = $CH_3\text{-}CH_2\text{-}CH_2$ S = $CH_3\text{-}CH\text{-}CH_3$

All A factors are in cc.mole^{-1}sec^{-1} or sec-1; E in kcal.mole^{-1}.

(a) These values are assumed to be approximately equal to the collision frequency at 500°K. The rate constants of cracking and combination reactions are combined in one.

(b) Calculated from intercombination ratio.

(c) Assumed value.

(d) This work, high-pressure value.

In order to have a better insight into the reaction conditions, it will be useful to assesss the concentrations of reactive species in the reaction cell. This is done for propane pressure of 10 mm Hg and 700 mm Hg at five different temperatures. The estimates are summarized in Table 12.

With increasing concentration of propane the concentrations of propyl radicals also increase, whereas the concentrations of ethyl, methyl and hydrogen atoms decrease at the same time. The change of propyl-radical concentration is about 10 to 100 times less than the change in concentration of propane, while the change of concentrations of hydrogen, methyl and ethyl radicals is comparable with that of propane.

The total concentration of radicals in the system $[R]_{total}$ is, within the experimental error, independent of temperature. This is to be expected since the total radical concentration depends only on the rate of quenching of the excited mercury by propane. Once complete quenching is achieved the total radical concentration is also independent of propane pressu

The overall dependence of the rates of product formation on the pressure of propane, shown in Figures 4 - 10, has been attributed to the complete quenching of the excited mercury atoms at certain propane pressure, so that further increase in concentratinn of propane does not noticeably affect the rate of reaction [2]. If this were true, then the introduction of some other gas of comparable quenching cross-section would cause a decrease of the rate of reaction [2] and complete quenching would occur at lower propane pressure. Carbon dioxide has a quenching cross-section of about 3 A^2, comparable with that for propane of about 2 A^2 (47), and it successfully competes for quenching of mercury. The effect of added carbon dioxide on the quenching of mercury becomes evident upon inspection of Table 10 and Figure 37.

The rates of formation of all products fall off rapidly with increasing pressure of added carbon dioxide, owing to its quenching of excited mercury.

TABLE 12

Approximate estimates of concentrations of the reactive species in the reaction cell*

	$P_{C_3H_8}$ = 10 mm Hg				
T [°C] →	252	276	301	325	350
$[C_3H_8]$	3.0×10^{-7}	2.9×10^{-7}	2.8×10^{-7}	2.7×10^{-7}	2.6×10^{-7}
$[n\text{-}C_3H_7]$	0.7×10^{-14}	0.6×10^{-14}	0.6×10^{-14}	0.5×10^{-14}	0.5×10^{-14}
$[i\text{-}C_3H_7]$	0.7×10^{-13}	0.7×10^{-13}	0.7×10^{-13}	0.7×10^{-13}	0.7×10^{-13}
$[C_2H_5]$	1.2×10^{-15}	1.6×10^{-15}	2.4×10^{-15}	2.6×10^{-15}	3.2×10^{-15}
$[CH_3]$	2.8×10^{-15}	3.8×10^{-15}	4.6×10^{-15}	6.6×10^{-15}	8.0×10^{-15}
[H]	2.0×10^{-17}	1.4×10^{-17}	1.3×10^{-17}	1.2×10^{-17}	2.0×10^{-17}
$[R]_{total}$	0.81×10^{-13}	0.81×10^{-13}	0.83×10^{-13}	0.84×10^{-13}	0.86×10^{-13}
	$P_{C_3H_8}$ = 700 mm Hg				
T [°C] →	252	276	301	325	350
$[C_3H_8]$	2.1×10^{-5}	2.0×10^{-5}	2.0×10^{-5}	1.9×10^{-5}	1.8×10^{-5}
$[n\text{-}C_3H_7]$	1.4×10^{-14}	1.3×10^{-14}	1.1×10^{-14}	1.0×10^{-14}	0.9×10^{-14}
$[i\text{-}C_3H_7]$	1.3×10^{-13}	1.3×10^{-13}	1.3×10^{-13}	1.3×10^{-13}	1.3×10^{-13}
$[C_2H_5]$	0.5×10^{-16}	0.9×10^{-16}	1.7×10^{-16}	2.6×10^{-16}	4.2×10^{-16}
$[CH_3]$	0.8×10^{-16}	2.0×10^{-16}	4.0×10^{-16}	8.9×10^{-16}	17×10^{-16}
[H]	1.1×10^{-18}	0.7×10^{-18}	0.6×10^{-18}	0.5×10^{-18}	0.7×10^{-18}
$[R]_{total}$	1.44×10^{-13}	1.43×10^{-13}	1.41×10^{-13}	1.41×10^{-13}	1.41×10^{-13}

*All concentrations are quoted in mole cc^{-1}.
$[R]_{total}$ denotes total concentration of radicals and hydrogen atoms in the system.
The following expressions were used for estimations:

$[H] = v_{H_2}/k_3[C_3H_8]$: $[CH_3] = v_{CH_4}/k_{15}[C_3H_8]$:

$[C_2H_5] = (v_{C_2H_6} - k_{19}[CH_3]^2)/k_{16}[C_3H_8]$:

$[n\text{-}C_3H_7] = (v_{n\text{-}C_6H_{14}}/k_4)^{1/2}$: $[i\text{-}C_3H_7] = (v_{2,3\text{-DMB}}/k_5)^{1/2}$.

4.2 Steady-state Equations

The steady-state condition for hydrogen atoms, and methyl, ethyl, n-propyl and i-propyl radicals, yields:

(1) $$v_{2p} + v_{2s} + v_{20a} + v_{21a} = v_{3p} + v_{3s} + v_{10a} + v_{10b} + v_{11} + v_{12} + v_{13} + v_{14p} + v_{14s}$$

(2) $$v_{10a} + v_{10b} + 2v_{11} + v_{20b} + v_{21b} = v_{12} + v_{15p} + v_{15s} + v_{17} + v_{18} + 2v_{19}$$

(3) $$v_{10a} + v_{10b} = v_{11} + v_{13} + v_{16p} + v_{16s}$$

(4) $$v_{2p} + v_{3p} + v_{15p} + v_{16p} = 2v_4 + v_6 + 2v_7 + v_9 + v_{10a} + v_{14p} + v_{17} + v_{20a} + v_{20b}$$

(5) $$v_{2s} + v_{3s} + v_{15s} + v_{16s} = 2v_5 + v_6 + 2v_8 + v_9 + v_{10b} + v_{14s} + v_{18} + v_{21a} + v_{21b}$$

$v_{2p} = \phi I_a \alpha$ and $v_{2s} = \phi I_a(1-\alpha)$, α being the fraction of n-propyl radicals produced in reaction [2]. From the above equations the following expressions can be derived:

(6) $$[H] = \frac{F_1}{k_3 [C_3H_8] + F_2}$$ where $k_3 = k_{3p} + k_{3s}$

(7) $$[CH_3] = \frac{F_3}{k_{15} [C_3H_8] + F_4}$$ where $k_{15} = k_{15p} + k_{15s}$ and v_{19} is neglected

(8) $$[C_2H_5] = \frac{F_5}{k_{16} [C_3H_8] + F_6}$$ where $k_{16} = k_{16p} + k_{16s}$

(9) $$[P] = \frac{-F_7 + (F_7^2 + 2C_1F_8)^{1/2}}{C_1} \quad \text{where } C_1 = 2(2k_4+2k_7-k_6-k_9)$$

(10) $$[S] = \frac{-F_9 + (F_9^2 + 2C_2F_{10})^{1/2}}{C_2} \quad \text{where } C_2 = 2(2k_5+2k_8-k_6-k_9)$$

(11) $$[C_3H_7]_{total} \approx \frac{-F_{11} + (F_{11}^2 + 2C_3F_{12})^{1/2}}{C_3} \quad \text{where } C_3 = 2(2k_4+2k_7)$$

(12) $$F_1 = \phi I_a + k_{20a}[P] + k_{21a}[S] .$$

(13) $$F_2 = k_{10a}[P] + k_{10b}[S] + k_{11}[C_2H_5] + k_{12}[CH_3] + k_{13}[C_2H_5] + k_{14p}[P] + k_{14s}[S]$$

(14) $$F_3 = k_{10a}[H][P] + k_{10b}[H][S] + 2k_{11}[H][C_2H_5] + k_{20b}[P] + k_{21b}[S].$$

(15) $$F_4 = k_{12}[H] + k_{17}[P] + k_{18}[S].$$

(16) $$F_5 = k_{10a}[H][P] + k_{10b}[H][S].$$

(17) $$F_6 = k_{11}[H] + k_{13}[H].$$

(18) $$F_7 = k_6[T] + k_9[T] + k_{10a}[H] + k_{14p}[H] + k_{17}[CH_3] + k_{20a} + k_{20b},$$

where $[T] = [C_3H_7]_{total}$.

(19) $$F_8 = \phi I_a{}^a + k_{3p}[H][C_3H_8] + k_{15p}[CH_3][C_3H_8] + k_{16p}[C_2H_5][C_3H_8].$$

(20) $F_9 = k_6[T] + k_9[T] + k_{10b}[H] + k_{14s}[H] + k_{18}[CH_3] + k_{21a} + k_{21b}$

where $[T] = [C_3H_7]_{total}$.

(21) $F_{10} = \emptyset I_a(1-a) + k_{3s}[H][C_3H_8] + k_{15s}[CH_3][C_3H_8] + k_{16s}[C_2H_5][C_3H_8]$.

(22) $F_{11} = k_{10}[H] + k_{14}[H] + k_{17}[CH_3] + k_{20} + k_{21}$

(23) $F_{12} = \emptyset I_a + k_3[H][C_3H_8] + k_{15}[CH_3][C_3H_8] + k_{16}[C_2H_5][C_3H_8]$.

4.3 Production of Hydrogen

The rate of hydrogen production as a function of propane pressure is:

(24) $$v_{H_2} = \frac{F_1}{1 + \frac{F_2}{k_3[C_3H_8]}}$$

The change of propane pressure causes a much smaller change of F_1 and F_2 than of $k_3[C_3H_8]$ (see Table 12), and the following approximate equations can be derived:

(25) $$v_{H_2} \approx \frac{F_1}{F_2} k_3[C_3H_8]$$

at low pressures of propane, and

(26) $$v_{H_2} \approx F_1$$

at high pressures of propane.

At high propane pressure the total concentration of propyl radicals and of the n- and i-propyl radicals approaches a constant value; F_1 thus also approaches a constant value. Experimentally, the order of hydrogen production with respect to propane changes from unity at low propane pressures to zero at high pressures of propane (see Figure 12). This is in agreement with the present results, provided that $F_1/F_2 \approx$ constant at low propane pressures and $F_1 \approx$ constant at high pressures of propane.

In the high-pressure region, reactions [10a], [10b], [11], [12], [13] and [14] can be neglected. At low temperatures, reactions [20a] and [21a] are also negligible. Under these conditions $v_{H_2} = v_2 = \phi I_a$: i.e., at low temperatures and high propane pressures the rate of hydrogen production is constant and independent of temperature.

At high temperatures, reactions [20a] and [21a] are additional sources of hydrogen and the rate of hydrogen production becomes strongly dependent on temperature. In the high temperature region, reactions [20a] and [21a], together with reactions [3p] and [3s] constitute reaction chains producing hydrogen without a net consumption of propyl radicals. In order to have some idea of chain lengths, we may define chain length as the number of H atoms released by the decomposition of propyl radicals per propyl radical formed, i.e. approximately $v_{H_2(\text{chain})}/v_{C_6H_{14}}$. The actual situation is far more complicated than this. Nevertheless this rough approximation indicates that chain lengths are of the order of magnitude of 10^0 and that they increase with increasing temperature. The activation energy for the chain hydrogen production was found to be 38.7 kcal.mole^{-1}, in good agreement with 38 and 37 kcal. mole^{-1} found by Steacie (28) and Back (34) respectively. This will be discussed later, together with the decomposition of propyl radicals.

4.4 Production of Methane and Ethene

According to the proposed mechanism, the rates of methane and ethene production should be approximately equal, because their main sources are reactions [20b] and [21b]. (As will be seen later, only reaction [20b] is of much importance). Experimentally these rates were found to be approximately equal. At low propane pressures up to about 40 mm Hg, the rate of methane production is slightly higher; on the other hand, above 40 mm Hg the rate of ethene production predominates. These results can be explained as follows. At low pressures of propane, reactions [10a] and [10b] and, to a smaller extent, [11] and [12], might play a role of some importance. They represent an additional source of methyl radicals over reactions [20b] and [21b] and more than compensate for the loss of methyl radicals through reactions [17], [18] and [19]. At higher propane pressures, reactions [10] - [12] diminish in importance and they less than compensate for the loss of methyl radicals, which results in a lower velocity of production of methane than of ethene. Nevertheless it should be emphasized that reaction [20b] is the main source of methyl and ethene at both low and high propane pressures and that reactions [10] - [12] represent only the minor contribution which can be neglected if only the major points of the mechanism are discussed.

The rate of methane production may be expressed as a function of propane concentration:

$$v_{CH_4} = \frac{F_3}{1 + \frac{F_4}{k_{15}[C_3H_8]}} \qquad (27)$$

As in the case of hydrogen, F_3 and F_4 change much less than $k_{15}[C_3H_8]$ with change of propane pressure, and the following approximations can be derived:

$$v_{CH_4} \approx \frac{F_3}{F_4} k_{15}[C_3H_8] \tag{28}$$

at low pressures of propane, and

$$v_{CH_4} \approx F_3 \tag{29}$$

at high pressures of propane.

Since $k_{15} \ll k_3$, the pressure of propane at which the rate of methane production becomes independent of propane pressure should be higher than that for hydrogen production. Experimentally this was found to be so.

Furthermore, according to the scheme for unimolecular decompositions,

$$R + M \rightleftharpoons R^* + M$$

$$R^* \rightarrow R^{\neq} \rightarrow \text{Products},$$

the propane pressure at which the equilibrium between the energized propyl radicals and the propane molecules isestablished depends on temperature. With increasing temperature the rate of decomposition of propyl radicals increases, and a higher propane pressure is required to establish the equilibrium between the energized radicals and the propane. Consequently, the propane pressure at which the rate of methane production approaches a constant value will also increase with increasing temperature.

Since the concentrations of ethyl, methyl and hydrogen atoms change inversely to that of propane, the order of F_3/F_4 with respect to propane at low pressures is expected to be negative, and consequently the order of methane production with respect to propane is expected to be less than unity at low propane pressures. At high propane pressure F_3 approaches a constant value and v_{CH_4} also becomes constant. The order of methane production with respect to propane was found to change from 0.8 at low propane pressures to zero at high pressures of propane (see Figure 16).

Reactions [20b] and [21b], together with reactions [15p] and [15s] constitute reaction chains producing methyl and ethene without a net consumption of propyl radicals. In order to have some idea of chain lengths for methyl radicals and ethene production, we may define chain length as the number of methyl radicals or ethene molecules released per n-propyl radical formed, i.e. approximately $v_{C_2H_4}/(v_{n\text{-}C_6H_{14}} + v_{2\text{-MP}})$. This rough approximation tells us that chain lengths increase from the order of magnitude of 10^0 at 250°C to the order of magnitude of 10^2 at 350°C.

The activation energy for methane production was found to change from an extrapolated value at zero propane pressure of 15 kcal. $mole^{-1}$ to 29.5 kcal.$mole^{-1}$ at high pressures of propane (see Figure 18). The change in the activation energy for methane production is most probably due to the pressure dependence of the first-order rate coefficient for the decomposition of a propyl radical into a methyl radical and ethene. This will be discussed later together with the decomposition of propyl radicals. However, there is also a possibility that quenching of the excited mercury by propane produces hot propyl radicals, which

decompose more readily than cold radicals in thermal equilibrium with their surroundings. With increasing pressure of propane hot radicals are deactivated and become thermalized. Correspondingly, the activation energy is increased until it reaches the high-pressure constant value. Since the activation energy of hydrogen production by the chain mechanism does not show the same behavior, it could imply that excess energy in hot radicals is distributed in such a way that it helps to break the C-C bond and does not affect the C-H bond. This does not seem unreasonable if one considers that the C-C bond breaks with lower activation energy than the C-H bond.

The same arguments apply to the production of ethene, for which the activation energy changes from an extrapolated value at zero propane pressure of 15 kcal $mole^{-1}$ to 29.7 kcal $mole^{-1}$ at high pressures of propane (see Figure 22). The corresponding values found by Steacie (28) and Back (34) were 20 and 22 kcal $mole^{-1}$ respectively. The big difference may be accounted for by the change of activation energy with the change of propane pressure. Their values were obtained at a single pressure and there was no mention of the dependence of the rate constant on the pressure of propane.

The rate of ethene production may be expressed as a function of propane concentration:

$$v_{C_2H_4} = k_{20b} \frac{-F_7 + (F_7^2 + 2C_1F_8)^{1/2}}{C_1} \qquad (30)$$

At high propane pressures, F_7 and F_8 approach constant values, and consequently $v_{C_2H_4}$ also becomes constant. It is more difficult to describe the behavior of this function at low pressures of propane. Because of the square-root dependence one could expect the order of ethene production with respect to propane to be less than unity. Experimentally the order was found to change from 0.8 at low propane pressures to zero at high pressures of propane, as in the case of methane (see Figure 20).

4.5 Production of Ethane

The mechanism of the ethane production seems to be more complicated. The following expression may be written for the rate of ethane production:

$$(31) \qquad v_{C_2H_6} = \frac{\dfrac{F_5}{F_6}}{1 + \dfrac{}{k_{16}[C_3H_8]}} + k_{19}\left(\frac{F_3}{k_{15}[C_3H_8] + F_4}\right)^2$$

Because of the complexity of the function, it is difficult to describe its behavior upon the change of propane pressure. Nevertheless, it might be approximated by the following expression:

$$(32) \qquad v_{C_2H_6} \approx \frac{F_5}{F_6}\, k_{16}[C_3H_8] + k_{19}\left(\frac{F_3}{F_4}\right)^2$$

at low pressures of propane, and

$$(33) \qquad v_{C_2H_6} \approx F_5$$

at high pressures of propane.

From the known rate constants k_{13}, k_{16} and k_{19} (see Table 11), and estimated concentrations of hydrogen atoms and methyl and ethyl radicals (see Table 12), the rate of ethane production by reactions [13], [16] and [19] may be estimated. The rate estimated in this way does not account for the total ethane production. However, it should be pointed out that the rate constants used to evaluate the velocities and the radical concentrations are not so well known that accurate estimates of velocities could be made. It is conceivable that an error of a few orders of magnitude could be involved and that all of the ethane is produced by reactions [13], [16] and [19].

The change of activation energy of ethane production with the change of propane pressure also suggests a complicated mechanism of ethane production (see Figure 26). The increase of the energy of activation could be explained on the same basis as in the case of methane and ethene.

4.6 Production of Hexanes

The rates of production of the three isomeric hexanes may be expressed as follows:

$$v_{2,3\text{-DMB}} = k_5\left(\frac{-F_9 + (F_9^2 + 2C_2F_{10})^{1/2}}{C_2}\right)^2 \tag{34}$$

$$v_{2\text{-MP}} = k_6\left(\frac{-F_7 + (F_7^2 + 2C_1F_8)^{1/2}}{C_1}\right)\left(\frac{-F_9 + (F_9^2 + 2C_2F_{10})^{1/2}}{C_2}\right) \tag{35}$$

$$v_{n\text{-}C_6H_{14}} = k_4\left(\frac{-F_7 + (F_7^2 + 2C_1F_8)^{1/2}}{C_1}\right)^2 \tag{36}$$

The functions are complex and it is difficult to describe their behavior upon the change of propane pressure. At high pressures of propane, the functions F_7, F_8, F_9 and F_{10} approach constant values and consequently the rates of production of the three isomeric hexanes also become constant. It is difficult to say anything about the behavior at low propane pressures. The order of formation of the three isomeric hexanes with respect to propane was found to change from 0.5 at about 10 to 50 mm Hg propane pressures to zero at high pressures of propane (see Figures 28, 30 and 34). It should be pointed that the orders for the formation of the three isomeric hexanes with respect to propane change considerably at low propane pressures up to 5 mm Hg.(see Figures 8, 9 and 10) and the orders for the formation of the three isomeric hexanes with respect to propane might be considerably higher than 0.5 at low pressures of propane.

No significant change in the rate of 2,3-DMB production was detected when the temperature was changed from 250°C to 350°C (see Figure 8), while the rates of 2-MP and n-C_6H_4 diminished on raising the temperature (see Figures 9, 10, 31 and 35). This implies that the concentration of i-propyl radicals remains essentially constant, while the concentration of n-propyl radicals decreases on raising the temperature. The reactions of propyl radicals will be considered in the next section.

4.7 Combination and Disporportionation of Propyl Radicals

It is reasonable to assume that combinations of propyl radicals occur by an energy-transfer mechanism (48). If for the moment only combinations of propyl radicals are considered, the following general scheme may be put forward:

$$2C_3H_7 \underset{-1}{\overset{1}{\rightleftharpoons}} C_6H_{14}^*$$

$$C_6H_{14}^* + C_3H_8 \overset{2}{\rightarrow} C_6H_{14} + C_3H_8$$

where C_3H_8 acts as a third body. The steady-state treatment of the scheme of reactions leads to the rate of disappearance of propyl radicals:

(37) $$-d[C_3H_7]/dt = 2k_1k_2[C_3H_7]^2[C_3H_8]/(k_{-1} + k_2[C_3H_8]).$$

At low pressure of propane when $[C_3H_8]$ is sufficiently small,

(38) $$-d[C_3H_7]/dt = (2k_1k_2/k_{-1})[C_3H_7]^2[C_3H_8]$$

i.e. the rate of disappearance of propyl radicals is proportional to the propane concentration. The rate-controlling step is deactivation of $C_6H_{14}^*$.

At sufficiently high pressures of propane,

(39) $$-d[C_3H_7]/dt = 2k_1[C_3H_7]^2$$

The overall rate is controlled by the frequency of collision of propyl radicals.

Under the present reaction conditions one cannot expect to observe the pressure dependence of propyl radical combination. Measurements of the rate of combination of methyl radicals at temperatures in the neighborhood of 250°C have indicated that pressure dependence begins to occur at pressures below about 10 mm Hg of acetone and also below 200 mm Hg of ethane at about 600°C (49). The combination of ethyl radicals at 250°C was found to be pressure independent to as low as 0.01 mm Hg of diethyl ketone (50). Because of the greater number of vibrational degrees of freedom in hexane molecules the pressure independence of the propyl radical combination is expected to hold to still lower pressures.

The quantity of interest in the combination reactions of alkyl radicals is often the ratio $k_{ab}/(k_{aa}k_{bb})^{1/2}$, where k_{aa} and k_{bb} are for the combination of like radicals and k_{ab} is for their cross-combination. According to the simple collision theory of chemical rates, this ratio should be 2 for reactions with no activation energy. The same value of the ratio could be predicted on the basis of activated-complex theory (51). In this case, the ratio of statistical factors or symmetry numbers (52) has to be introduced into the rate equation. In the case of two identical reactant molecules, the statistical factor is taken as the number of equivalent products divided by 2. The ratio of rate constants was verified by measuring the ratio of velocities, $v_{2\text{-MP}}/(v_{n\text{-}C_6H_{14}} \times v_{2,3\text{-DMB}})^{1/2}$. The results are in good agreement with the predicted value and with the values determined for other alkyl radicals (39) (see Table 9).

On the assumption that every collision results either in combination or in disproportionation, and that disproportionation requires no activation energy, the statistical formulation should be (53):

(40) $$(k_6 + k_9)/(k_4 + k_7)^{1/2} (k_5 + k_8)^{1/2} = 2.$$

From this and the experimental data:

(41) $$k_6/(k_4 k_5)^{1/2} = 2.$$

The ratio for the cross-disproportionation

(42) $$k_9/k_6 = (1 + \frac{k_7}{k_4})^{1/2} (1 + \frac{k_8}{k_5})^{1/2} - 1.$$

can be derived; this cannot be accurately measured. With the values of $k_7/k_4 = 0.16$ and $k_8/k_5 = 0.63$ (39) the value of $k_9/k_6 = 0.38$ is obtained, which compares with the value 0.41 ± 0.02 obtained by Terry and Futrell (70).

If we assume that $k_4 = k_5$, the ratio of i-propyl to n-propyl radicals can be directly monitored by the relationship:

(43) $$[S]/[P] = (v_{2,3\text{-DMB}}/v_{n\text{-}C_6H_{14}})^{1/2}$$

which yields the values quoted in Table 13.

TABLE 13

The ratios of i-propyl to n-propyl radicals as a function of temperature at propane pressure of 300 mm Hg

T [°C]	252	276	301	325	350
[S]/[P]	9.5	10.6	12.2	13.4	15.0

The ratios do not change on change of propane pressure, and are close to the value of 9.1 obtained by Gunning and co-workers (18) for the i-propyl to n-propyl split in the primary step of the mercury-photosensitized decomposition of propane. The data in Table 13 are plotted in Figure 38. From the plot the following expression was obtained:

$$[S]/[P] = 1.7 \times 10^{2} \exp(-3.1/RT) \qquad (44)$$

This result shows that in the temperature range of the present investigation the concentrations of propyl radicals differ from the equilibrium concentrations, in qualitative agreement with the earlier findings by Lin and Laidler (3). If the radicals were at equilibrium the n-propyl radical concentration would be reduced to a few percent of that of i-propyl, which is more stable by 3.5 kcal.mole^{-1}. The temperature coefficient of the ratio [S]/[P] is related to the increasing rate of removal of the n-propyl radicals as the temperature increases.

FIGURE 38

Plot of the logarithms of i-propyl to n-propyl ràtios against reciprocal temperature at propane pressure of 300 mm Hg.

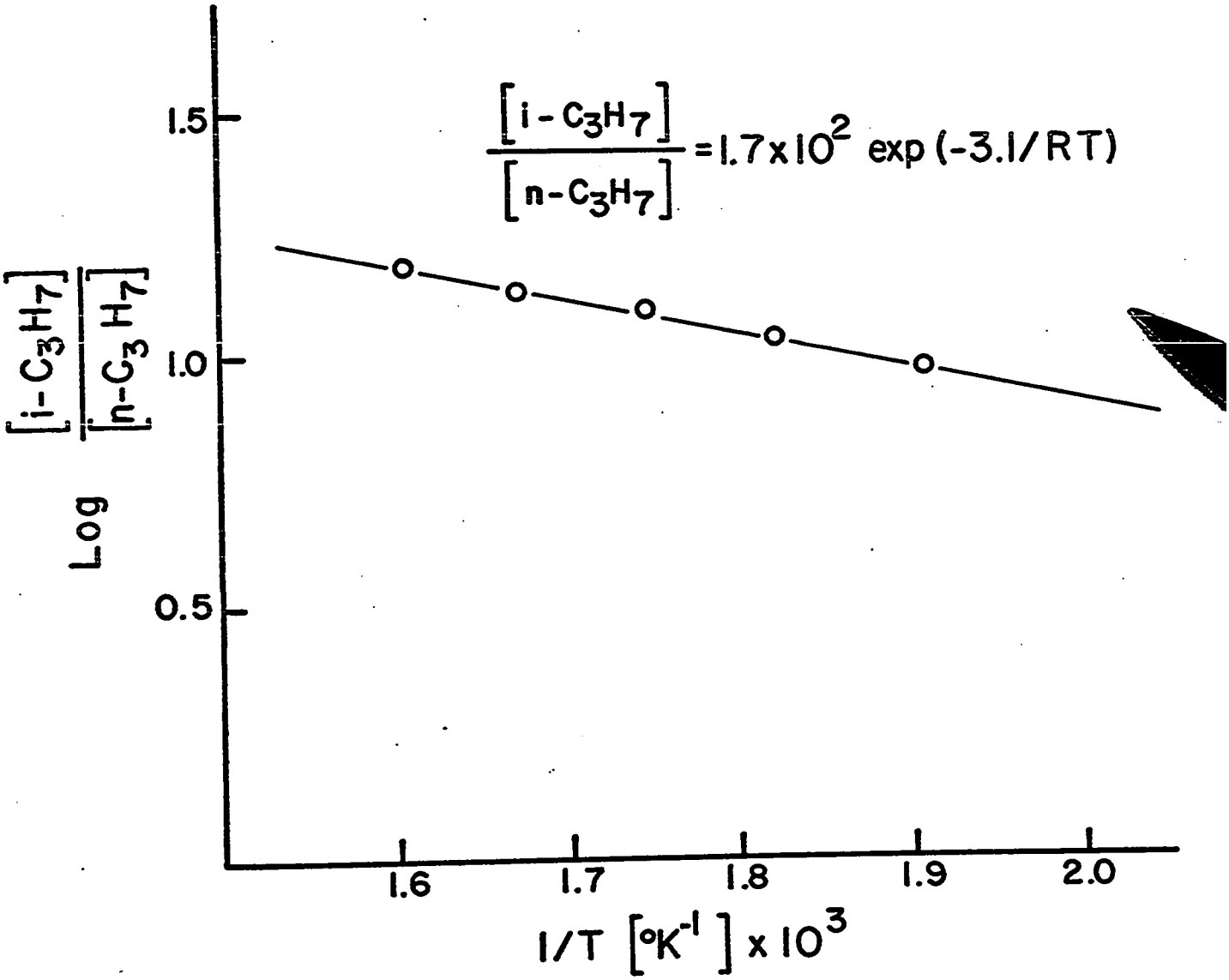
$\frac{[i\text{-}C_3H_7]}{[n\text{-}C_3H_7]} = 1.7 \times 10^2 \exp(-3.1/RT)$
Log $\frac{[i\text{-}C_3H_7]}{[n\text{-}C_3H_7]}$
1.5
1.0
0.5
1.6
1.7
1.8
1.9
2.0
$1/T\ [^\circ K^{-1}] \times 10^3$

4.8 Decomposition of Propyl Radicals

The decomposition to ethene: The decomposition of n-propyl radicals to ethene is about 10^3 times faster than the decomposition of i-propyl radicals to ethene (46), and under the present conditions one can assume that all ethene results from the decomposition of n-propyl radicals. Also, the decomposition of n-propyl radicals to propene is about 10^3 times slower than the decomposition to ethene (46) and in the present discussion the loss of n-propyl radicals by reaction [20a] may be neglected. In other words, the only important reaction in the production of ethene is reaction [20b]. It is more convenient to follow the decomposition of n-propyl to ethene and methyl by determining the ethene, since methyl radicals may disappear by several reaction paths.

From the reaction scheme the rate of decomposition of n-propyl radicals is given by:

$$v_{20b} = k_{20b}[P]$$

where k_{20b} is a defined first-order rate coefficient. With reference to reactions

[4] $2P \rightarrow n\text{-}C_6H_{14}$

and

[20b] $P \rightarrow CH_3 + C_2H_4$

the rate coefficient k_{20b} may be expressed as follows:

(45) $$k_{20b} = k_4^{1/2} v_{C_2H_4} / (v_{n\text{-}C_6H_{14}})^{1/2}$$

With k_4 taken as $10^{13.4}$ cc.mole^{-1}sec^{-1} and independent of temperature (37), k_{20b} can be evaluated. The resulting values of the rate constant k_{20b} at different temperatures and pressures are listed in Table 14.

TABLE 14

Values of the first-order rate coefficient k_{20b} at different temperatures and propane pressures*

T [°C] →	252	276	301	325	350
$P_{C_3H_8}$ [mm Hg]	k_{20b}	k_{20b}	k_{20b}	k_{20b}	k_{20b}
10	4.2	9.7	20.1	40.9	74.6
20	5.8	13.4	28.9	57.0	112
30	6.4	15.3	34.4	71.9	151
40	6.4	17.1	38.5	80.8	177
60	6.4	19.1	45.5	98.7	222
80	6.4	20.1	52.0	116	266
100	6.4	21.3	58.2	136	307
150	6.4	23.3	70.3	174	412
200	6.4	24.8	80.5	215	507
250	6.4	25.3	88.3	250	590
300	6.4	25.4	93.2	280	661
350	6.4	25.4	95.5	302	719
400	6.4	25.4	95.5	309	766
450	6.4	25.4	95.5	310	808
500	6.4	25.4	95.5	310	840
550	6.4	25.4	95.5	310	869
600	6.4	25.4	95.5	310	888
650	6.4	25.4	95.5	310	890
700	6.4	25.4	95.5	310	890

* The values of k_{20b} are quoted in $sec.^{-1}$.

The dependence of the first-order rate coefficient k_{20b} on the propane concentration at five different temperatures is shown in Figure 39.

The plots are in qualitative agreement with the predictions of the Lindemann theory, which gives the following expressions for the first-order rate coefficient.

(46) $$k^1 = \frac{k_\infty}{1 + \frac{k_2}{k_{-1}[M]}}$$

and

(47) $$\frac{1}{k^1} = \frac{1}{k_\infty} + \frac{1}{k^o[M]}$$

At high pressures of propane the first-order rate coefficient for the decomposition of n-propyl radicals becomes independent of pressure. The logarithms of the high-pressure rate coefficient against the reciprocal temperature are plotted in Figure 40. This plot yields the value of the high-pressure rate constant, which can be expressed as:

$$k_{20b} = 2.5 \times 10^{14} \exp(-32.6/RT) \text{ sec}^{-1}$$

The energy of activation for the production of ethene at high pressures of propane was found to be 29.7 kcal.mole^{-1} (see Figure 22), and the energy of activation in the expression for k_{20b} is 32.6 kcal.mole^{-1}. The difference of 2.9 kcal.mole^{-1} may be attributed to the temperature dependence of the concentration of n-propyl radicals. Since the ratio of i-propyl to n-propyl radicals is given by:

FIGURE 39

Double logarithmic plots of the rate constant k_{20b} against the propane concentration at five different temperatures:

A	252°C
B	276°C
C	301°C
D	325°C
E	350°C

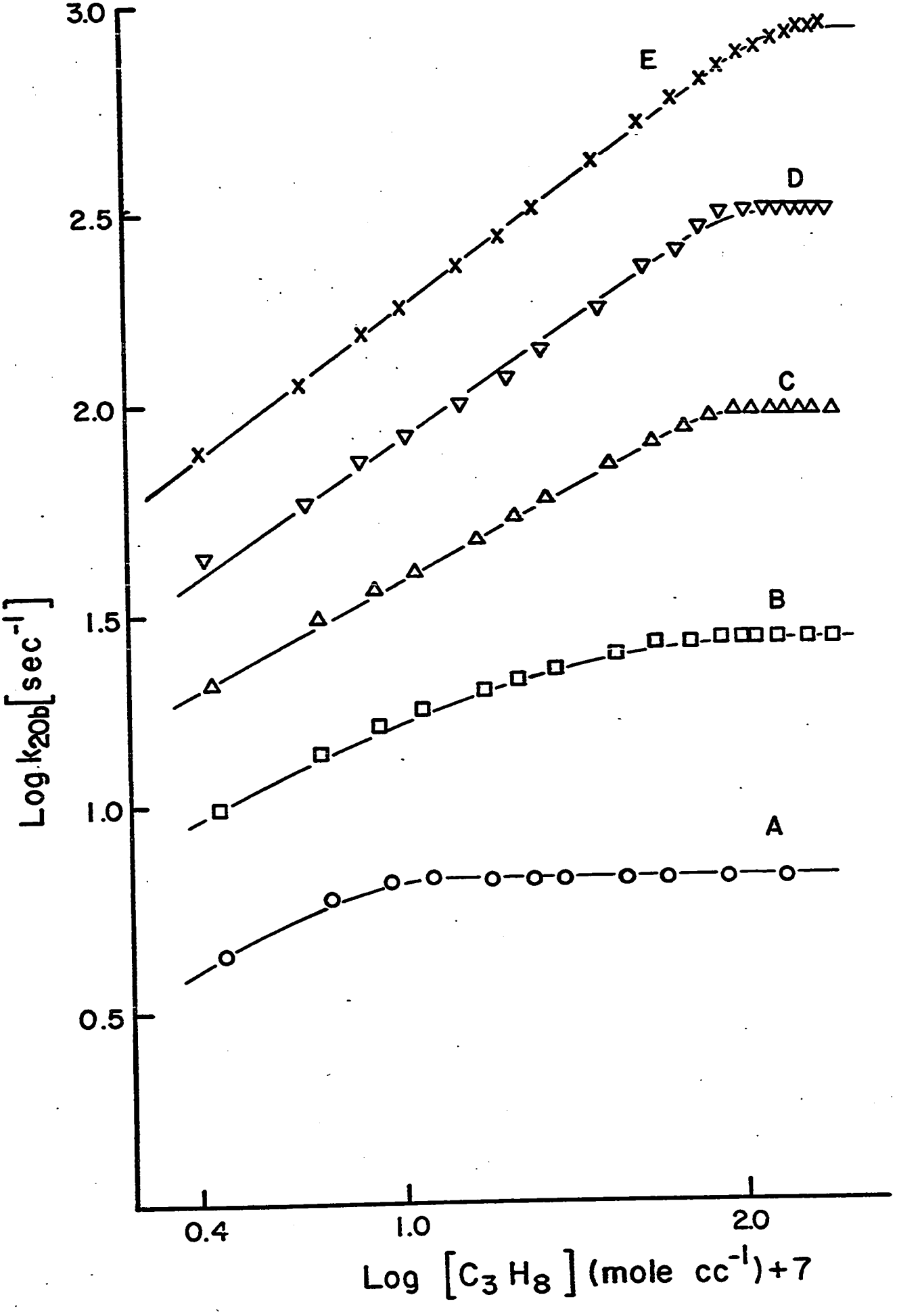
3.0
2.5
2.0
1.5
1.0
0.5
E
D
C
B
A
Log k_{20b} [sec^{-1}]
0.4
1.0
2.0
Log [C_3H_8] (mole cc^{-1})+7

FIGURE 40

An Arrhenius plot of k_{20b} at propane pressure of 700 mm Hg.

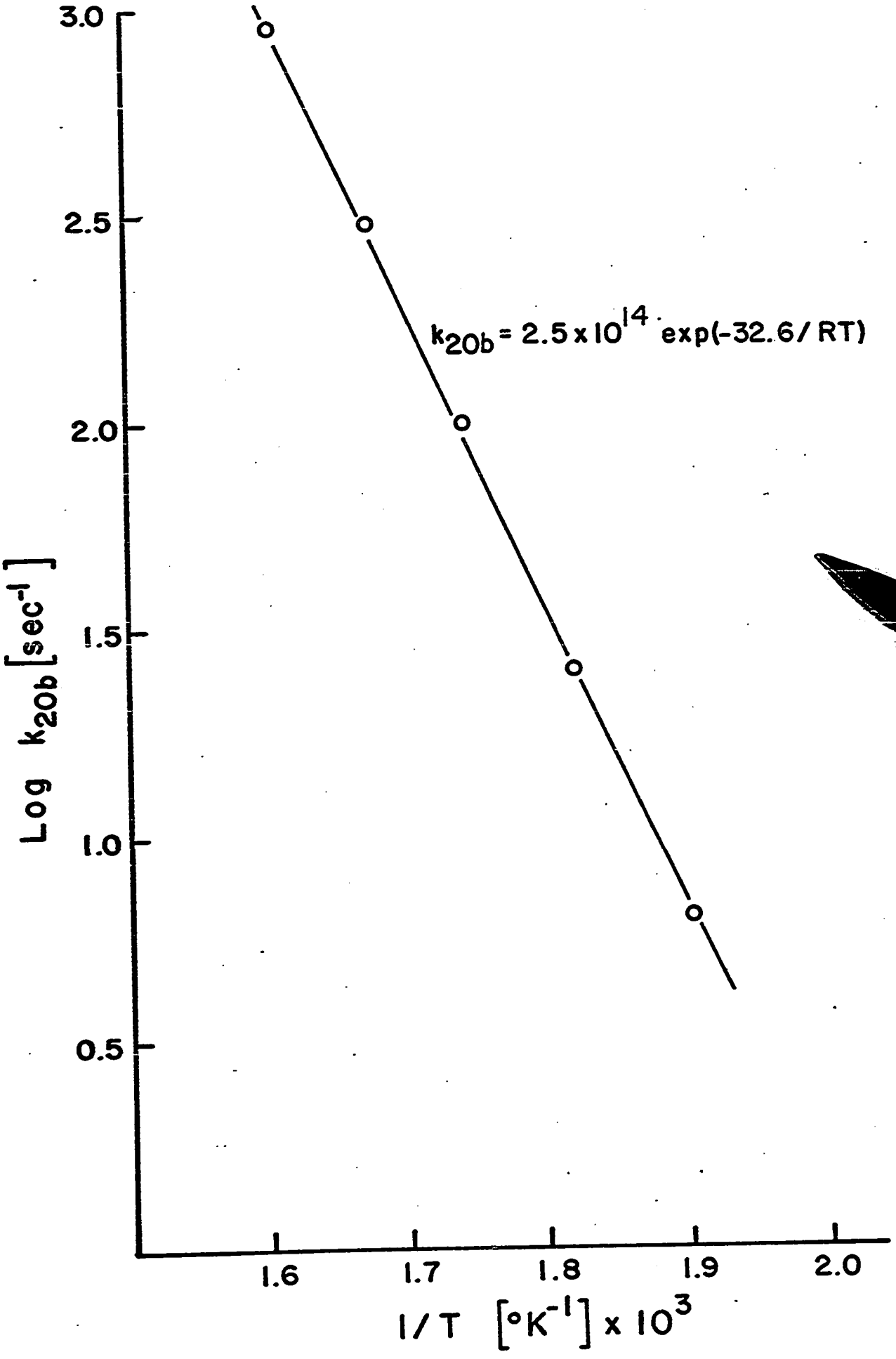
3.0
2.5
2.0
1.5
1.0
0.5
Log k_{20b} [sec^{-1}]
$k_{20b} = 2.5 \times 10^{14} \cdot \exp(-32.6/RT)$
1.6
1.7
1.8
1.9
2.0
1/T [$°K^{-1}$] x 10^3

$$[S]/[P] = 1.7 \times 10^2 \exp(-3.1/RT)$$

the concentrations of n-propyl and i-propyl radicals as a function of temperature may be expressed as:

$$[n\text{-}C_3H_7] = \text{const.} \exp(2.9/RT)$$

and

$$[i\text{-}C_3H_7] = \text{const.} \exp(-0.2/RT)$$

which is consistent with the finding that the concentration of i-propyl radicals is practically independent of temperature and that the concentration of n-propyl radicals decreases with increasing temperature.

Figure 41 shows a Lindemann plot of the reciprocal of the rate coefficient k_{20b} against the reciprocal of the propane concentration at 301°C.

At lower $[C_3H_8]^{-1}$ values a typical deviation from linearity is observed. Similar plots were obtained at other temperatures. From the intercepts of the Lindemann plots at 276°C, 301°C, 325°C and 350°C the values of the high-pressure limiting rate constant k_{20b}^{∞} were obtained. The values are listed in Table 15.

Figure 42 shows an Arrhenius plot of the results. From the plot an expression for k_{20b}^{∞} was obtained:

$$k_{20b}^{\infty} = 1.6 \times 10^{15} \exp(-34.4/RT) \text{ sec}^{-1}.$$

From the slopes of Lindemann plots at 252°C, 276°C, 301°C, 325°C and 350°C the values of the low-pressure limiting rate constant k_{20b}^{o} were obtained. The values are listed in Table 15. An Arrhenius plot of the results is shown in Figure 43.

TABLE 15

Values of k_{20b}^{∞} and k_{20b}^{o} obtained from the intercepts and slopes of the Lindemann plots

T[°C]	252	276	301	325	350
k_{20b}^{∞} [sec^{-1}]		28.6	125	500	1330
k_{20b}^{o} [$cc.mole^{-1}sec^{-1}$]	2.8	6.1	11.4	23.0	37.0

FIGURE 41

A Lindemann plot of the k_{20b}^{-1} against $[C_3H_8]^{-1}$ at 301°C.

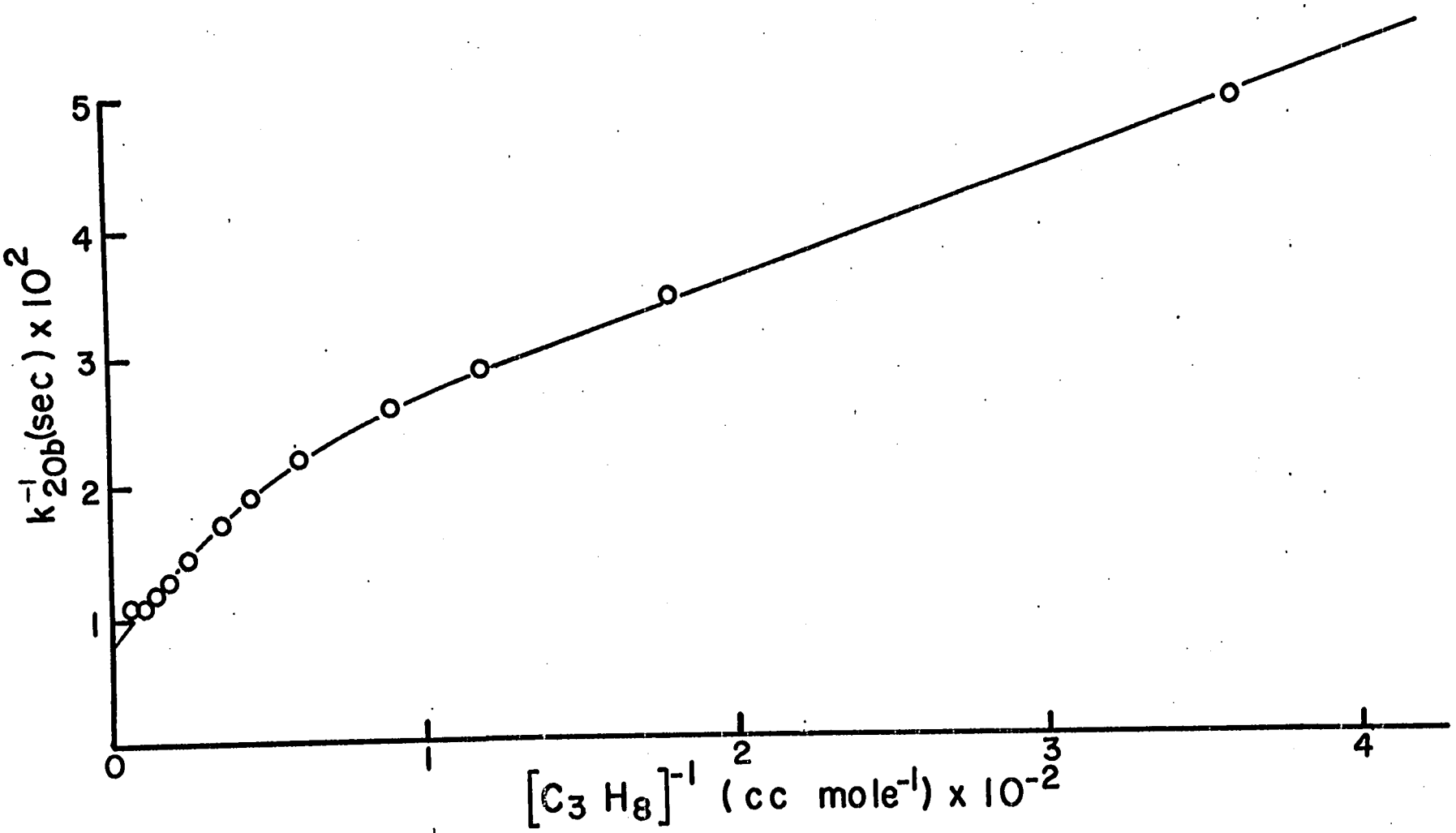
5
4
3
2
1
0
$k^{-1}_{20b}(sec) \times 10^2$
1
2
3
4
$[C_3 H_8]^{-1}$ (cc mole^{-1}) x 10^{-2}

FIGURE 42

An Arrhenius plot of k_{20b}^{∞} obtained from intercepts of the Lindemann plots.

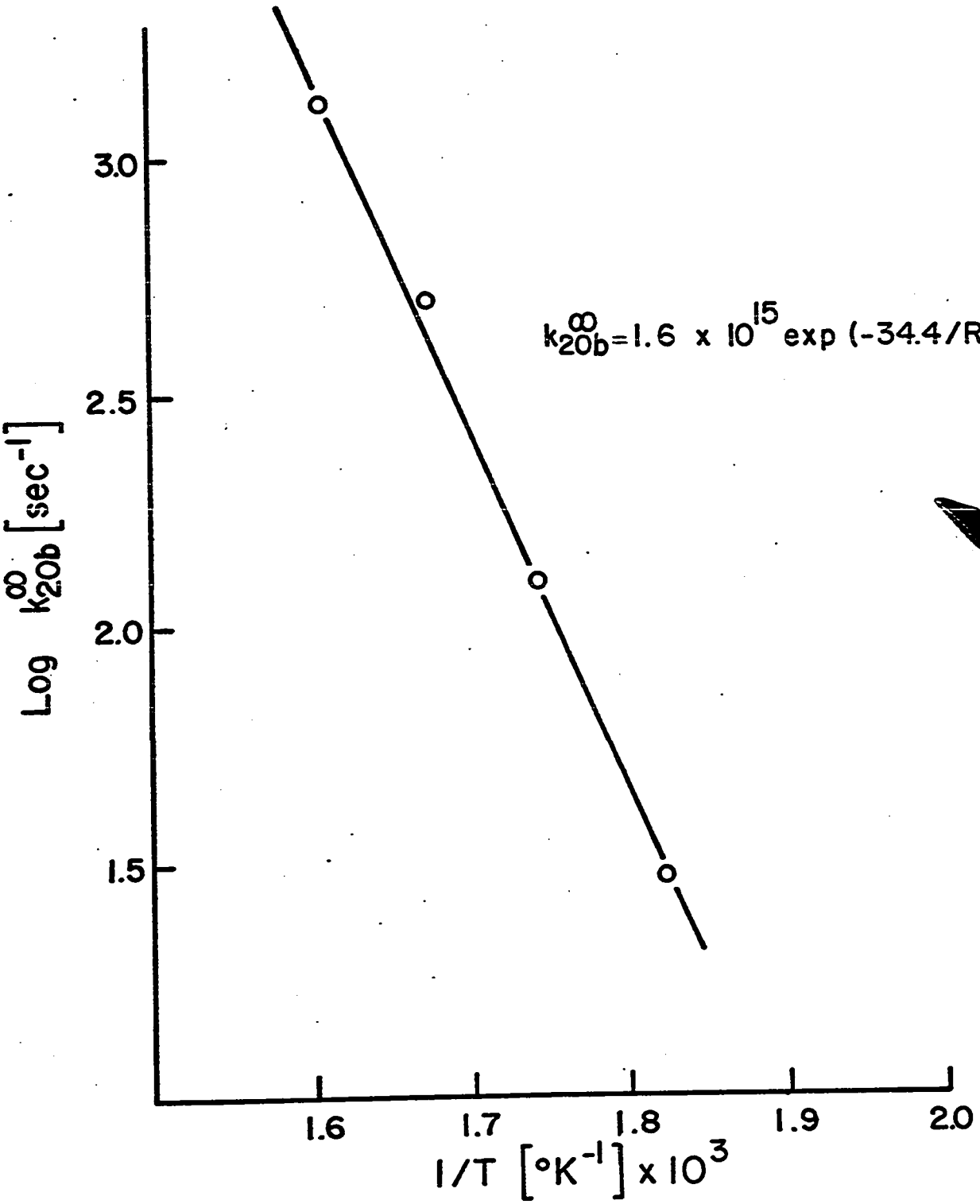
$k_{20b}^{\infty}=1.6 \times 10^{15} \exp(-34.4/RT)$
Log k_{20b}^{∞} [sec^{-1}]
3.0
2.5
2.0
1.5
1.6
1.7
1.8
1.9
2.0
1/T [°K^{-1}] x 10^{3}

FIGURE 43

An Arrhenius plot of k^{o}_{20b} obtained from the slopes of the Lindemann plots.

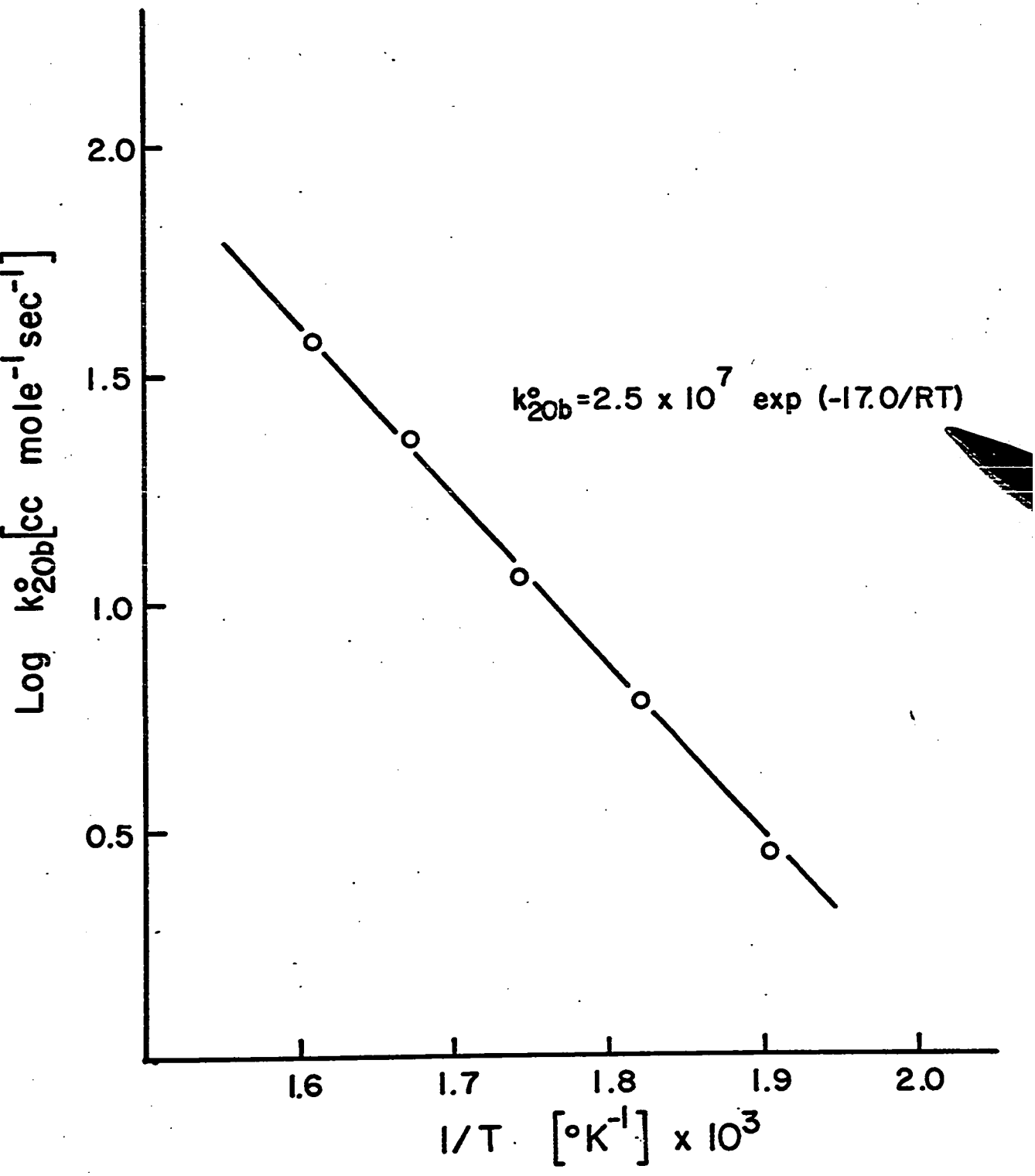
2.0
1.5
1.0
0.5
Log k°_{20b}[cc mole^{-1}sec^{-1}]
k°_{20b}=2.5 x 10^{7} exp (-17.0/RT)
1.6
1.7
1.8
1.9
2.0
1/T [°K^{-1}] x 10^{3}

From the plot an expression for k^{o}_{20b} was obtained:

$$k^{o}_{20b} = 2.5 \times 10^{7} \exp(-17.0/RT) \text{cc.mole}^{-1}\text{sec}^{-1}.$$

The modern theories of unimolecular reactions are based on the following scheme of reactions:

$$A + A \underset{k_{-1}}{\overset{k_1}{\rightleftharpoons}} A^{*} + A$$

$$A^{*} \xrightarrow{k_2} A^{\neq} \rightarrow \text{Products}$$

From the Hinshelwood expression for the rate of energization the number of normal modes of vibration contributing to the energization of the molecule is given by the expression:

$$E^{\infty} - E^{o} = (s-1)RT$$

Insertion of the values of 32.6 kcal.mole^{-1} and 17.0 kcal.mole^{-1} for the limiting high-pressure and low-pressure energies of activation respectively, gives s = 15 for the decomposition of the n-propyl radical into the methyl radical and ethene. It is frequently found that for relatively complex molecules

$$\frac{2}{3}n > s > \frac{1}{2}n$$

where n is the total number of vibrational degrees of freedom (54). The present result is also within the same limits.

Table 16 lists the values for the rate constant for the decomposition of n-propyl radicals into CH_3 and C_2H_4 obtained by other authors.

TABLE 16

Kinetic parameters for the decomposition of n-C_3H_7 into $CH_3 + C_2H_4$

Method of investigation	log k[sec^{-1}]	References
Photolysis of n-C_3H_7CHO	11.7-25.2/2.3 RT	Kerr and Trotman-Dickenson (43)
Photolysis of n-$C_3H_7N_2C_3H_7$	15.4-34.5/2.3 RT	Kerr and Calvert (55)
Photolysis of $CH_3N_2CH_3$ in the presence of n-C_3H_7CHO	15.3-34.9/2.3 RT	Calvert and Sleppy (56)
Thermochemical estimate based on the results of ref. (43)	13.9-31/2.3 RT	Jackson and McNesby (45)
$CH_3N_2CH_3$-sensitized decomposition of C_3H_8	13.5-31.4/2.3 RT	Lin and Laidler (57)
Hg-photosensitized decomposition of C_3H_8	9.2-20/2.3 RT	Bywater and Steacie (28)
Hg-photosensitized decomposition of C_3H_8	9.6-22/2.3 RT	Back and Takamuku (34)
Hg-photosensitized decomposition of C_3H_8	14.4-32.6/2.3 RT	This work; high pressure value
Hg-photosensitized decomposition of C_3H_8	15.2-34.4/2.3 RT	This work; k^{∞}_{20b} from the intercepts of Lindemann plots
Hg-photosensitized decomposition of C_3H_8	7.4-17.0/2.3RT	This work; k^{o}_{20b} from the slopes of Lindemann plots

In the work of Kerr and Trotman-Dickenson (43) the photolysis of n-butyraldehyde was investigated in the temperature range 270 - 420°C at an n-butyraldehyde pressure of about 25 mm Hg. They noticed that a three-fold increase of pressure caused the rate constant to increase by a factor of about 1.6. A similar increase was obtained by adding some 60 mm Hg of carbon dioxide. A reduction in the aldehyde pressure by a factor of 20 considerably lowered the rate constant. This aspect of the investigation was not carried further. It is conceivable that these measurements were carried out in the pressure-dependent region, which explains the somewhat lower Arrhenius parameters.

Kerr and Calvert (55) studied the vapor phase photolysis of azo-n-propane from 24°C to 290°C at a wave length of 3660 A. The pressure of azo-n-propane was about 25 mm Hg. When the initial pressure of azo-n-propane was approximately doubled the rate constant was increased by a factor of about 1.4. The addition of about 450 mm Hg of carbon dioxide also increased the rate constant. The more efficient activator, trimethylamine, caused the same increase at about 70 mm Hg. A quantitative study of the pressure dependence of the rate constant was not carried out. Since the reaction was studied at relatively low temperatures, and azo-n-propane is an efficient energizer, it may be expected that the reaction was being studied close to the pressure-independent region. However, it should be pointed out that reactions such as

$$C_3H_6N_2C_3H_7 \rightarrow C_2H_4 + CH_2N_2C_3H_7$$

may represent an additional source of ethene in their system, thus causing an apparent increase of the rate constant.

In the work by Calvert and Sleppy (56) thermally-equilibrated n-propyl radicals were generated homogeneously by the selective photolysis of azomethane at 3660 A in n-butyraldehyde-azomethane mixtures. The reaction was studied in the temperature range 200 to 280°C at total pressures from 80 to 100 mm Hg. This investigation was probably also carried out in the pressure-independent region. When the pressure was halved, however, the calculated rate constant increased somewhat (55). The apparent increase of the rate constant with decrease in pressure was most surprising; non-homogeneous light absorption in the azomethane mixtures may explain these results. A possible source of error in the aldehyde work is the presence of the radicals $CH_2CH_2CH_2CHO$ and CH_3CH_2CHCHO, which may decompose into $C_2H_4 + CH_2CHO$ and $CH_3 + CH_2CHCHO$ respectively: there would therefore be higher rates of formation of methane and ethene.

Lin and Laidler (57) investigated the thermal decomposition of propane sensitized by azomethane in the temperature range from 260 to 300°C at a pressure of about 190 mm Hg. The decomposition of n-propyl radicals occurred close to the pressure-independent region, so that the high-pressure Arrhenius parameters were obtained.

The measurements of Bywater and Steacie (28) and of Back and Takamuku (34) were most probably carried out in the pressure-dependent region so that low values for Arrhenius parameters were obtained. Their values fall between the values for the low pressure limiting rate constant and the high-pressure limiting rate constant obtained in this work.

The present data are compared with those of the previous studies in Figure 44.

FIGURE 44

Arrhenius plots of the rate constant, k_{20b}, obtained in several different studies.

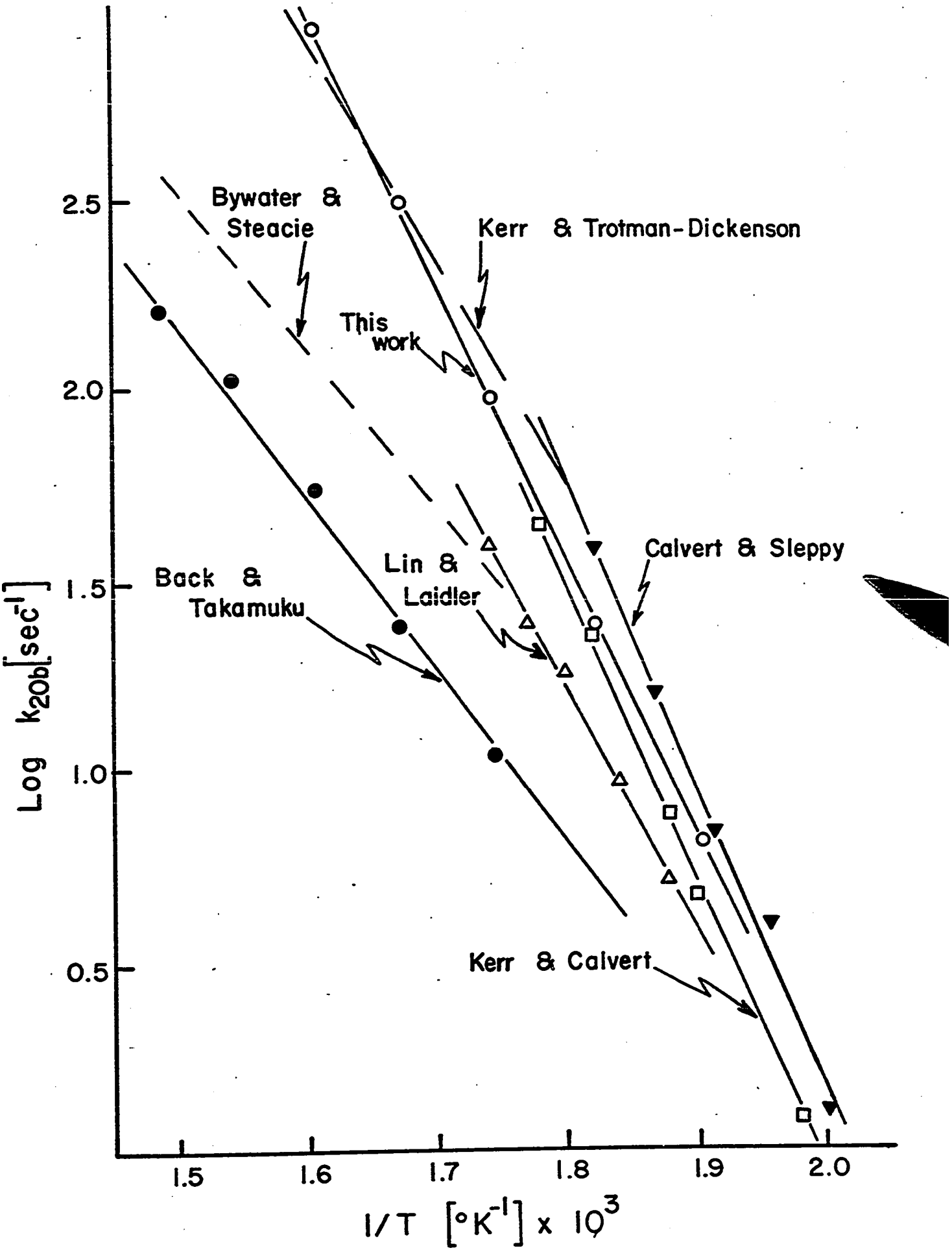
Bywater &
Steacie
Kerr & Trotman-Dickenson
This
work
Calvert & Sleppy
Lin &
Laidler
Back &
Takamuku
Kerr & Calvert
Log k20b[sec-1]
2.5
2.0
1.5
1.0
0.5
1.5
1.6
1.7
1.8
1.9
2.0
1/T [°K-1] x 10^3

Thermochemistry: - With the high pressure value of E_{20b} it is possible to calculate the bond dissociation energy of the C-C bond in the n-propyl radical, the standard enthalpy of formation of the n-propyl radical, and the primary C-H bond dissociation energy in the propane molecule.

The activation energy $E_{20b} = 32.6$ kcal.mole^{-1} is related to the standard enthalpy change ΔH^{o}_{20b} for the reaction [20b] at a given temperature T by:

$$(48) \qquad \Delta H^{o}_{20b} = E_{20b} - E_{-20b} + RT = \Delta H^{o}_{20bO} + \int_{o}^{T} \Delta C_p dT$$

where ΔH^{o}_{20bO} is the standard enthalpy change at $0^{o}K$. By definition

$$(49) \qquad \Delta H^{o}_{20bO} = D_o(n\text{-}CH_3\text{-}CH_2CH_2)$$

where D_o denotes the dissociation energy at $0^{o}K$. Therefore

$$(50) \qquad D_o(n\text{-}CH_3\text{-}CH_2CH_2) = E_{20b} - E_{-20b} + RT - \int_{o}^{T} \Delta C_p dT$$

The integral $\int_{o}^{T} \Delta C_p dT$ presents the net enthalpy change in raising the system from $0^{o}K$ to $T^{o}K$. To evaluate the integral the heat capacities of CH_3, C_2H_4 and C_3H_7 should be known as a function of temperature. Since the heat capacities as a function of temperature are not known over a wide enough range of temperatures, it is easier to evaluate the net enthalpy change from the listed values for the heat contents. On the assumption that the enthalpy of $n\text{-}C_3H_7$ is the same as

for C_3H_8 and using the values for heat contents of C_2H_4 and C_3H_8 (58) and of CH_3 (59) the net enthalpy change in raising the system from 0°K to 600°K (approximately the middle of the present temperature range) is 1.3 kcal.mole^{-1}. The value of RT at 600°K is 1.2 kcal.mole^{-1}. Taking the value for E_{-20b} = 8.6 kcal.mole^{-1} obtained by Brinton (60), the bond dissociation energy at 0°K, $D_o(n\text{-}CH_3\text{-}CH_2CH_2)$ is obtained:

$$D_o(n\text{-}CH_3\text{-}CH_2CH_2) = 23.9 \text{ kcal.mole}^{-1}$$

The standard bond dissociation energy DH^o at 25°C then amounts to

$$DH^o(n\text{-}CH_3\text{-}CH_2CH_2) = 24.3 \text{ kcal.mole}^{-1}$$

which compares well with 23.0 kcal.mole^{-1} and 25.5 kcal.mole^{-1} obtained by Lin and Laidler (57) and Benson (61) respectively.

From the relation

$$(51) \qquad DH^o(n\text{-}CH_3\text{-}CH_2CH_2) = \Delta H_f^o(CH_3) + \Delta H_f^o(C_2H_4) - \Delta H_f^o(n\text{-}C_3H_7)$$

the standard heat of formation $\Delta H_f^o(n\text{-}C_3H_7)$ for the n-propyl radical may be obtained. If the standard heat of formation for the methyl radical, $\Delta H_f^o(CH_3)$ is 32.0 kcal.mole^{-1}, and that for ethene $\Delta H_f^o(C_2H_4)$ is 12.5 kcal.mole^{-1} (17), the standard heat of formation for the n-propyl radical is:

$$\Delta H_f^o(n\text{-}C_3H_7) = 20.2 \text{ kcal.mole}^{-1}.$$

This is to be compared with 20.9 kcal.mole^{-1} listed by Calvert and Pitts (17).

The primary C-H standard bond dissociation energy in propane may be obtained from the relation

(52) $$DH^{o}(CH_3CH_2CH_2\text{-}H) = \Delta H_f^{o}(n\text{-}C_3H_7) + \Delta H_f^{o}(H) - \Delta H_f^{o}(C_3H_8)$$

With $\Delta H_f^{o}(H) = 52.1$ kcal.mole^{-1}, $\Delta H_f^{o}(C_3H_8) = -24.8$ kcal. mole^{-1} (17), and $\Delta H_f^{o}(n\text{-}C_3H_7) = 20.2$ kcal.mole^{-1}, obtained in this work,

$$DH^{o}(CH_3CH_2CH_2\text{-}H) = 97.1 \text{ kcal.mole}^{-1}$$

This is to be compared with the value 98 ± 2 kcal.mole^{-1} listed by Kerr (62).

The thermodynamical formulation of reaction rates gives the unimolecular rate coefficient in the form

(53) $$k = e\frac{kT}{h}\, e^{\Delta S^{\neq}/R} e^{-E_{exp}/RT} \text{ sec}^{-1}$$

where $\Delta S^{\neq}$ is the entropy of activation, and other symbols have their usual meaning. Comparison with the Arrhenius equation

(54) $$k = Ae^{-E_{exp}/RT} \text{ sec}^{-1}$$

gives

(55) $$A = e\frac{kT}{h}\, e^{\Delta S^{\neq}/R} \text{ sec}^{-1}$$

and

(56) $$\Delta S^{\neq} = R(\ln A - \ln \frac{ekT}{h}) \text{ cal.deg.}^{-1}\text{mole}^{-1}.$$

For the decomposition of n-propyl radicals into methyl and ethene at 600°K we obtain

$$\Delta S^{\neq} = 4.1 \text{ cal.deg.}^{-1}\text{mole}^{-1},$$

and at 25°C

$$\Delta S^{\neq} = 5.4 \text{ cal.deg.}^{-1}\text{mole}^{-1}.$$

These values indicate a loose structure of the activated complex.

The entropy change for the reaction [20b] may be evaluated from the expression:

(57) $\Delta S_{20b} = R \ln (A_{20b}/A_{-20b})$ cal.deg.$^{-1}$mole^{-1}

With Brinton's (60) data for $A_{-20b} = 10^{12.1}$ cc.mole^{-1}sec^{-1}

$$\Delta S_{20b} = 10.6 \text{ cal.deg.}^{-1}\text{mole}^{-1}$$

if the standard state is taken as 1 mole cc^{-1} of ideal gas. This value compares well with $\Delta S_{20b} = 12.0$ cal.deg.$^{-1}$mole^{-1} calculated from listed entropies (17) for ethene, methyl and n-propyl radicals at 25°C.

Decomposition to propene: There is some uncertainty about the relative rates of decomposition of i-propyl radicals into ethene and methyl radicals, and into propene and hydrogen atoms respectively. Also, if decomposition of i-propyl radicals into ethene occurs under given conditions, it is not certain whether it occurs directly or via the isomerization into n-propyl radicals. The activated complex is probably the same for the isomerization reaction and the direct decomposition: $CH_3 - \underset{\diagdown\ \diagup}{CH} - CH_2$ (H). However, there is no direct evidence of the isomerization process. Billinge and Gowenlock (63) pyrolyzed separately di-n-propylmercury and di-i-propylmercury in order to investigate the isomerization of propyl radicals. In neither case did the products reveal the occurrence of the isomeric propyl radicals.

Jackson and McNesby (64) found the ratio of the rate constants k_{21b}/k_{21a} for the i-propyl radical decomposition into ethene and methyl and into propene and hydrogen atoms respectively to be about 0.04 at 500°C, with no evident temperature trends. If the isomerization of i-propyl to n-propyl is simultaneous with, or is an immediate precursor of decomposition, they concluded that $k_{21b}/k_{21a} \approx 0.07$. Falconer, Rabinovitch and Cvetanovic (65) pointed out that this value must be accepted as an upper limit, and that C-H rupture is the predominant path for the i-propyl decomposition, possibly to the exclusion of the C-C rupture. On the other hand, Kerr and Trotman-Dickenson (44) give expressions for the corresponding rate constants, from which the ratio $k_{21b}/k_{21a} \approx 1$ in the temperature range from 250°C to 350°C may be evaluated. From the results of Heller and Gordon (66) the ratio k_{21b}/k_{21a} in the temperature range from 250°C to 350°C is again close to unity.

The percentage conversion in the work of Kerr and Trotman-Dickenson (44) and of Heller and Gordon (66) was not mentioned. It should be pointed out that in some instances the ethene in the isopropyl systems might arise from the reactions:

$$H + C_3H_6 \rightarrow n\text{-}C_3H_7$$

$$n\text{-}C_3H_7 \rightarrow CH_3 + C_2H_4$$

Although the non-terminal addition of hydrogen atoms to propene amounts to only 6% (67), continued attack by the H atoms may eventually lead to substantial C-C rupture via n-propyl radicals.

From the point of view of hydrogen production in the present system, the eventual loss of i-propyl radicals via reaction [21b] tends to be compensated by the occurrence of the reaction [20a]. The present discussion will therefore be based on the assumption that all

hydrogen comes from the decomposition of i-propyl radicals and that all i-propyl radicals decompose via reaction [21a], bearing in mind the uncertainties involved. If the assumption proved to be incorrect, then the derived kinetic parameters would correspond to some average value for n- and i-propyl radicals. The kinetic parameters for the decomposition of n- and i-propyl radicals into propene are very close (46) (see also Table 11) and the eventual error involved cannot be of much significance.

From the reaction scheme the rate of decomposition of i-propyl radicals is given by:

$$v_{21a} = k_{21a}[S]$$

where k_{21a} is a defined first order rate coefficient. The rate of propene production was not measured in the present work. The rate of hydrogen production by reaction [21a] (chain hydrogen) may be obtained by subtracting the rate of the low-temperature hydrogen production, v_3, from the rate of the total hydrogen production. The rate coefficient k_{21a} is then given by:

$$k_{21a} = \frac{v_{21a}}{[S]} = \frac{v_{H_2(\text{chain})}}{[S]} \qquad (58)$$

The rate of 2, 3-DMB production is given by:

$$v_{2,3\text{-DMB}} = k_5[S]^2$$

The concentrations of i-propyl radicals can be expressed in terms of the rate of 2, 3-DMB production and the following expression is obtained for the rate coefficient k_{21a}:

(59) $$k_{21a} = k_5^{1/2} v_{H_2(chain)} / (v_{2,3\text{-DMB}})^{1/2}$$

With $k_5 = 10^{13.4}$ cc.mole^{-1}sec^{-1} and temperature independent (37), k_{21a} can be evaluated. The obtained values of the rate constant k_{21a} at different temperatures and pressures are listed in Table 17.

The rate coefficient k_{21a} does not show any regular dependence on the propane pressure at pressures above about 10 mm Hg. If there is a fall off of k_{21a} with decreasing propane pressure it must then take place in the pressure region below 10 mm Hg. The plot of the logarithms of the high-pressure rate coefficient against the reciprocal temperature is shown in Figure 45. From the plot the value of the high-pressure rate constant can be expressed as:

$$k_{21a} = 2.0 \times 10^{14} \exp(-38.7/RT) \text{ sec}^{-1}$$

The values of the rate constant for the decomposition of i-propyl radicals into propene and hydrogen obtained by other authors are listed in Table 18.

TABLE 17

Values of the first-order rate coefficient k_{21a} at different temperatures and propane pressures*

T[°C]	301	325	350
$P_{C_3H_8}$[mm Hg]	k_{21a}	k_{21a}	k_{21a}
5	0.29	0.98	3.6
10	0.38	1.5	5.7
20	0.42	1.8	6.6
30	0.45	1.8	6.0
40	0.40	1.7	6.5
60	0.33	1.5	5.8
80	0.35	1.5	5.5
100	0.38	1.5	5.3
150	0.37	1.4	5.1
200	0.37	1.4	5.1
250	0.37	1.4	5.1
300	0.37	1.4	5.1

* The values for k_{21a} are quoted in sec^{-1}.

TABLE 18

Kinetic parameters for the decomposition of i-C_3H_7 into H + C_3H_6

Method of investigation	log k [sec^{-1}]	References
Photolysis of i-C_3H_7CHO	13.8-36.9/2.3 RT	Kerr and Trotman-Dickenson (44)
Photolysis of $(i\text{-}C_3H_6D)_2CO$	13.1-35/2.3 RT	Heller and Gordon (66)
Thermochemical estimate based on results of ref. (28, 44, 66)	15.0-42/2.3 RT	Leathard and Purnell (68)
Hg-photosensitised decomposition of C_3H_8	14.6-38/2.3 RT	Bywater and Steacie (28)
Hg-photosensitized decomposition of C_3H_8	14.0-37/2.3 RT	Back and Takamuku (34)
Hg-photosensitized decomposition of C_3H_8	14.3-38.7/2.3 RT	This work; k_{21a} high pressure value

FIGURE 45

An Arrhenius plot of k_{21a} at a propane pressure of 300 mm Hg.

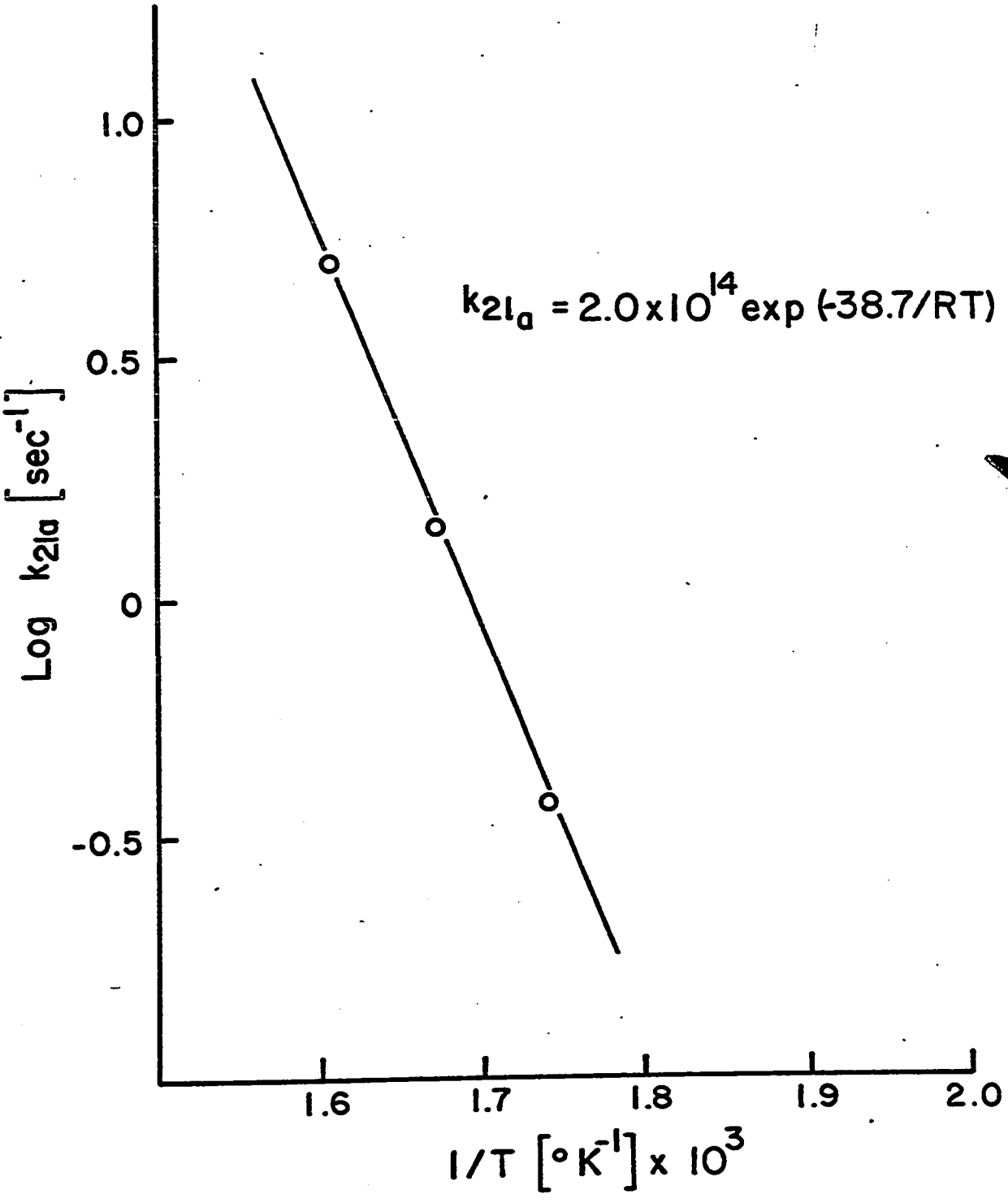
$k_{21a} = 2.0 \times 10^{14} \exp(-38.7/RT)$
Log k_{21a} [sec^{-1}]
1.0
0.5
0
-0.5
1.6
1.7
1.8
1.9
2.0
$1/T$ [$°K^{-1}$] x 10^3

Kerr and Trotman-Dickenson (44) investigated the photo-initiated chain decomposition of i-butyraldehyde between 20°C and 500°C. The rate of formation of propene by decomposition of i-propyl radicals was obtained as a difference between the rate of total propene production and the rate of propene production by disproportionation of i-propyl radicals and decomposition of i-butyryl radicals. The amounts of 2, 3-DMB were estimated from measurements of the rate of propane production. In view of the complexities the agreement with present work is very good.

Heller and Gordon (66) studied the photolysis of di-i-propylketone-d2 over the temperature range from 100°C to 500°C. In their work the rate of production of propene by decomposition of i-propyl radicals was obtained by subtraction from the total propene produced of the propene produced by disproportionation of i-propyl radicals and by decomposition of ketonyl radicals. This procedure could involve some error which may be reflected in a somewhat lower activation energy.

Leathard and Purnell (68) obtained an expression for the rate constant, k_{21a}, from a thermochemical estimate of $E_{21a} - E_{-21a}$ as 38.8 kcal.mole^{-1} near 800°K, and by taking the value of k_{21a} at 800°K as $10^{13.5}$ (our value at 800°K is $10^{13.8}$). For the activation energy, E_{-21a}, they assumed the value of 3 kcal. mole^{-1}, and they obtained the E_{21a} as 42 kcal.mole^{-1}. Yang (69) suggested 1.5 or 2.2 kcal.mole^{-1} for E_{-21a}. The value of 42 kcal. mole^{-1} can be in error by any error in the value for E_{-21a}.

The studies of Bywater and Steacie (28) and of Back and Takamuku (34) on the mercury-photosensitized decomposition of propane have been discussed earlier. It should be noted that here, in contrast with the case of decomposition of n-propyl radicals, good agreement exists between their results and the results obtained in the present work. Here the agreement is to be expected since both measurements were carried out in the pressure-independent region.

The position of the present data relative to those of the previous studies is shown in Figure 46.

Thermochemistry: With the high pressure value of E_{21a} it is possible to calculate the bond dissociation energy of the C-H bond in the i-propyl radical, the standard enthalpy of formation of the i-propyl radical and the secondary C-H bond dissociation energy in the propane molecule.

The activation energy $E_{21a} = 38.7$ kcal.mole^{-1} is related to the standard enthalpy change ΔH^{o}_{21a} for the reaction [21a] at a given temperature T by

$$\Delta H^{o}_{21a} = E_{21a} - E_{-21a} + RT \tag{60}$$

$$= \Delta H^{o}_{21aO} + \int_{o}^{T} \Delta C_p dT$$

where ΔH^{o}_{21aO} is the [illegible] enthalpy change at $0^{o}K$. By definition

$$\Delta H^{o}_{21aO} = D_o(i\text{-}CH_3CHCH_2\text{-}H) \tag{61}$$

where D_o denotes the dissociation energy at $0^{o}K$. Therefore,

FIGURE 46

Arrhenius plots of the rate constant, k_{21a}, obtained in several different studies.

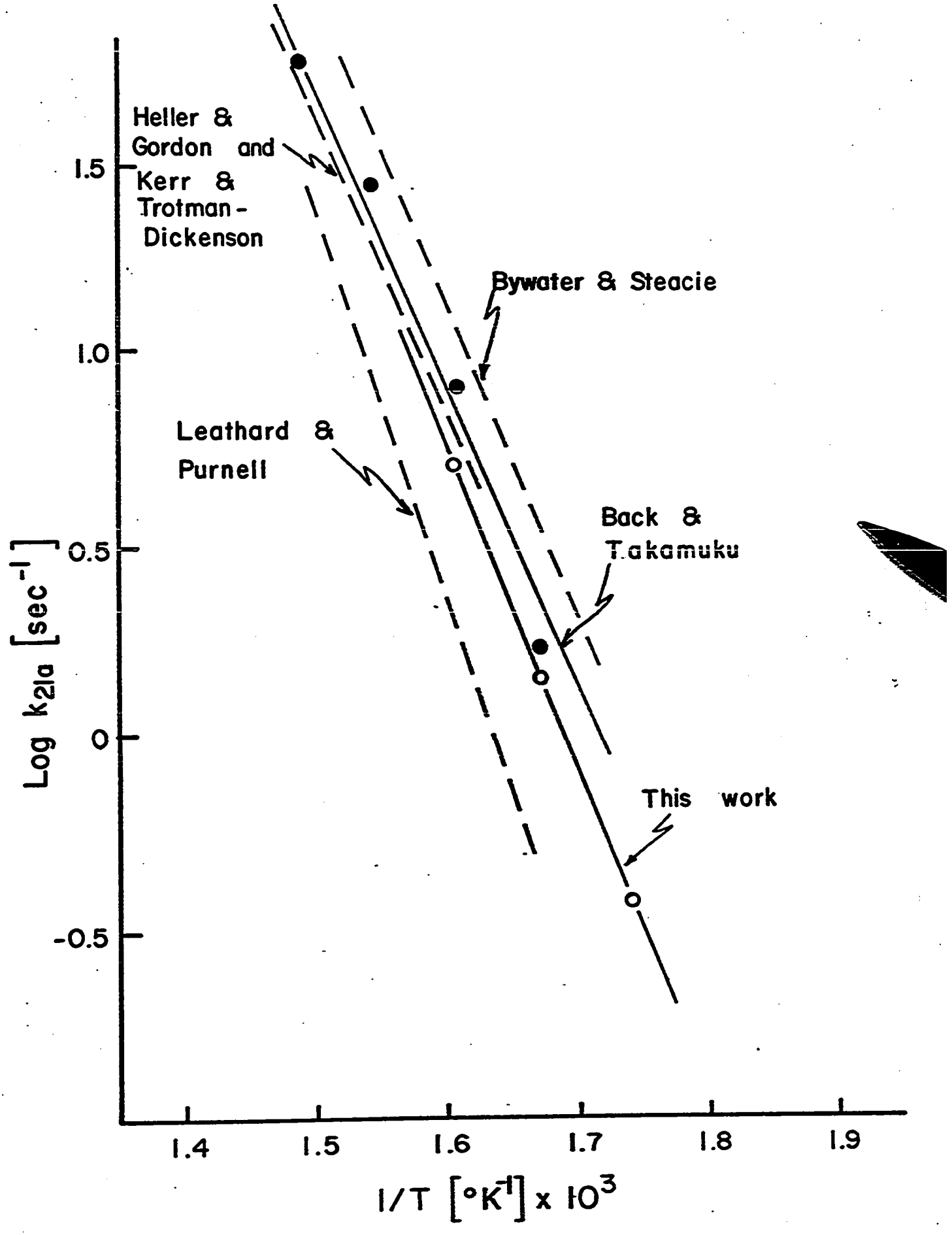
Heller &
Gordon and
Kerr &
Trotman-
Dickenson
Bywater & Steacie
Leathard &
Purnell
Back &
Takamuku
This work
Log k_{21a} [sec^{-1}]
1.5
1.0
0.5
0
-0.5
1.4
1.5
1.6
1.7
1.8
1.9
1/T [$°K^{-1}$] x 10^3

(62) $$D_o(i\text{-}CH_3CHCH_2\text{-}H) = E_{21a}\text{-}E_{-21a} + RT - \int_o^T \Delta C_p dT$$

Here again, the integral $\int_o^T \Delta C_p dT$ represents the net enthalpy change in raising the system from 0^oK to T^oK. To evaluate the integral, the heat capacities of H, C_3H_6 and C_3H_7 should be known as a function of temperature. Since the heat capacities as a function of temperature are not known over a wide enough range of temperatures, it is easier to evaluate the net enthalpy change from the listed values for the heat contents. On the assumption that the enthalpy of $i\text{-}C_3H_7$ is the same as for C_3H_8 and using the values for the heat contents of C_3H_6 and C_3H_8 (58) and of H (59), the net enthalpy change in raising the system from 0^oK to 600^oK (approximately the middle of the present temperature range) is 1.5 kcal.mole^{-1}. The value of RT at 600^oK is 1.2 kcal.mole^{-1}. With the value E_{-21a} = 1.5 kcal. mole^{-1} (69), the bond dissociation energy at 0^oK, $D_o(i\text{-}CH_3CHCH_2\text{-}H)$ is obtained:

$$D_o(i\text{-}CH_3CHCH_2\text{-}H) = 36.9 \text{ kcal.mole}^{-1}$$

The standard bond dissociation energy DH^o at 25^oC then amounts to

$$DH^o(i\text{-}CH_3CHCH_2\text{-}H) = 38.1 \text{ kcal.mole}^{-1}$$

which can be compared with 39 kcal.mole^{-1} listed by Kerr (62).

From the relation

(63) $$DH^o(i\text{-}CH_3CHCH_2\text{-}H) = \Delta H_f^o(H) + \Delta H_f^o(C_3H_6) - \Delta H_f^o(i\text{-}C_3H_7)$$

the standard heat of formation $\Delta H_f^o(i\text{-}C_3H_7)$ for the i-propyl radical may be obtained. If the standard heat of formation for the hydrogen atom, $\Delta H_f^o(H)$ is 52.1 kcal.mole^{-1}, and that for propene, $\Delta H_f^o(C_3H_6)$ is 4.9 kcal.mole^{-1} (17), the standard heat of formation for the i-propyl radical is

$$\Delta H_f^o(i\text{-}C_3H_7) = 18.9 \text{ kcal.mole}^{-1}$$

compared with 17.6 kcal.mole^{-1} listed by Benson (61).

The secondary C-H standard bond dissociation energy in the propane molecule may be obtained from the relation

$$(64) \quad DH^o[(CH_3)_2CH\text{-}H] = \Delta H_f^o(i\text{-}C_3H_7 + \Delta H_f^o(H) - \Delta H_f^o(C_3H_8)$$

With $\Delta H_f^o(H)$ = 52.1 kcal.mole^{-1}, $\Delta H_f^o(C_3H_8)$ = -24.8 kcal.mole^{-1} (17) and $\Delta H_f^o(i\text{-}C_3H_7)$ = 18.9 kcal.mole^{-1}, obtained in this work,

$$DH^o[(CH_3)_2CH\text{-}H] = 95.8 \text{ kcal.mole}^{-1}$$

This is to be compared with the value 94.5 kcal.mole^{-1} listed by Kerr (62).

The thermodynamical formulation of the reaction rates gives the unimolecular rate coefficient in the form

$$(65) \qquad k = e \frac{kT}{h} e^{\Delta S^{\neq}/R} e^{-Eexp/RT} \text{ sec}^{-1}$$

where $\Delta S^{\neq}$ is the entropy of activation, and other symbols have their usual meaning. Comparison with the Arrhenius equation

$$(66) \qquad k = Ae^{-E_{exp}/RT} \text{ sec}^{-1}$$

gives

$$(67) \qquad A = e \frac{kT}{h} e^{\Delta S^{\neq}/R} \text{ sec}^{-1}$$

and

(68) $$\Delta S^{\neq} = R(\ln A - \ln \frac{ekT}{h}) \text{cal deg.}^{-1}\text{mole}^{-1} \quad .$$

For the decomposition of i-propyl radicals into hydrogen atoms and propene at 600°K we obtain

$$\Delta S^{\neq} = 3.7 \text{ cal.deg.}^{-1}\text{mole}^{-1}$$

or at 25°C

$$\Delta S^{\neq} = 5.0 \text{ cal.deg.}^{-1}\text{mole}^{-1} \ .$$

These values indicate a loose activated complex for the decomposition of i-propyl radicals into H and C_3H_6.

The entropy change for the reaction [21a] may be evaluated from the expression:

(69) $$\Delta S_{21a} = R \ln (A_{21a}/A_{-21a}) \text{ cal.deg.}^{-1}\text{mole}^{-1}$$

With Yang's (69) value of 10^{13} cc.mole^{-1}sec^{-1} for A_{-21a}, it is found that

$$\Delta S_{21a} = 6.0 \text{ cal.deg.}^{-1}\text{mole}^{-1} \ ,$$

the standard state being taken as 1 mole cc^{-1} of ideal gas. This value compares well with $\Delta S_{21a} = 5.2$ cal.deg.$^{-1}$mole^{-1} calculated from listed entropies (17) for propene, hydrogen atoms and i-propyl radicals at 25°C.

CLAIMS TO ORIGINAL RESEARCH

1. The mercury-photosensitized decomposition was re-investigated at 252°C, 276°C, 301°C, 325°C and 350°C and in the pressure range from 5 mm Hg to 700 mm Hg. The kinetics of the formation of hydrogen, methane, ethene, ethane, 2, 3-dimethylbutane, 2-methylpentane and n-hexane have been studied in detail.

2. The rates of formation of all measured products were found to be pressure dependent. The rates approached constant values at high pressures of propane. The influence of CO_2 as a foreign gas has been examined to check this pressure dependence.

3. On the basis of the proposed mechanism a semi-quantitative discussion of the pressure dependence of the rates of the product formation has been given.

4. The pressure dependence of the energy of activation for the production of methane and ethene has been examined, and the formation of hot propyl radicals in the first elementary act has been considered.

5. From the measurements of the rates of 2, 3-DMB, 2-MP and n-C_6H_{14} production, the cross-combination ratio $k_{ab}/(k_{aa} \times k_{bb})^{1/2}$ was found to be close to 2. The ratio k_9/k_6, for the cross-disproportionatinn has been derived; the value of 0.38 has been obtained. The ratio of i-propyl to n-propyl radicals at propane pressure of 300 mm Hg has been found to be given by the expression $[S]/[P] = 1.7 \times 10^2 \exp(-3.1/RT)$.

6. The pressure dependence of the first-order rate coefficient for the unimolecular decomposition of the n-propyl radical into methyl radical and ethene has been examined. The limiting high-pressure and low-pressure Arrhenius parameters for the thermal decomposition of the n-propyl radical have been deduced from a temperature and pressure study. The number of normal modes of vibration contributing to the energization of the n-propyl radical has been estimated.

7. From the limiting high-pressure Arrhenius parameters for the n-propyl radical decomposition, and from the high-pressure energy of activation for the ethene production, the temperature dependences of the concentrations of n-propyl and i-propyl radicals were obtained.

8. From the kinetic measurements the C-C bond dissociation energy in the n-propyl radical has been calculated. The standard enthalpy of formation of the n-propyl radical, and the primary C-H bond dissociation energy in the propane molecule, have been derived. The entropy of activation for the unimolecular decomposition of the n-propyl radical into a methyl radical and ethene has been estimated. The entropy change in the decomposition reaction of n-propyl radical has been evaluated.

9. The pressure dependence of the first-order rate coefficient for the unimolecular decomposition of the i-propyl radical into a hydrogen atom and propene has been examined. The high-pressure Arrhenius parameters for the thermal decomposition of the i-propyl radical have been deduced from a temperature and pressure study.

10. From the kinetic measurements the C-H bond dissociation energy in the i-propyl radical has been calculated. The standard enthalpy of formation of the i-propyl radical, and the secondary C-H bond dissociation energy in the propane molecule, have been derived. The entropy of activation for the unimolecular decomposition of the i-propyl radical into a hydrogen atom and propene has been estimated. The entropy change in the decomposition reaction of i-propyl radical has been evaluated.

REFERENCES

1. E. W. R. Steacie, Atomic and Free Radcial Reactions, Reinhold Publishing Corp., New York, 1954, p. 494.
2. N. N. Semenov, Some Problems of Chemical Kinetics and Reactivity, Pergamon Press, New York, 1958, p. 1.
3. M. C. Lin and K. J. Laidler, Can. J. Chem., 44 (1966) 2927.
4. R. A. Back and S. Takamuku, J. Am. Chem. Soc., 86 (1964) 2558.
5. J. A. Kerr and J. G. Calvert, J. Am. Chem. Soc., 83 (1961) 3391.
6. W. M. Jackson and J. R. McNesby, J. Am. Chem. Soc., 83 (1961) 4891.
7. J. A. Kerr and A. F. Trotman-Dickenson, Trans. Faraday Soc., 55 (1959) 592.
8. J. G. Calvert and W. C. Sleppy, J. Am. Chem. Soc., 81 (1959) 1544.
9. S. Bywater and E. W. R. Steacie, J. Chem. Phys., 19 (1951) 319.
10. E. W. R. Steacie and D. J. Dewar, J. Chem. Phys., 8 (1940) 571.
11. K. J. Laidler, J. Chem. Phys., 15 (1947) 712.
12. E. W. R. Steacie, Ann. N. Y. Acad. Sci., 41 (1941) 187.
13. K. J. Laidler, J. Chem. Phys., 10 (1942) 43.
14. C. R. Masson and E. W. R. Steacie, J. Chem. Phys., 18 (1950) 210.

15. E. W. R. Steacie and D. J. LeRoy, J. Chem. Phys., 12 (1944) 34.

16. H. E. Gunning and O. P. Strausz, Mercury Photosensitization, Advances in Photochemistry, Vol. 1, eds. W. A. Noyes Jr., G. S. Hammond and J. N. Pitts Jr., Intersci. Pub., a division of John Wiley and Sons, New York, 1963.

17. J. G. Calvert and J. N. Pitts Jr., Photochemistry, John Wiley and Sons, New York, 1966.

18. E. Jakubowski, P. Kebarle, O. P. Strausz and H. E. Gunning, Can. J. Chem. 45 (1967) 2287.

19. R. A. Holroyd and G. W. Klein, J. Phys. Chem., 67 (1963) 2273.

20. B. deB. Darwent, J. Chem. Phys., 18 (1950) 1532.

21. G. N. C. Woodall and H. E. Gunning, Bull. Soc. Chim. Belges., 71 (1962) 725.

22. M. Avrahami and P. Kebarle, Can. J. Chem., 41 (1963) 347.

23. Y. Russeau, G. N. C. Woodal and H. E. Gunning, J. Chem. Phys., 37 (1962) 2722.

24. Y. Russeau and H. E. Gunning, Can. J. Chem., 41 (1963) 465.

25. B. deB. Darwent, E. W. R. Steacie, J. Chem. Phys., 16 (1948) 381.

26. S. Bywater, and E. W. R. Steacie, J. Chem. Phys., 19 (1951) 326.

27. B. deB. Darwent and E. W. R. Steacie, J. Chem. Phys., 13 (1945) 563.

28. S. Bywater, and E. W. R. Steacie, J. Chem. Phys., 19 (1951) 319.

29. R.A. Back, Can.J.Chem., 37 (1959) 1834.

30. R.A. Back, Trans.Faraday Soc., 54 (1958) 512.

31. R.J. Cvetanovic, J.Chem.Phys., 23 (1955) 1208.

32. R.J. Cvetanovic, W.E. Falconer and K.R. Jennings, J.Chem.Phys., 35 (1961) 1225.

33. R. Payette, M. Bertrand and Y. Rousseau, J.Am.Chem. Soc., 90 (1968) 5341.

34. R.A. Back and S. Takamuku, J.Am.Chem.Soc., 86 (1964) 2558.

35. M. Papic, J.Gas Chromatogr. 6 (1968) 493.

36. L.F. Loucks and K.J. Laidler, Can.J.Chem., 45 (1967) 2795.

37. A.F. Trotman-Dickenson and G.S. Milne, Tables of Bimolecular Gas Reactions, NSRDS-NBS 9, U.S.Department of Commerce, Washington, D.C. 1967.

38. A.D. Stepukhovich and V.A. Ulitskii, Uspekhi Khimii, 35 (1966) 487.

39. J.A. Kerr and A.F. Trotman-Dickenson, The Reactions of Alkyl Radicals, Prog.Reac.Kinetics, Vol. 1, Ed. G.Porter, Pergamon Press, 1961.

40. A.F. Trotman-Dickenson, Ann.Rep.Chem.Soc., 1958, 36

41. A.F. Trotman-Dickenson, Adv.Free Radical Chem., 1 (1965) 1.

42. E.L. Metcalfe and A.F. Trotman-Dickenson, J.Chem.Soc., 1962, 4620.

43. J.A. Kerr and A.F. Trotman-Dickenson, Trans.Faraday Soc., 55 (1959) 572.

44. J.A. Kerr and A.F. Trotman-Dickenson, Trans.Faraday Soc., 55 (1959) 921.

45. W.M. Jackson and J.R. McNesby, J.Am.Chem.Soc., 83 (1961) 4891.

46. J.A. Kerr and A.C. Lloyd, Quart.Rev., 22 (1968) 549.

47. R.J. Cvetanovic, Mercury Photosensitized Reactions, Prog.Reac.Kinetics, Vol. 2, Ed. G. Porter, Pergamon Press, 1964.

48. K.J. Laidler, Chemical Kinetics, McGraw-Hill Book Co., New York, 1965.

49. M.C. Lin and M.H. Back, Can.J.Chem., 44 (1966) 2357.

50. R.K. Brinton and E.W.R. Steacie, Can.J.Chem., 33 (1955) 1840.

51. K.J. Laidler, Theories of Chemical Reaction Rates, McGraw Hill Book Co., New York, 1969.

52. D.M. Bishop and K.J. Laidler, J.Chem.Phys., 42 (1965) 1688.

53. A.R. Blake, J.F. Henderson and K.O. Kutschke, Can.J.Chem. 39 (1961) 1920.

54. E.K. Gill and K.J. Laidler, Proc.Roy.Soc. A251 (1959) 66.

55. J.A. Kerr and J.G.Calvert, J.Am.Chem.Soc., 83 (1961) 3391.

56. J.G. Calvert and W.C. Sleppy, J.Am.Chem.Soc., 81 (1959) 1544.

57. M. C. Lin and K.J. Laidler, Can.J. Chem., 44 (1966) 2927.

58. F.D. Rossini, K.S. Pitzer, R.L. Arnett, R.M. Braunaud and G.C. Pimentel, Selected Values of Physical and Thermodynamic Properties of Hydrocarbons and Related Compounds, American Petroleum Institute Research Project 44, Carnegie Press, Pittsburgh, 1953.

59. JANAF Interim Thermochemical Tables, The Dow Chemical Comp., Midland, Michigan.

60. R.K. Brinton, J. Chem. Phys., 29 (1958) 781.

61. S.W. Benson, J. Chem. Ed., 42 (1965) 502.

62. J.A. Kerr, Chem. Rev., 66 (1966) 465.

63. B.H.M. Billinge and B.G. Gowenlock, J. Chem. Soc., 1962, 3252

64. W.M. Jackson and J.R. McNesby, J. Chem. Phys., 36 (1962) 2272.

65. W.E. Falconer, B.S. Rabinovitch and R.J. Cvetanovic, J. Chem. Phys., 39 (1963) 40.

66. C.A. Heller and A.S. Gordon, J. Phys. Chem., 62 (1958) 709.

67. R.J. Cvetanovic, Addition of Atoms to Olefins in the Gas Phase, Advances in Photochemistry, Vol, 1, Ed. W.A. Noyes Jr., G.S. Hammond and J.N. Pitts Jr. Intersci. Pub., a division of John Wiley and Sons, New York, 1963.

68. D.A. Leathard and J.H. Purnell, Proc.Roy.Soc., A306 (1968) 553.

69. K. Yang, J.Am.Chem.Soc., 84 (1962) 719; 3795.

70. J.O. Terry and J.H. Futrell, Can.J.Chem., 45, (1967) 2327.